THESIS

DIRECTED EXPRESSION OF R2R3 MYB TRANSCRIPTION FACTORS FOR ECTOPIC SUBERIN DEPOSITION

Submitted by

Angel McKay Whiteman

Graduate Degree Program in Cell and Molecular Biology

In partial fulfillment of the requirements

For the Degree of Master of Science

Colorado State University

Fort Collins, Colorado

Fall 2022

Master's Committee:

Advisor: June Medford

Marc Nishimura
Christie Peebles

ABSTRACT

DIRECTED EXPRESSION OF R2R3 MYB TRANSCRIPTION FACTORS FOR ECTOPIC SUBERIN DEPOSITION

Plants are susceptible to many stresses, which can lead to reduced growth, decreased crop yield, or even plant death. Plants contain natural barriers to protect them from stresses, including the hydrophobic biopolymer suberin. Suberin protects plants against a variety of factors, including water loss, toxic ions, loss of essential nutrients, and entry of microorganisms. Plant roots contain a suberized barrier called the endodermis, which regulates the entry and exit of materials from the cortex to the vascular cylinder. While the endodermis protects the vascular cylinder, the cortex is left susceptible to stresses. Engineering a suberized barrier in the root epidermis could protect the cortex and provide an additional point of regulation.

Multiple R2R3 type MYB transcription factors have been found to be involved in suberin biosynthesis. Expressing these transcription factors in the root epidermis could provide a suberin barrier for protection. I expressed five R2R3 MYB transcription factors in the root epidermis of *Arabidopsis thaliana* to determine whether their expression led to suberization of the root epidermis. Constitutive expression of one transcription factor, MYB84, led to increased epidermal suberin. Two homozygous lines were further analyzed and found to have decreased root growth. Gene expression results from one homozygous line suggest that MYB84 overexpression may lead to increased expression of suberin biosynthetic genes involved in synthesis of aliphatic suberin monomers and monomer transport. Further analysis of these transgenic plants could provide insight into the potential protective barrier the root epidermal suberin provides.

TABLE OF CONTENTS

LIST OF TABLES

LIST OF FIGURES

Chapter 1: Introduction

Function of Suberin

Plants are susceptible to many biotic and abiotic stresses, such as insects, microorganisms, drought, and salinity. These stresses can cause decreased growth, lower crop yields, or even death (Atkinson and Urwin, 2012). Plants contain natural barriers to protect them against stresses. One such barrier, the cuticle, is deposited on the surface of epidermal cells of leaves, fruit, and primary shoots. The cuticle consists of cutin and cuticular waxes. The cuticular waxes are deposited both within the cutin polymer as intracuticular wax and outside of the cutin polymer, in direct contact with the environment, as epicuticular wax (Schreiber, 2010). The cuticle, namely the cuticular waxes, functions primarily as a barrier to protect the plant against water loss. Removal of these waxes leads to an increase in permeability of water and solutes from 100 to 1000-fold (Schreiber, 2010).

Another biopolymer, suberin, plays a similarly protective role in plants. While similar to cutin, suberin differs in its location and composition. Suberin is an important lipophilic biopolymer deposited in the cell walls of certain plant cells, including the endodermis, root exodermis, periderm, seed coat, and occasionally the skin of fruits and vegetables (Fich et al., 2016; Schreiber, 2010; Graça, 2015). Suberin is also present in abscission zones and deposited in response to wounding (Graça, 2015). Depositions of suberin can provide barriers to regulate transport of materials through cells, which function to protect the plant against a variety of factors, including water loss (Ranathunge et al., 2011), toxic ions (such as salt stress; Beisson et al., 2007), loss of essential nutrients (Barberon et al., 2016; Doblas et al., 2017), and entry of microorganisms (Lulai and Corsini, 1998).

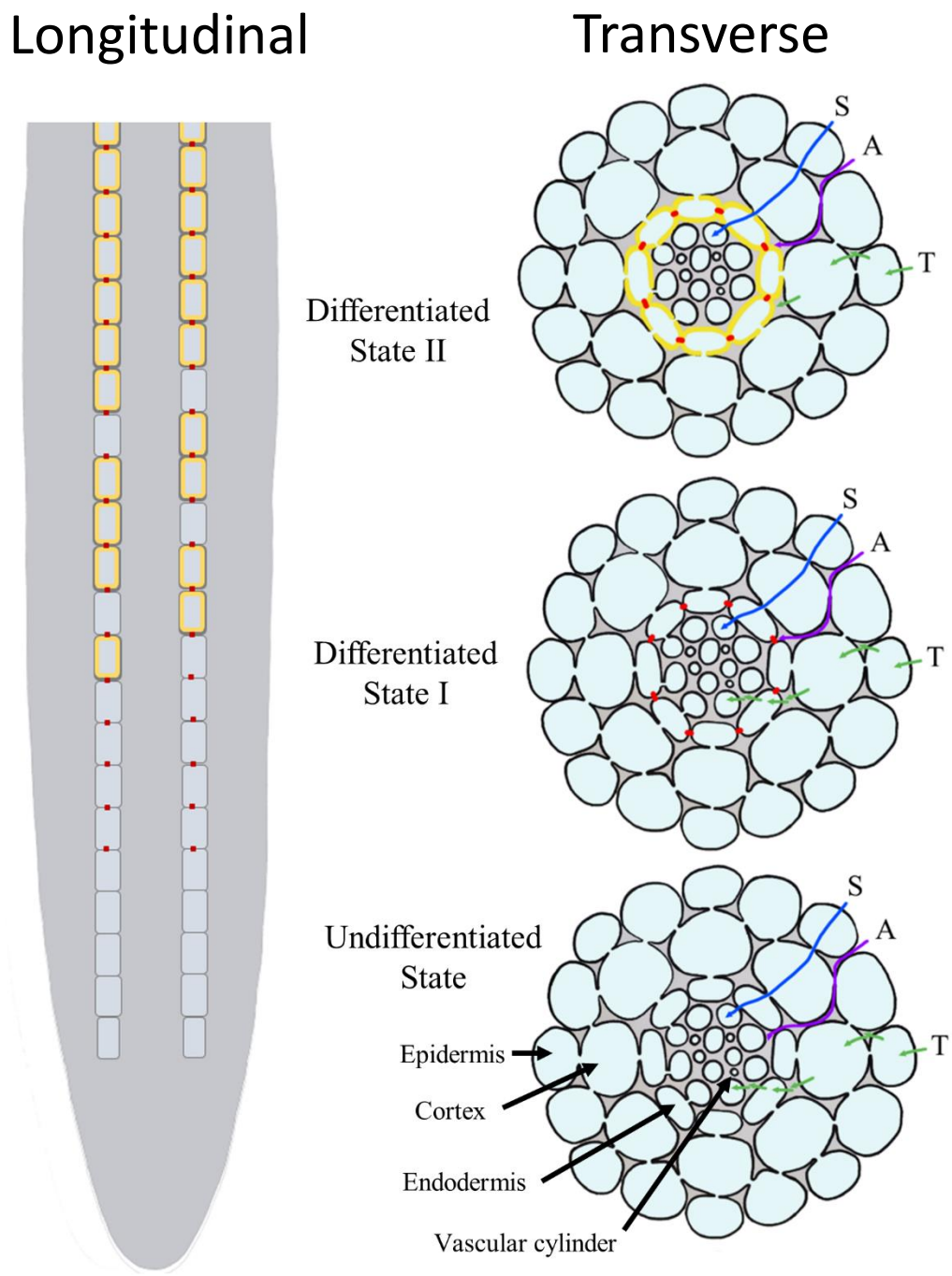

Figure 1.1. Differentiation of endodermal barriers in *Arabidopsis* roots. Diagram of longitudinal (left) and transverse views (right) of endodermal differentiation. In the undifferentiated state, there are three pathways for the transport of materials into the vascular cylinder: the symplastic pathway (S), apoplastic pathway (A), and coupled transcellular pathway (T). During state I, the Casparian strip (red) is formed by lignin deposited between adjacent endodermal cells, forming a continuous ring around endodermal cells within the apoplast and blocking the apoplastic pathway. During state II, suberin (yellow) is deposited between the cell wall and plasma

membrane, blocking the coupled transcellular pathway. Suberin deposition begins in individual cells, resulting in a patchy appearance. As the endodermis continues to differentiate, suberin is deposited continuously, resulting in a fully formed suberin lamellae and fully differentiated endodermis. The symplastic pathway, whereby materials move from cell to cell through plasmodesmata, is not blocked by endodermal barriers. Figure 1.1 adapted from Barberon et al. (2017), Doblas et al. (2017), and Vishwanath et al. (2015).

Molecules are transported from outside of the root into the vascular cylinder, and thereby the rest of the plant, through three pathways: the symplastic, the apoplastic, and the transcellular pathways (Figure 1.1). In the symplastic pathway, materials move from the cytoplasm of one cell to another through the plasmodesmata. Materials move through the area outside of the plasma membrane through the apoplastic pathway. In the transcellular pathway, materials move from the apoplast, through the plasma membrane, into the cytoplasm of a cell.

In the root, a layer of cells between the cortex and pericycle called the endodermis acts as a permeable barrier, regulating the entry of materials into the vascular cylinder during primary development. During secondary growth, the endodermis is replaced with a suberized periderm (Ranathunge and Schreiber, 2011). The endodermal barrier consists of the Casparian strip and the suberin lamellae. The Casparian strip is composed of lignin deposited between adjacent endodermal cells, forming a continuous ring around endodermal cells within the apoplast and blocking apoplastic movement (Figure 1.1) (Naseer et al., 2012; Doblas et al., 2017). The suberin lamellae consists of suberin deposited at the inner surface of primary cell walls, between the primary cell wall and plasma membrane of the cell (Doblas et al., 2017; Nawrath et al. 2013). This creates a barrier to the transcellular pathway as opposed to the apoplastic barrier the Casparian strip provides (Figure 1.1).

In addition to being deposited in different locations, the Casparian strip and suberin lamellae are deposited at different time points during root development. Differentiation of the

endodermal barrier has been defined in two steps: state I, during which the Casparian strip is formed, and state II, during which the suberin lamellae is formed (Doblas, et al., 2017; Barberon et al., 2016; Ranathunge and Schreiber, 2011; Naseer et al., 2012; Robards and Robb, 1974). During state I, lignin (or at least a lignin-like polymer) is deposited (Figure 1.1) (Naseer et al., 2012). It was long thought that the Casparian strip was composed of both lignin and suberin; however, suberin is deposited much later during endodermal differentiation (Naseer et al., 2012). During state II, suberin deposition begins in the elongation zone of the root and occurs in individual cells, resulting in a patchy appearance. As the endodermis continues to differentiate, suberin is deposited continuously, resulting in a fully formed suberin lamellae and fully differentiated endodermis (Figure 1.1) (Wang et al., 2020; Naseer et al., 2012). Due to the delayed formation of the endodermal barrier, the root tip and elongation zone are not fully protected, leaving this area of the root more susceptible to stresses. Within the mature endodermis, some non-suberized cells called passage cells can be found. Due to the absence of suberin, which acts as a transcellular barrier, these cells are thought to provide areas of unobstructed transcellular movement of water and ions (Holbein et al., 2020; Doblas, et al., 2017; Peterson and Enstone, 1996).

While both the Casparian strip and suberin lamellae constitute the endodermal barrier, they each have different functions. The suberin lamellae is thought to provide a barrier against transcellular movement of materials whereas the Casparian strip is thought to provide an apoplastic barrier (Barberon et al., 2016; Ranathunge and Schreiber, 2011). Propidium iodide is a red fluorescent dye commonly used to test cell viability and trace apoplastic movement as it flows through the apoplast but cannot pass through the plasma membrane in viable cells (Alassimone et al., 2010; Pecková, et al., 2016). In endodermal cells that contain the Casparian

strip but are not suberized, propidium iodide cannot pass through the endodermis into the vascular cylinder (Naseer et al., 2012). This supports the Casparian strip as a sufficient barrier to apoplastic movement without the presence of the suberin lamellae. Fluorescein diacetate dye (FDA) enters cells through the cell membrane and fluoresces within viable cells (Barberon et al., 2016; Huang et al., 1986). When only the Casparian strip is present, FDA can enter endodermal and pericycle cells after one minute of incubation but takes eight minutes to enter endodermal cells when the endodermis contains both the Casparian strip and suberin lamellae. Casparian strip defective mutants with normal suberization do not affect FDA staining (Barberon et al., 2016).

Similarly, analysis of root water transport capacity of multiple mutants with altered endodermal barriers showed that the suberin lamellae impacts root water transport whereas the Casparian strip does not (Calvo-Polanco et al., 2021). The shoots of plants were removed and the root hydraulic conductivity measured using pressure chambers containing hydroponic solution. The hydrostatic conductivity was determined by dividing the root hydraulic conductivity by the root dry weight and the osmotic conductivity was calculated based on sap exudation rate and the osmotic potential gradient between the sap and hydroponic solution. Generally, mutants with disrupted Casparian strip and increased suberization (*myb36-1*, *myb36-2*, *esb1-1*, *esb1-2*, and *casp1-1 casp3-1*) had a reduction in root water transport. Mutants with disrupted Casparian strip and normal suberization (*sgn3-3*, *sgn3-4*, and *sgn3-3 esb1-1*) or normal Casparian strip and enhanced suberization (*gelp51-2*, *anac038-1* and *anac38-2*) had no difference in root water transport compared to wild type. Mutants with normal Casparian strips and reduced suberization (*horst-1*, *horst-2*, *horst-1 ralph-1*, *pCASP1::CDEF1)* or altered suberin composition (*ralph-1* and *ralph-2*) had increased water transport capacity (Table 1.1) (Calvo-Polanco et al., 2021).

Mutants with disrupted Casparian strip and enhanced suberization had a reduction in root water transport but plants with a normal Casparian strip and enhanced suberization had normal water transport capacity. Calvo-Polanco et al. (2021) suggest that normal suberization blocks water in wild type and increasing suberization doesn't change this; however, this doesn't explain the reduction in root water transport for the plants with enhanced suberization and a disrupted Casparian strip. The reduction in root water transport may be due to differences in suberin composition for these mutants, such as in *esb1* mutants (Ranathunge and Schreiber, 2011). This suggests that the composition of suberin, not just the amount, plays a role in the permeability.

Table 1.1. Effects of altered suberin lamellae and/or Casparian strips on root water transport capacity. Root water transport capacity of multiple *Arabidopsis* mutants with normal (=), increased (+), reduced (-), or altered composition (~) of suberin lamellae and Casparian strips. Table created from results reported by Calvo-Polanco et al. (2021).

	Suberin	*Casparian strip*	*Root water transport*
myb36-1, myb36-2, esb1-1, esb1-2, and casp1-1 casp3-1	+	-	-
sgn3-3, *sgn3-4*, and *sgn3-3 esb1-1*	=	-	=
gelp51-2, *anac038-1,* and *anac38-2*	+	=	=
horst-1, *horst-2*, *horst-1 ralph-1*, *pCASP1::CDEF1*	-	=	+
ralph-1 and *ralph-2*	~	=	+

The reasoning behind the permeability of suberin is not known, but may be due to the composition, including suberin-associated waxes, or pores within the suberin lamellae. Suberin-associated waxes are thought to play a large role in the permeability of suberin (Li et al., 2007b;

Schreiber, 2010). The permeability of the endodermis may be due to the reduced wax content in endodermal suberin compared to cuticle and suberized potato periderm, a well-studied model for suberized tissue, which both have much lower permeability. It has been suggested that a waxy composition similar to the cuticle would block the necessary movement of water into roots (Schreiber, 2010). The permeability may be due to pores through the suberin lamellae. Confocal laser scanning microscopy of isolated onion endodermal cells showed pores through the suberin lamellae (Waduwara et al., 2008). These pores may be present in suberin lamellae of other plants as well. Waduwara et al. speculated that these pores act as passages for water and ions into endodermal cells. An intriguing possibility is that these pores may be responsible for the selective permeability of the endodermis. The suberin lamellae blocks access to the plasma membrane besides where these pores are present, which may allow the cell to regulate the entry and exit of materials due to the reduced surface area of the plasma membrane. Since both these pores and passage cells in the mature endodermis are thought to provide pathways for water and ions (Waduwara et al., 2008; Holbein et al., 2020; Doblas, et al., 2017; Peterson and Enstone, 1996), passage cells may have a similar function; by providing points where the plant can regulate the entry of materials.

Due to the decreased barrier properties at pores and passage cells, I suggest that these sites are also entry points for stresses such as toxic ions and microorganisms. While suberin pores may seem like weak points within the barrier, limiting access to endodermal cells besides where pores and passage are present could provide a huge advantage. For example, if the plant encounters toxic ions or microorganisms, it could respond by taking protective measures at these transport sites, thereby conserving resources since the rest of the endodermal cells are protected by the suberin lamellae. Further studies may elucidate this important function. Another role for

suberized barriers is when plants encounter specific nutrient deficiencies, they increase endodermal suberization to prevent loss of these nutrients (see Abiotic stress responses section; Barberon et al., 2016). An intriguing possibility is that this type of increased suberization may block pores and/or passage cells, and/or prevent movement through the suberin lamellae itself by thickening or tightening the suberin matrix; however, this is currently only speculation.

Overall, the suberin lamellae is sufficient to provide a highly organized barrier against the movement of water and ions. The amount and composition of suberin affect this barrier; increased suberization reduces permeability and altered composition increases permeability.

Composition of Suberin

The structure and composition of suberin is important as it impacts the barrier properties (Ranathunge and Schreiber, 2011); however, determination of the exact composition and structure of suberin has not yet been possible as suberin cannot be isolated without altering it (Vishwanath et al., 2015). The advent of gas chromatography mass spectrometry (GC-MS) allowed for the identification of monomers from partially depolymerized suberins (Kolattukudy et al., 1975; Holloway, 1983) while transmission electron microscopy (TEM) and nuclear magnetic resonance (NMR) based methods have made it possible to visualize suberin structure in cell walls and further elucidate the structure and composition of suberin (Graça et al., 2015; Correia et al., 2020), yet the exact structure is still unknown. Studying the properties of endodermal suberization is problematic due to difficulty in extraction from other root tissues, therefore the composition of suberin has primarily been derived through studying cork and potato tuber periderm due to the higher suberin content (Graça, 2015; Schreiber, 2010). Potato tuber skin is highly suberized, consisting of 8-12 suberized cell layers, and is easily isolated (Schreiber, 2010; Schreiber et al., 2005).

Suberin is a hydrophobic biopolymer composed of an aliphatic domain and an aromatic domain (Kolattukudy et al., 1974; Kolattukudy et al., 1980; Schreiber et al., 1999). It has been proposed that the term "suberin" should be reserved for the aliphatic domain due to their independent structures (Graça, 2015); however, this is not commonly accepted in the literature. Therefore, the term suberin in my thesis includes both the aliphatic and aromatic domains unless specified.

The aliphatic domain is primarily responsible for the barrier properties of the suberin lamellae due to its hydrophobic nature (Ranathunge and gSchreiber, 2011; Schreiber et al., 1999). It consists primarily of α,ω-diacids, ω-hydroxyacids, and glycerol (Kolattukudy et al., 1975; Holloway, 1983; Graça and Pereira, 2000). The proportions of these molecules and the monomer compositions vary in suberins by plant developmental stage, tissue type, and species, resulting in different arrangements of suberin monomers (Ranathunge et al., 2011; Holloway, 1983; Kolattukudy, 2002). It is not clear why suberin varies so greatly. It has been proposed that there are two main kinds of suberin: one in which the more polar C18 epoxide (cyclic ether with a three atom ring) and *vic*-diol (two vicinal hydroxyl groups) α,ω-diacids and ω-hydroxyacids are dominant, and another in which the mono-unsaturated and saturated C18 monomers are dominant, although there are suberins that do not fit in either category (Holloway, 1983; Graça, 2015). The aliphatic carbon chain lengths range from C16 to C32 with C16 and C18 predominant (Schreiber et al., 1999). The suberin backbone is composed of glycerol linked to α,ω-diacids (Franke and Schreiber, 2007; Correia et al., 2020) and ω-hydroxyacids have been found linked to glycerol as well (Graça and Pereira, 2000; Graça and Santos, 2006). Glycerol comprises 5% to 20% of suberin monomers (Graça and Pereira, 2000).

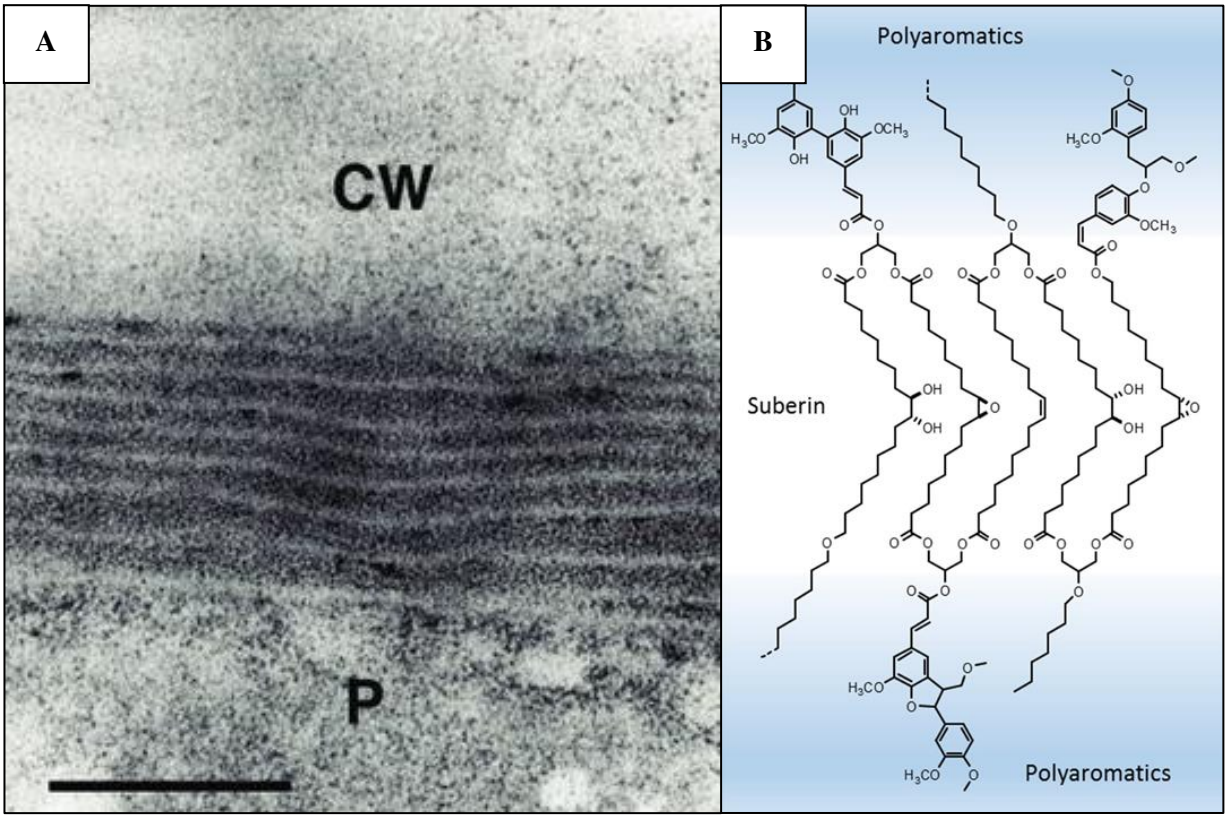

Figure 1.2. Structure and organization of suberin. (**A)** Suberized root periderm cell of wild type *Arabidopsis* with alternating light, electron translucent, and dark, electron dense, layers typical of suberin (TEM picture by Martine Schorderet, University of Fribourg; Nawrath et al., 2013). Scale bar: 100 nm. P: peridermal cell, CW: cell wall. (**B)** Hypothetical structure of suberin proposed by Graça (2015). The aromatic domain (blue) corresponds to the dark layers in (**A)**. The aliphatic domain (white) corresponds to the light layers in (**A**). The more regular thickness of the light layer is due to an orderly arrangement of glycerol, α,ω-diacids, and ω-hydroxyacids. Ferulic acid links the two domains together.

The linking groups of suberin monomers allow them to join together to form the aliphatic suberin polymer. The α and ω positions of α,ω-diacids contain carboxylic acids and ω-hydroxyacids contain carboxylic acid in the α position and a hydroxyl group in the ω position (Kolattukudy et al., 1975; Holloway, 1983). Ester linkages of ω-hydroxyacids and α,ω-diacids may allow for formation of a two- and three-dimensional matrix (Franke and Schreiber, 2007). Other fatty acids, including α-hydroxyacids, α,ω-alkanediols, and C16 ω-dihydroxyacids have also been found in suberins (Kolattukudy, 2002), as have alkanoic acids and alkanols, but as less

than 10% compared to α,ω-diacids and ω-hydroxyacids. Alkanoic acids and alkanols are monofunctional, meaning they contain a single linking group, preventing them from linking to more than one molecule. Therefore they can only be found at the ends of suberin polymers (Graça, 2015).

The aromatic domain is primarily composed of hydroxycinnamates, namely ferulic acid and coumaric acid. Ferulic acids have been found linked to ω-hydroxyacids (Graça and Pereira, 2000). The ferulic acid amides feruloyltyramine and feruloyloctopamine have also been found within suberin polyaromatics of potato periderm but have not been proven to link to suberin (Negrel, 1996). Suberin is thought to bind the cell wall via covalent linkages with its aromatic monomers (Kolattukudy 2001; Bernards 2002). Transmission electron microscopy has shown the suberin lamellae to be composed of electron-dense and translucent layers, providing alternating light and dark layers (Figure 1.2A) (Nawrath et al., 2013; Graça, 2015; Bernards, 2002). Nuclear magnetic resonance-based techniques of suberin within cell walls showed the aliphatic and aromatic domains to be physically separated, with one group of aromatics near the aliphatic polyester and another close to polysaccharides of the cell wall (Yan and Stark, 1998; Neto et al., 1995). Graça (2015) hypothesized that the more regular thickness of the light lamellae is due to an orderly arrangement of glycerol, α,ω-diacids, and ω-hydroxyacids and the dark lamellae is mostly polyaromatics, with ferulic acid linking the two domains together (Figure 1.2B).

Suberin from *Arabidopsis* is similar in composition to that of other species (Franke et al., 2005). TEM of endodermal suberization showed light and dark layers typical of lamellate suberin (Figure 1.2A) (Nawrath et al., 2013). Due to the difficulty in isolating endodermal cells from the rest of the root, Franke et al. analyzed suberin composition in whole roots treated

with polysaccharide hydrolases, cellulase, and pectinase to remove much of the unsuberized cell walls, reducing background. This method did not remove lignin. Similar to other species, ω-hydroxy acids and α,ω-dicarboxylic acids were the primary monomers detected through GC-MS (43% and 24%, respectively). Carboxylic acids (10%), alcohols (6%), and 2-hydroxyacids (<1%) were also detected, as were the aromatics ferulic acid and *p*-coumaric acid. Chain lengths varied from C16 to C24 with C18 the dominant length, particularly for ω-hydroxy acids and α,ω-diacids (Franke et al., 2005). Glycerol was also present, supporting glycerol as the backbone linking monomers together.

Waxes are also associated with suberin and are thought to be embedded within the aliphatic domain, although there is even less knowledge on these waxes than on suberin. Waxes are hydrophobic, non-polymeric long chain lipids. Compared to the cuticle and potato periderm, *Arabidopsis* roots contain much less wax, and the composition of these waxes is different (Schreiber, 2010). This is thought to be due to the necessity of the permeability of root suberin for water and nutrient uptake (Schreiber, 2010). In *Arabidopsis* root periderm, the composition of waxes also differs from that of suberin found in other locations (Li et al., 2007b). These waxes share characteristic with aliphatic suberin monomers (Li et al., 2007b; Franke et al., 2005), including a connection in the biosynthesis of both (see Biosynthesis of Suberin below; Li et al., 2007b). This may be due to suberin and its associated waxes being part of the same biosynthetic pathway, or these monoacylglycerols, free fatty acids, primary alcohols, and alkyl ferulates may be precursors to suberin monomers (Li et al., 2007b).

Like suberin, cutin composition varies across species and between different tissues of the same plant (Beisson et al., 2012). While suberin and cutin share many monomers, the proportions of individual monomers vary between them (Graça, 2015; Franke et al., 2005;

Vishwanath et al., 2015). Suberin generally contains longer chain saturated aliphatics and higher levels of hydroxycinnamic acids and fatty alcohols (Beisson et al., 2012). In *Arabidopsis*, root suberin was found to contain more longer chain monomers than leaf cutin and the dominant C18 monomer for suberin is monounsaturated ω-hydroxyacid and in cutin is double unsaturated α,ω-diacid (Franke et al., 2005). While similar in function, these two polymers are distinct from each other in composition and where in the plant they act as barriers.

Biosynthesis of Suberin

Much is still unknown about the biosynthesis of suberin. How the suberin monomers assemble to create the macromolecular structure remains largely unknown, as do the transport processes involved (Graca, 2015). The following includes the known biosynthesis of suberin in *Arabidopsis thaliana*.

Fatty acids, the precursors for suberin biosynthesis, are synthesized in the plastid by the fatty acid synthase complex (Li-Beisson et al., 2013). The fatty acids are then conjugated to acyl-CoA by long-chain acyl-CoA synthetase (LACS). LACS2 loss of function mutants indicated this enzyme may be involved in suberin biosynthesis (Li-Beisson et al., 2013), suggesting that this and possibly other LACS enzymes may activate fatty acids in the suberin biosynthesis pathway. LACS1 and LACS2 are involved in fatty acid activation in the biosynthesis of cutin. Due to the many shared monomers in cutin and suberin, LACS1 may be involved in suberin biosynthesis as well. Fatty acyl-CoAs are then exported to the endoplasmic reticulum (ER), where they are elongated by β-ketoacyl-CoA synthase (KCS). KCS is the first of four enzymes in the fatty acid elongase (FAE) complex (Millar and Kunst, 1997), a complex embedded within the ER membrane (Batsale et al., 2021; Serra & Geldner, 2022). Two of the twenty-one *Arabidopsis* KCSs, DAISY/AtKCS2 and AtKCS20, have been implemented in the elongation of C_{20} acyl

chain suberin precursors (Franke et al. 2009; Lee et al. 2009). Biochemical studies of yeast expressing DAISY previously showed that DAISY was capable of elongating saturated C_{16}-C_{20} acyl-CoA substrates into C_{22}, along with saturated C_{22} and unsaturated C_{16}-C_{18} substrates but with lower activity (Paul et al., 2006). Disruption of transcription through knock-outs of DAISY in *Arabidopsis* showed significantly reduced root aliphatic suberin monomers with chain lengths longer than C_{20} (Franke et al., 2008). This supports the involvement of DAISY in elongation of C_{20} suberin precursors, which was further supported by an accumulation of monomers shorter than C_{22}. Surprisingly, a β-glucuronidase (GUS) reporter line showed DAISY expression in cells of the stele, including the pericycle and xylem parenchyma cells, but not the endodermis, cortex, or epidermis. Besides the root, signal was found in flowers and siliques but in lower amounts than in roots (Franke et al., 2008).

KCS20 was found to have a similar, likely partially redundant role to KCS2 and is also expressed in high amounts in the roots of *Arabidopsis* (Lee et al., 2009). Double knockouts of KCS2/DAISY and KCS20 had 27% less C_{22} and C_{24} very long chain fatty acids compared to KCS20 single knockout (*kcs20*) and 18% less than KCS2/DAISY knockout (*kcs2/daisy*). The double mutant had about 51% more C_{20} very long chain fatty acids than *kcs20* and 24% more than *kcs2/daisy* (Lee et al., 2009). Due to the more extreme effect on aliphatic suberin monomers in the double knockout than either single mutant, these two enzymes are likely partially redundant. Additionally, the double knockout had an 8% decrease in total aliphatic suberin and the lamellate structure of suberin in the endodermis was disrupted whereas the single mutants had total suberin amounts comparable to wild type and a typical suberin lamellae (Lee et al., 2009), further supporting the necessity of KCSs in suberin biosynthesis. Similarly, in potato

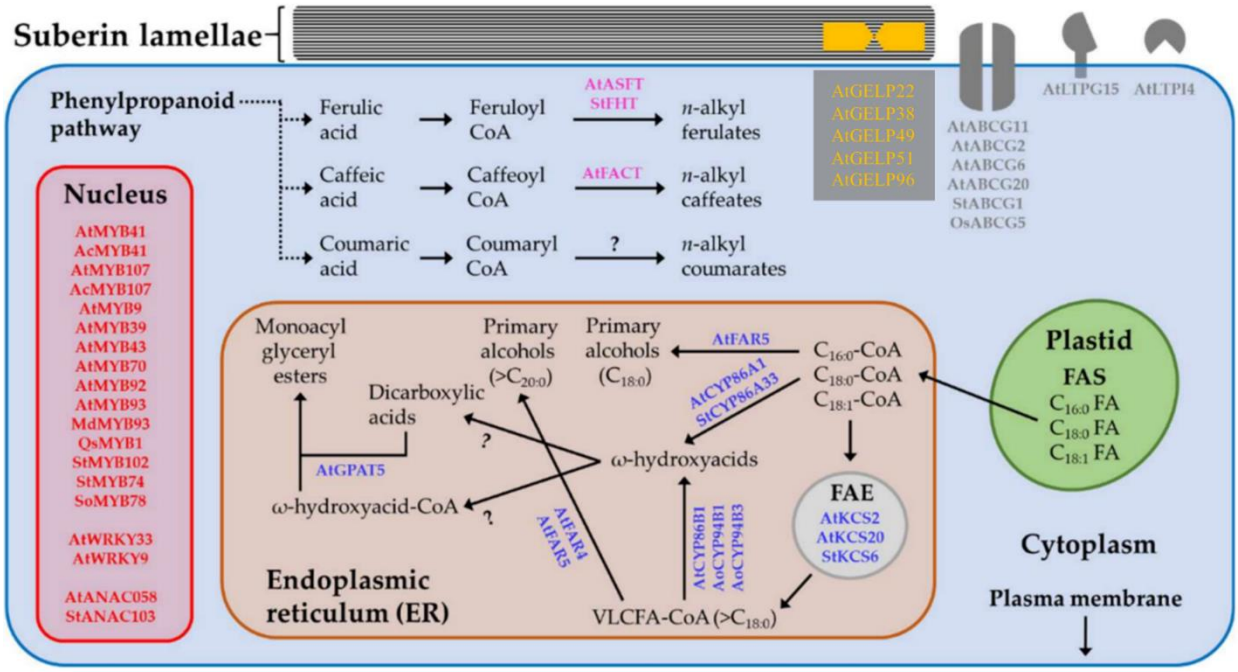

Figure 1.3. Suberin biosynthesis pathway, showing genes/proteins involved in the biosynthesis of suberin aliphatic monomers (blue), aromatic monomers (pink), monomer polymerization (orange), monomer transport (gray), and regulation of the suberin pathway (Nomberg et al., 2022). This figure includes enzymes from plants other than *Arabidopsis thaliana*, which are not the focus of my thesis. Genes/enzymes involved in the regulation of suberin are reviewed in the Regulation of Suberin section.

knockdowns of StKCS6 resulted in a significant decrease in very long chain fatty acids with C_{28} and higher and an increase in C_{26} and lower (Serra et al., 2009a). The mutant also had a decrease in wax and an increase in peridermal transpiration.

After elongation, hydroxylation of the very long chain fatty acids is catalyzed by Cytochrome P450 (CYP) oxygenases in the CYP86 subfamily. In *Arabidopsis*, CYP86A1 and CYP86B1 are involved in root suberin biosynthesis (Gaca, 2015; Vishwanath, 2015). CYP86A1 preferentially oxygenates C_{16}–C_{18} fatty acids and CYP86B1 preferentially oxygenates C_{22}–C_{24} fatty acids (Pinot & Beisson, 2011). Genes encoding ω-hydroxylases were more highly associated with either CYP86A1 or CYP86B1(Beisson et al., 2012).

CYP86A1 is a hydrolase in *Arabidopsis* roots (Höfer, et al., 2008). Two T-DNA insertional mutants resulting in loss of function of CYP86A1 named *horst* (hydroxylase of root suberized tissue) had significant decreases in suberin monomers in *Arabidopsis* roots (60.86% and 63.4%) compared to wild type (Höfer, et al., 2008). These reductions were primarily in ω-hydroxyacids of chain length C_{16} and C_{18} and α,ω-diacids with chain length C_{16}–C_{20}. Transformation of *horst-1* with wild type CYP86A1 coding sequence and 1.4kb upstream of the start codon resulted in wild type levels of aliphatic suberin, supporting that loss of CYP86A1 was responsible for the alteration in suberin monomer composition in the horst mutants. There were no significant differences in suberin monomer compositions in the leaves and seeds of the mutants compared to wild type. A GUS reporter line showed expression of CYP86A1 in the root endodermis and not in above ground organs of seedlings or mature plants. Fusion of GFP to CYP86A1 showed accumulation at the ER and CYP86A1 has been predicted to have a transmembrane domain (Höfer, et al., 2008; Schwacke et al. 2003), further supporting that the biosynthesis of suberin monomers takes place at the ER membrane (Höfer, et al., 2008).

In potato, the *Arabidopsis* CYP86A1 homolog CYP86A33 (88% homology) functions similarly to CYP86A1 (Serra et al., 2009), further supporting the role of CYP86A1 in suberin biosynthesis. Knockdown of CYP86A33 through RNA interference had a 60% reduction in aliphatic suberin monomers in potato periderm, especially *ω*-hydroxyacids and *α*,*ω*-diacids, while increasing the wax fraction. The lamellate structure of suberin was also severely impacted, as seen through TEM, and glycerol was reduced by 60% (Serra et al., 2009). The knock down also resulted in higher water permeability (Serra et al., 2009).

CYP86B1 functions similarly to CYP86A1, except it preferentially oxidizes C_{22}-C_{24} monomers instead of C_{16}-C_{18} (Pinot & Beisson, 2011). T-DNA insertional knockout of

CYP86B1 resulted in a reduction in very long chain monomers in roots and seeds, along with an increase in unsubstituted fatty acids in seeds (Molina et al., 2009). This was further supported by additional CYP86B1 knockouts, which had a reduction in C_{22} and C_{24} hydroxyacids and α,ω-diacids in roots and seed coats along with an increase in C_{22} and C_{24} fatty acids, the proposed precursors (Compagnon et al., 2009).

Two other Cytochrome P450 enzymes, CYP94B1 and CYP94B3, have more recently been found to be involved in suberin biosynthesis (Krishnamurthy et al., 2020; Krishnamurthy et al., 2021). Knockout of CYP94B1 led to reduced ω-hydroxy acids, α,ω-diacids, and alcohols. These levels (except for C_{18} octadecanol) were restored by crossing these mutant plants with plants expressing CYP94B1 under its native promoter, restoring CYP94B1 levels (Krishnamurthy et al., 2020). Knockout of CYP94B3 also lead to decreased suberin content, which was rescued when the mangrove homolog, AoCYP94B3, was expressed in these plants (Krishnamurthy et al., 2021).

Activated fatty acids are reduced by fatty acyl reductases (FARs), producing fatty alcohols. Three of the eight FARs in *Arabidopsis* (FAR1, FAR4, and FAR5) are expressed in the endodermis (Domergue et al., 2010). FAR1 and FAR4 were also found in seeds, another tissue known to be suberized (Domergue et al., 2010). T-DNA insertion mutants of each FAR had altered monomer lengths (Domergue et al., 2010; Vishwanath et al., 2013). FAR5 mutants had decreased C_{18} alcohols and an increase in C_{20} and C_{22} alcohols. FAR4 mutants had decreased C_{20} alcohols but no significant change in C_{18} or C_{22} alcohols. FAR1 mutants did not have altered C_{18} alcohols but had reduced C_{20} and C_{22} alcohols (Domergue et al., 2010; Vishwanath et al., 2013). The reductions in different fatty alcohols for the FAR T-DNA insertion mutants suggests that each FAR is responsible for reducing fatty acids of different lengths, with partial overlap of

FAR1 and FAR4 but no overlap with FAR5 (Vishwanath et al., 2013). FAR5 produces C_{18} fatty alcohols, FAR4 produces C_{20}, and FAR1 produces C_{22} and C_{20} fatty alcohols. Additionally, triple mutants reduce fatty alcohols (70-80%) without impacting other suberin monomers (Vishwanath et al., 2013). The decrease in specific fatty alcohols for each FAR was similar both for the polymeric and the soluble fatty alcohols (Vishwanath et al., 2013).

Glycerol-3-phosphate acyltransferases (GPATs) promote the esterification of fatty acids to glycerol, the backbone of suberin (Graça, 2015; Beisson et al., 2012). Of the eight GPATs found in *Arabidopsis,* GPAT5 is primarily responsible for suberin biosynthesis (Yang et al., 2012). GPAT5 esterifies ω-hydroxyacids and α,ω-diacids at the sn-2 position of glycerol-3-phosphate (Yang et al., 2010). GPAT5 accepts a wide range of acyl chain lengths, including C_{16}-C_{24}, but is most active with C_{22} substrates (Yang et al., 2012). GPAT5 is expressed in tissues known to be suberized, including flowers, seeds, and roots, but not in stems and rosette leaves (Beisson et al., 2007). Within the root, GPAT5 expression matches deposition of suberin within the differentiated endodermis, supporting its role in endodermal suberin biosynthesis (Beisson et al., 2007; Naseer et al., 2012). Additionally, knockouts of GPAT5 lead to reduced fatty acids (Beisson et al., 2007) and reduced monoacylglycerides (MAGs) in roots (Li et al., 2007b), while overexpression of GPAT5 results in the accumulation of MAGS (Li et al., 2007b).

GPAT7 may also be involved in suberin biosynthesis. GPAT7 has similar substrate specificity to GPAT5 and produces suberin-like precursors in overexpression lines (Yang et al., 2012). GPAT7 expression is induced by wounding in leaf tissues. GPAT7 knockout mutants do not have altered suberin composition, suggesting that this enzyme may only be involved in suberin biosynthesis in response to wounding (Yang et al., 2012).

Enhanced Suberin1 (ESB1) is another protein found to be involved in suberin biosynthesis, although how it is involved remains to be elucidated (Baxter et al., 2009; Nomberg et al., 2022). ESB1 is primarily expressed in the root endodermis, and knockout mutants have twice as much aliphatic suberin as wild type (Baxter et al., 2009). This suggests that ESB1 isn't directly involved in the synthesis of suberin, and may be involved in preventing suberin deposition.

Recently, five GDSL-type-esterase/lipase proteins (GELPs), have been found to be involved in suberin polymerization (Ursache et al., 2021). All five, GELP38, GELP51, GELP96, GELP22, and GELP49, are expressed in the endodermis, with GELP22 and GELP49 showing expression in the epidermis as well (Ursache et al., 2021). Quintuple knockout mutants had loss of the lamellate suberin structure and reductions in aliphatic suberin monomers (85%). Additionally, Ursache et al. (2021) found five GELPs involved in the degradation of endodermal suberin: GELP12, GELP55, GELP72, GELP73, and GELP81, suggesting that these proteins are involved in the regulation of suberin biosynthesis.

Aliphatic suberin feruloyl transferase (ASFT), a member of the BAHD family, links ferulic acid to ω-hydroxyacids, connecting the aliphatic suberin polymer to the aromatic domain (Graça, 2015, Molina et al., 2009; Nomberg et al., 2022; Philippe et al., 2020). ASFT is expressed in seed coats and roots, known locations of suberin deposition. Similar to CYP86A1 expression (Höfer, et al., 2008), ASFT is expressed in the root endodermis during primary development and in the periderm during secondary development (Molina et al., 2009). T-DNA insertional knockouts of ASFT resulted in decreased ferulate and ω-hydroxyacids (C_{20}-C_{24}) and an increase in α,ω-diacids in seeds. In roots, ferulate levels were also highly reduced but the aliphatic monomer composition wasn't significantly affected (Molina et al., 2009). Surprisingly,

the lamellate structure of suberin in the root periderm was not affected in the mutants, suggesting that the ferulate released through transmethylation does not play a part in the root periderm (Molina et al., 2009). ASFT mutants do not have altered root hydroxycinnamate ester wax composition, suggesting that this enzyme is not responsible for synthesis of these molecules (Molina et al., 2009).

Fatty alcohol:caffeoyl-CoA caffeoyl transferase (FACT), another transferase in the BAHD family, is responsible for synthesis of a subclass of hydroxycinnamate esters, alkyl caffeate. FACT knockout mutants lead to reduced alkyl caffeate but not reduced alkyl coumarate levels in roots (Kosma et al., 2012). There is not yet a known enzyme responsible for synthesis of alkyl coumarates (Kosma et al., 2012; Nomberg et al., 2022).

The mechanism(s) of transport of suberin to its site of deposition, between the plasma membrane and cell wall, is not well known (Nomberg et al., 2022). In addition, there are no known transporters of suberin building blocks from their major site of biosynthesis, within the endoplasmic reticulum, to the cytosol. Transporters from the ATP-Binding Cassette (ABCG) and Lipid Transfer Protein (LTP) families have been found to be involved in transport of these molecules through the plasma membrane (Nomberg et al., 2022). ABCG2, ABCG6, and ABCG20 triple mutants had reduced aliphatic suberin, and a distorted suberin lamellae with increased permeability in roots and seed coats (Yadav et al., 2014). The analysis of the mutant *awake1*, an allele of ABCG20, further supported its role in transport of suberin fatty acids (Fedi et al., 2017). ABCG1 has been found to be involved in the transport of longer chain aliphatic monomers (Shanmugarajah et al., 2019). ABCG1 mutants had reduced longer chain dicarboxylic acids, fatty alcohols (C_{26}-C_{30}), and fatty acids (C_{24}-C_{30}) (Shanmugarajah et al., 2019). LTPI4 is involved in suberin in crown galls that develop in response to *Agrobacterium tumefaciens*, which

are covered in suberin. LTPI4 mutants have smaller crown galls with reduced long chain fatty acids (Deeken et al., 2014). LTPG15 is expressed in the root endodermis and seed coat. LTPG15 knockout mutants had decreased C_{20}-C_{24} fatty acids, C_{20} and C_{22} primary alcohols, C_{22}-C_{24} ω-hydroxy fatty acids, and C_{20}-C_{22} α,ω-alkanediols (Lee and Suh, 2018). Due to expression of LTP15 in the root endodermis, this protein may be involved in the transport of suberin monomers in the endodermis as well. After transport through the plasma membrane, it is not known how the suberin monomers are polymerized into the macromolecular structure (Graca, 2015).

Regulation of Suberin

Hormonal responses

The hormones abscisic acid (ABA) and ethylene regulate the deposition and degradation of endodermal suberin, respectively. ABA treatment of plant roots induces endodermal suberization. ABA treatment results in suberization at the root tip without the usual patchy zone between the tip and zone of maturation (Shukla et al., 2021). Similarly, Wang et al. (2020) found that treatment of a pGPAT5::GFP-GUS reporter line with ABA for two days resulted in a small level of suberization. Using fluorol yellow (FY) staining, they found that ABA induced high levels of suberization after six hours, which leveled out between twelve and twenty-four hours, after which suberin levels began to decrease. Suberin biosynthetic enzyme gene expression was examined with qPCR and showed the same response pattern (Wang et al., 2020), supporting that ABA induces suberization by activating transcription of suberin biosynthesis genes.

Using a GPAT5::mCITRINE-SYP122 reporter line, Barberon et al. (2016) found increased GPAT5 expression in the endodermis three hours after treatment with ABA. GPAT5 expression extended toward the root tip and formed an early and continuous expression pattern

after twenty hours compared to the patchy expression in untreated plants. GPAT5 expression extended into the cortex and in some cases into epidermal cells. This was confirmed by FY staining, which showed suberization in the cortex and root tip. Additionally, root suberin monomers increased 43% compared to nontreated roots. Casparian strip formation was not affected (Barberon et al. 2016). This further supports ABA's role in inducing suberization, without affecting the Casparian strip.

The role of ABA as a regulator of suberin deposition was confirmed through disrupting the response to, or biosynthesis of ABA, which decreases endodermal suberin. Mutants with disruptions in ABA response and biosynthesis showed delayed suberization and increased patchy suberization with less continuous suberization (Barberon et al., 2016). Expression of the ABA response suppressor *aba-insensitive 1-1* in the endodermis resulted in delayed suberization. Treatment with ABA did not increase suberization in these plants (Barberon et al., 2016), supporting the necessity of ABA signaling for endodermal suberin development. Similarly, blocking ABA biosynthesis with fluridone results in lower levels of root suberin (Wang et al., 2020). This suggests that ABA is necessary for suberin deposition (Barberon et al., 2016).

Ethylene has the opposite response on suberization as ABA. Application of the ethylene precursor 1-aminocyclopropane-1-carboxylic acid (ACC) results in decreased suberization in new parts of roots and degradation in already suberized mature roots (Barberon et al., 2016). Increasing ACC resulted in a stronger reduction. Twenty-four-hour treatment of ACC resulted in patchy (and thinner) or absent suberin lamellae in mature endodermal cells, while whole roots had a 40% decrease in suberin monomers compared to untreated (Barberon et al., 2016). This supports ethylene as a negative regulator of suberin. The Casparian strip was not affected by ACC treatment (Barberon et al., 2016). Mutants with disrupted ethylene signaling (*etr1* and *ein3*)

had higher levels of suberin, and suberin was not affected by ACC treatment. This supports ethylene signaling in the degradation of suberin reported after ACC treatment (Barberon et al., 2016). A mutant with constitutive ethylene (*ctr1*) had similar effects to ACC treatment. ABA treatment of the mutant resulted in partial rescue (some endodermal suberin) (Barberon et al., 2016).

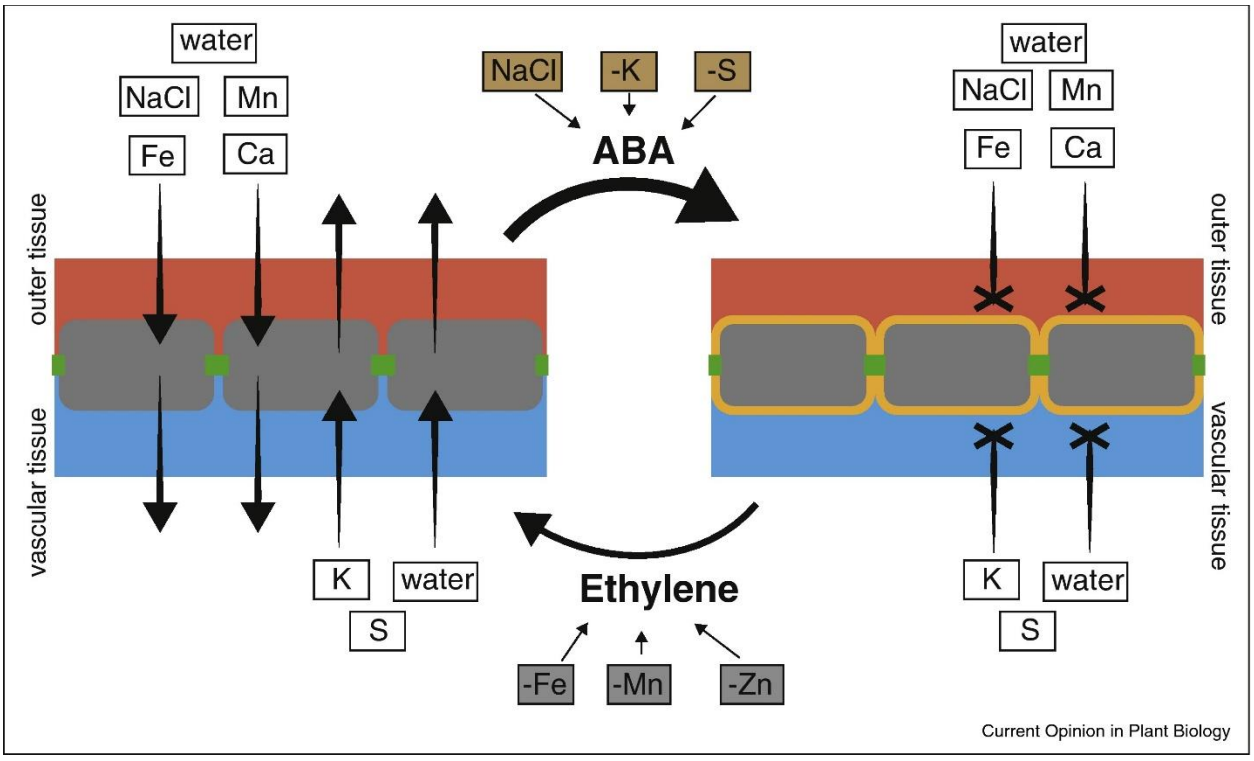

Figure 1.4. Endodermal suberin modulation in response to hormones and abiotic stresses. K^+ and S deficiencies and treatment with NaCl lead to increased suberization through the ABA pathway, preventing entry of NaCl into the vascular tissue and loss of K and S. Fe, Mn, and Zn deficiencies lead to reduced suberization through the ethylene pathway, allowing entry of NaCl, Mn, Fe, and Ca into the vascular tissue and exit of K and S. Increased suberization can also provide a barrier against water loss or entry (Doblas et al., 2017).

Abiotic stress responses

Suberin is regulated by a variety of environmental factors. Endodermal suberin levels are modified in response to abiotic stresses, including nutrient deficiencies, salt stress, and drought.

Increased endodermal suberin can prevent the exit of beneficial ions and water, and provide protection against the entry of unwanted ions, such as salt (Barberon et al., 2016; Silva et al., 2021).

Suberization is delayed in response to iron (Fe), magnesium (Mn), and zinc (Zn) deficiencies and enhanced under potassium (K) and sulfur (S) deficient conditions (Barberon et al., 2016). Barberon et al. (2016) examined the effects of impaired nutrient transporters on endodermal suberization in *Arabidopsis* mutants. The Fe transporter mutant *irt1* had a reduction in endodermal suberin with delayed and patchy suberization, as did the Fe and Mn-deficient mutant (*nramp1).* The K-deficient mutant (*skor*) had earlier development of suberin and differentiated into the continuous suberization earlier, as did the S-deficient double mutant (*sultr1;1 sultr1;2)*. This was further supported by growth under deficient conditions. Suberization is delayed in Fe, M, and Zn-deficient conditions and enhanced under K and S-deficient conditions.

The hormones ABA and ethylene regulate the altered suberin in response to these nutrient deficiencies (Figure 1.4). Fe, Zn, and Mn deficiency in the ethylene signaling *Arabidopsis* mutants *etr1* and *ein3* didn't change suberin levels, suggesting that ethylene signaling is responsible for the decreased suberin in response to these deficiencies (Figure 1.4) (Barberon et al., 2016). Fe deficiency has similar effects on suberization as ACC treatment. Fe deficiency led to loss of suberin in mature endodermal cells and reduction in new root growth, supported by a slight reduction of GPAT5 expression similar to that in response to ACC (Barberon et al., 2016). Additionally, the ethylene perception inhibitor $AgNO_3$ and the ethylene biosynthesis inhibitor aminoethoxyvinylglycine (AVG) can prevent decreased suberin in response to Fe deficiency, further supporting ethylene's role in reducing suberization in response

to Fe deficiency (Barberon et al., 2016). Increased suberization in response to S or K deficiency was not altered in the ethylene signaling mutants but is not seen in the ABA signaling repressor line (*abi 1-1*), suggesting that ABA signaling is responsible for the increased suberization in response to S or K deficiency (Figure 1.4) (Barberon et al., 2016). It is not yet known how nutrient levels lead to ABA or ethylene responses, or how these hormones lead to the transcriptional regulation of suberin biosynthesis genes (Barberon, 2016).

Mutant plants with decreased levels of endodermal suberin have increased lithium (Li), sodium (Na), and arsenic (As), and decreased K in leaves (Barberon et al., 2016). Baxter et al. (2009) analyzed mutants with increased suberization (*esb1-1* and *esb1-2*), and found they had increases in shoot Na, S, K, As, selenium (Se), and molybdenum (Mo) and reductions in Ca, Mn, Zn, and Fe. Similarly, Hosmani et al. (2013) found mutants with increased suberization (*esb1-1* and *casp1-1casp3*-1) had increased K, S, and Mo and reductions in Ca, Mn, and Fe. Additionally, suberization was found to prevent Ca^{2+} concentrations in endodermal cells (Moore et al., 2002). Together, this suggests that the suberin lamellae may function in prevention of the entry of some elements, such as Ca, and exit of others, such as K, supporting suberin as a bidirectional barrier (Baxter et al., 2009; Barbaron, 2016; Doblas et al., 2017).

Suberin deposition plays a role in protection against salt stress. Salt induces endodermal suberization in wild type *Arabidopsis* (Franke et al., 2009; Geng et al., 2013; Kosma et al., 2014; Barberon et al., 2016; Shukla et al., 2021; Silva et al., 2021). Barberon et al. (2016) found low levels of salt treatment resulted in increased suberization in *Arabidopsis* after twenty-four hours. Additionally, suberin defective mutants have increased Na accumulation (Barberon et al., 2016; de Silva et al., 2021), and when grown under salt conditions, have decreased root length and seed production compared to wild type (Barberon et al., 2016). This suggests that suberin protects the

plant against salt stress. Mutant plants with decreased endodermal suberin did not increase in suberization when treated with NaCl (de Silva et al., 2021). Similarly with the response to K and S deficiencies, increased suberization in response to salt treatment was found to be dependent on the ABA pathway, further supporting ABA as a regulator for suberin deposition (Figure 1.4) (Barberon et al., 2016).

In addition to salt stress and nutrient deficiencies, drought stress induces endodermal suberization. Drought stress was introduced to two-week-old wild type *Arabidopsis* for two or three weeks, which led to increased root suberin compared to non-treated plants (41% and 22%, respectively) (De Silva et al., 2021). While treated plants had higher levels of suberization when immature, once plants reached maturity (six-weeks-old), they had the same levels of suberin as non-treated plants of the same age, and no ectopic suberin was found (De Silva et al., 2021). This suggests that drought accelerates endodermal suberin formation, rather than increasing suberization (De Silva et al., 2021). Less than two weeks of drought treatment didn't result in differences in suberin compared to non-treated plants (De Silva et al., 2021). Suberin-associated waxes also increased after three weeks of drought treatment. Mutants with reduced suberin (*abcg2-1 abcg6-1 abcg20-1*, *far1-2 far4-1 far5-1*, *cyp86a1-1 cyp86b1-1*, and *myb92-1 myb93-1*) also had increased suberin in response to drought (De Silva et al., 2021).

Additionally, increased suberization has been found to confer drought resistance. Baxter et al. (2009) found mutants with increased suberization (*esb1-1* and *esb1-2*) had reduced wilting in response to water withdrawal compared to wild type. This was due to the roots; grafting of mutant roots to wild type shoots led to reduced wilting similar to self-grafted mutants whereas mutant shoots grafted to wild type roots wilted much sooner. The *esb1* mutants also had increased water use efficiency (Baxter et al., 2009). Similarly, analysis of root water transport

capacity of multiple mutants with altered Casparian strips and/or suberin lamellae found that the suberin lamellae impacts root water transport (Table 1; Composition of Suberin section) (Calvo-Polanco et al., 2021).

Both drought and NaCl induce suberization in wild type plants; however, drought increases suberization in suberin defective mutants, but NaCl does not increase suberin in these plants (de Silva et al., 2021). The suberin defective mutants contain high levels of Na when treated with NaCl (Barberon et al., 2016; de Silva et al., 2021), therefore the lack of increased suberization in response to NaCl may be because increased suberization would trap the Na already in the shoots, similarly to how K loss is prevented in K-deficient conditions (Barberon et al., 2016). This differs from drought as the increased suberization would protect the plant without trapping unwanted ions within the shoots. The difference in responses also presents the possibility that these environmental factors are not regulated by the same pathway since they have different responses.

Altogether, the induced suberization in response to abiotic stresses supports suberin as a bidirectional barrier for protection against stresses. The suberized endodermis protects the vascular cylinder, leaving the cortex, between the endodermis and the epidermis, susceptible to stresses outside of the root. Replicating endodermal suberin to the epidermis in plants lacking an exodermis could provide an additional protection for the vascular cylinder while also protecting the cortex. This has the potential to allow for plants to be grown in drought or saline environments.

R2R3 MYB transcription factors

Multiple R2R3 type MYB transcription factors have been found to be involved in suberin biosynthesis. Expressing these transcription factors in the root epidermis could provide a suberin

barrier for protection. MYB transcription factors contain the conserved MYB DNA-binding domain, which contains one to three imperfect repeats. Those with one repeat are in the MYB1R factor family, those with two repeats are in the R2R3-type MYB family, and those with three repeats are in the MYB3R family. Those with three repeats create a helix turn helix structure (Stracke et al., 2001).

The R2R3-type MYBs constitute the largest MYB family, with over one hundred different MYBs identified in *Arabidopsis thaliana*, and control plant-specific processes (Stracke et al. 2001). AtMYB41 was previously thought to regulate cutin deposition due to overexpression lines with altered cuticle (Cominelli et al., 2008); however, Kosma et al. (2014) found that MYB41 is involved in the regulation of suberin. MYB41 overexpression lines had ectopic suberin aliphatic monomers in leaves but did not have altered suberin in the endodermis, periderm, or seed coat. This was confirmed through transient expression of AtMYB41 in *Nicotiana benthamiana* (Kosma et al., 2014).

Analysis of previously published DNA microarray data from MYB41 overexpression lines (Cominelli et al., 2008) by Kosma et al. (2014) found that the most upregulated genes were involved in suberin biosynthesis, including ASFT, GPAT5, and FAR4. This was further confirmed in a MYB41 overexpression line with increased CYP86A1 (+18,000-fold), CYP86B1 (+7,000-fold), GPAT5 (+8,000-fold), FACT (+2,000-fold), ASFT (+3,000-fold), KCS2 (+100-fold), FAR5 (+400-fold), FAR4 (+1700-fold), and FAR1 (+10-fold) (Kosma et al., 2014).

Similarly to the induction of suberin deposition, ABA and salt treatment induce MYB41expression in the endodermis. Fusion of GUS to the MYB41 promoter resulted in gene expression in the endodermis and surrounding cortical cells in response to ABA and NaCl treatment (Kosma et al., 2014). While Kosma et al. (2014) did not find endodermal expression of

MYB41 in the absence of ABA or salt treatment, Shuckla et al. (2021) found that MYB41 was expressed in the endodermis in unstressed conditions in addition to in response to ABA treatment. ABA treatment led to an increase in MYB41 expression including expression closer to the root tip.

While MYB41 expression is found in the root endodermis, overexpression lines did not lead to suberization in any other root tissue. This is likely due to a lack of activation in other root tissues. MYB41 relies on phosphorylation of its serine 251 by MPK6 kinase for activation (Hoang et al., 2012). MYB41 may not be phosphorylated in the root epidermis.

Converting a serine to aspartic acid mimics phosphorylation because aspartic acid is chemically similar to phosphorylated serine (Figure 1.5) (Fodor-Dunai et al., 2011). The Medford lab created a phosphomimic mutant of MYB41 by mutating Ser251 to aspartic acid. Constitutive expression of this mutant resulted in suberin synthesis in root epidermal cells.

A functional redundancy between MYBs has been suggested due to little alteration in phenotype for knockouts (Stracke et al., 2001). MYB41 CRISPR knockouts do not have altered endodermal suberin (Shuckla et al., 2021), supporting this redundancy. Other MYBs in the R2R3 family have strong similarity to MYB41, both in sequence (Figure 1.6) and phylogenetically

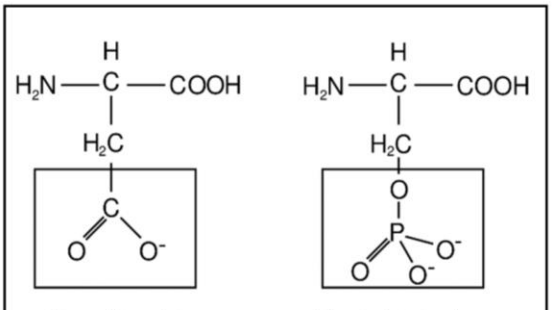

Figure 1.5. Chemical similarly between aspartic acid and phosphor-serine. Image from Wikipedia.

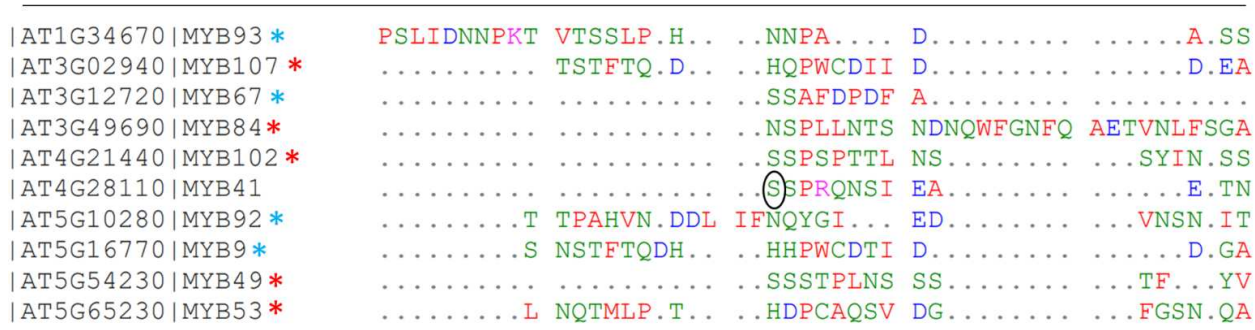

Figure 1.6. T-coffee amino acid alignment of MYB93, MYB107, MYB67, MYB84, MYB102, MYB41, MYB92, MYB9, MYB49, and MYB53. Red stars indicate MYBs analyzed in this thesis. Blue stars indicate MYBs recently analyzed in the Medford lab (Berning, 2022). MYB41 Ser251 circled in black.

(Figure 1.7), and may also have roles in controlling suberin biosynthesis and/or rely on phosphorylation for activation. This includes AtMYB49, AtMYB53, AtMYB84, AtMYB102, and AtMYB107 analyzed here. AtMYB9, AtMYB67, AtMYB92, and AtMYB93 were recently analyzed in the Medford lab (Berning, 2022).

AtMYB49 is involved in suberin biosynthesis in leaves (Zhang et al., 2020). Similarly to MYB41, MYB49 is induced by ABA and salt stress (Zhang et al., 2020). A MYB49 overexpression line led to higher salt tolerance while knockout and repression lines led to increased susceptibility. Genes involved in cutin, suberin, and wax biosynthesis were upregulated in Arabidopsis plants overexpressing MYB49 and downregulated in a MYB49 repressor line both under normal and salt stress conditions (Zhang et al., 2020). MYB49 was also found to directly bind to the promoters of genes involved in cutin, suberin, and root wax biosynthesis and activate their expression (Zhang et al., 2020). MYB49 was previously found to affect cadmium (Cd) accumulation in Arabidopsis, and to be induced by Cd (Zhang et al., 2019). This suggests that MYB49 regulates Cd accumulation through increased suberization in response to increased Cd. Additionally, the tomato ortholog SlMYB49 is involved in regulating stress responses (Cui et al., 2018).

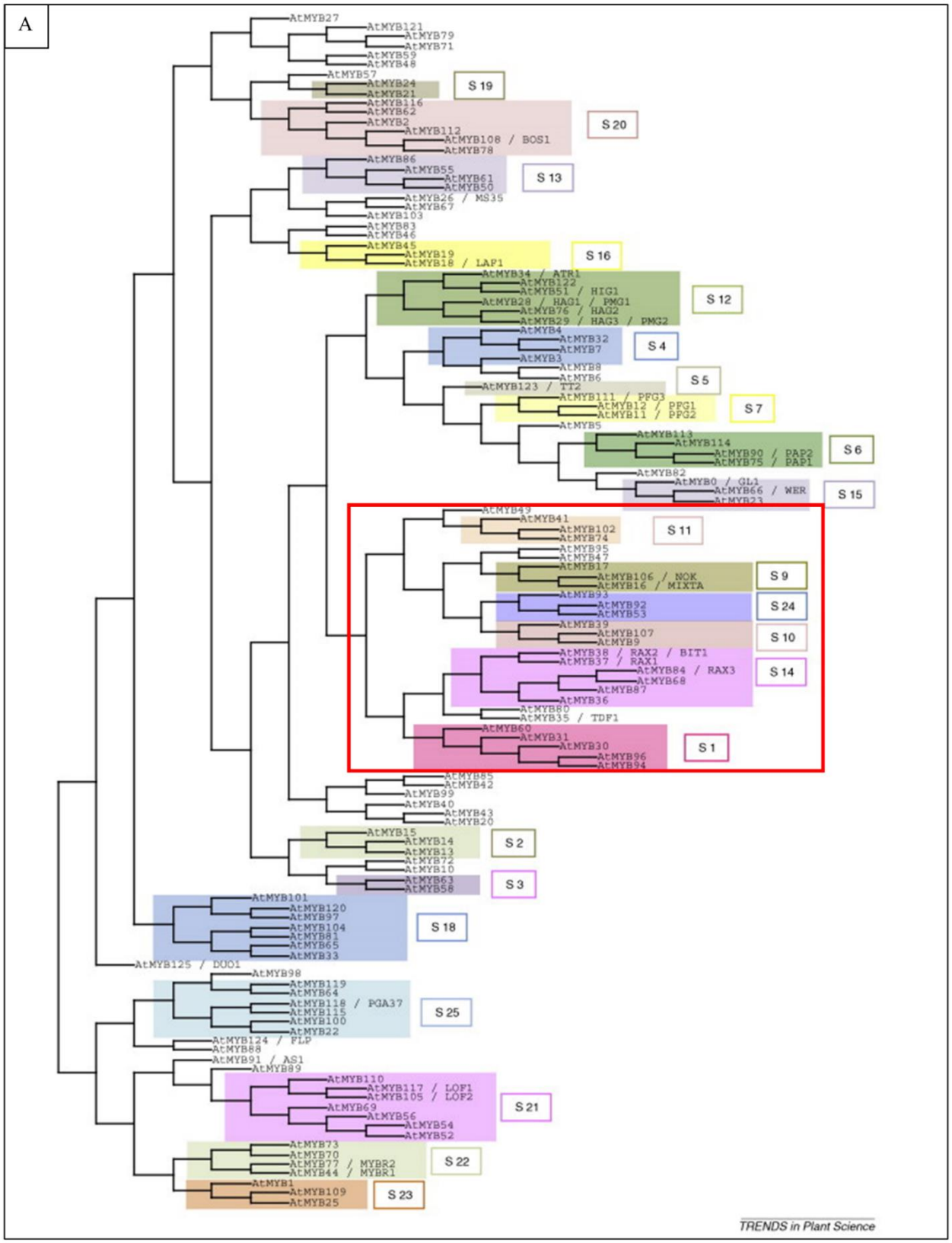
A
AtMYB27
AtMYB121
AtMYB79
AtMYB71
AtMYB59
AtMYB48
AtMYB57
AtMYB24
AtMYB21
S 19
AtMYB116
AtMYB62
AtMYB2
AtMYB112
AtMYB108 / BOS1
AtMYB78
S 20
AtMYB86
AtMYB55
AtMYB61
AtMYB50
S 13
AtMYB26 / MS35
AtMYB67
AtMYB103
AtMYB83
AtMYB46
AtMYB45
AtMYB19
AtMYB18 / LAF1
S 16
AtMYB34 / ATR1
AtMYB122
AtMYB51 / HIG1
AtMYB28 / HAG1 / PMG1
AtMYB76 / HAG2
AtMYB29 / HAG3 / PMG2
S 12
AtMYB4
AtMYB32
AtMYB7
S 4
AtMYB3
AtMYB8
AtMYB6
S 5
AtMYB123 / TT2
AtMYB111 / PFG3
AtMYB12 / PFG1
AtMYB11 / PFG2
S 7
AtMYB5
AtMYB113
AtMYB114
AtMYB90 / PAP2
AtMYB75 / PAP1
S 6
AtMYB82
AtMYB0 / GL1
AtMYB66 / WER
AtMYB23
S 15
AtMYB49
AtMYB41
AtMYB102
AtMYB74
S 11
AtMYB35
AtMYB47
AtMYB17
AtMYB106 / NOK
AtMYB16 / MIXTA
S 9
AtMYB93
AtMYB92
AtMYB53
S 24
AtMYB39
AtMYB107
AtMYB9
S 10
AtMYB38 / RAX2 / BIT1
AtMYB37 / RAX1
AtMYB84 / RAX3
AtMYB68
AtMYB87
AtMYB36
S 14
AtMYB80
AtMYB35 / TDF1
AtMYB60
AtMYB31
AtMYB30
AtMYB96
AtMYB94
S 1
AtMYB85
AtMYB42
AtMYB99
AtMYB40
AtMYB43
AtMYB20
AtMYB15
AtMYB14
AtMYB13
S 2
AtMYB72
AtMYB10
AtMYB63
AtMYB58
S 3
AtMYB101
AtMYB120
AtMYB97
AtMYB104
AtMYB81
AtMYB65
AtMYB33
S 18
AtMYB125 / DUO1
AtMYB98
AtMYB119
AtMYB64
AtMYB118 / PGA37
AtMYB115
AtMYB100
AtMYB22
S 25
AtMYB124 / FLP
AtMYB88
AtMYB91 / AS1
AtMYB89
AtMYB110
AtMYB117 / LOF1
AtMYB105 / LOF2
AtMYB69
AtMYB56
AtMYB54
AtMYB52
S 21
AtMYB73
AtMYB70
AtMYB77 / MYBR2
AtMYB44 / MYBR1
S 22
AtMYB1
AtMYB109
AtMYB25
S 23
TRENDS in Plant Science

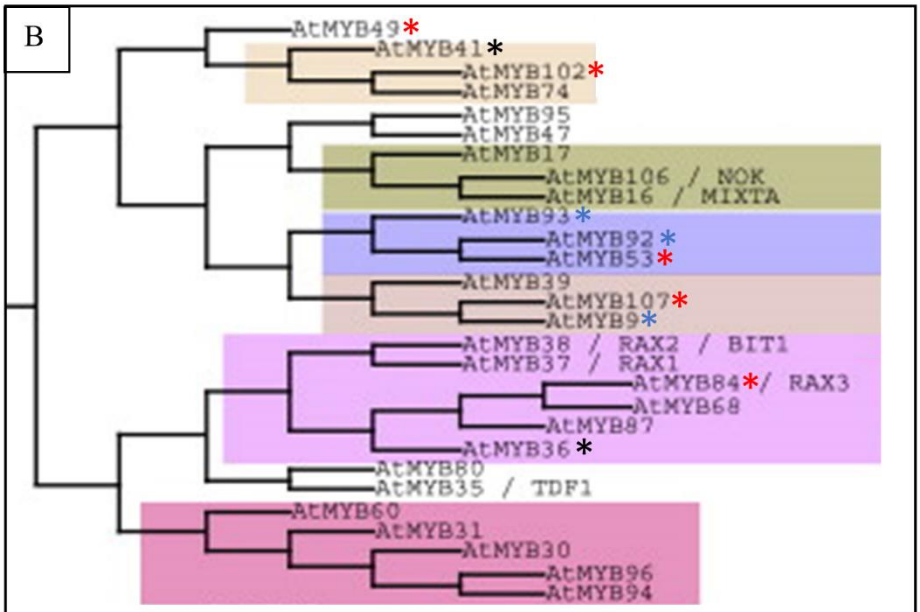

Figure 1.7. A. Phylogeny of *Arabidopsis thaliana* MYB transcription factors (Dubos et al., 2010). **B.** Close up of red box in **A.** Red stars indicate MYBs analyzed in this thesis. Black stars indicate MYBs with known functions relating to the endodermis. Blue stars indicate MYBs recently analyzed (Berning, 2022).

AtMYB53 is involved in endodermal suberin regulation. MYB53 is induced by ABA but at a lower level than MYB41 (Shuckla et al., 2021). Expression of MYB41 was found to reduce expression of MYB53 and knocking out MYB41 led to increased expression of MYB53, supporting redundancy between MYB41 and MYB53. A quadruple knockout of MYB41, MYB53, MYB92, and MYB93 led to almost complete absence of endodermal suberin, supporting that these four MYBs regulate endodermal suberin deposition (Shuckla et al., 2021). MYB92 and MYB93 are not described in my thesis.

AtMYB84 is involved in periderm formation and has been used as a periderm marker (Wei et al. 2020). MYB84 regulates phosphate (Pi) accumulation in a Zinc-dependent manner. Under Zinc deficiency, MYB84 (along with MYB15, bHLH35, and ICE1) represses expression of the Arabidopsis phosphate transporter PHO1;H3. MYB84 and MYB15 bind directly to each other and the PHO1;H3 promoter, repressing transcription (Bouain, 2019; Pal et al., 2017).

AtMYB102 is expressed in response to dehydration (Kranz et al., 1998), wounding, salt stress, and ABA (Denekamp and Smeekens, 2003). MYB102 is expressed at damage sites from insect feeding and knockout of MYB102 allows for *P. rapae* caterpillars to develop faster than Col-0 (De Vos et al., 2006). It has been suggested that MYB102 is involved in healing after wounding in Poplar stem bark by regulating suberin deposition at sites of wounding (Rains et al., 2022).

AtMYB107 is involved in suberin and wax deposition in seed coats (Lashbrooke et al., 2016), which may be suberin-associated waxes. Gou et al. (2020) also found MYB107 to be involved in the regulation of seed coat suberin. MYB107 knockouts have altered seed coat suberin with increased permeability. This leads to increased susceptibility to stresses (Gou et al., 2020).

These MYBs could regulate production of different suberin precursors or have functions overlapping with MYB41. Further characterizing these genes will give insight into their physiological roles in plants. We hypothesize that expressing the MYB genes described above under control of an epidermal-specific promoter will lead to suberization of the root epidermis (Figure 1.7), protecting the root cortex and providing a barrier against stresses.

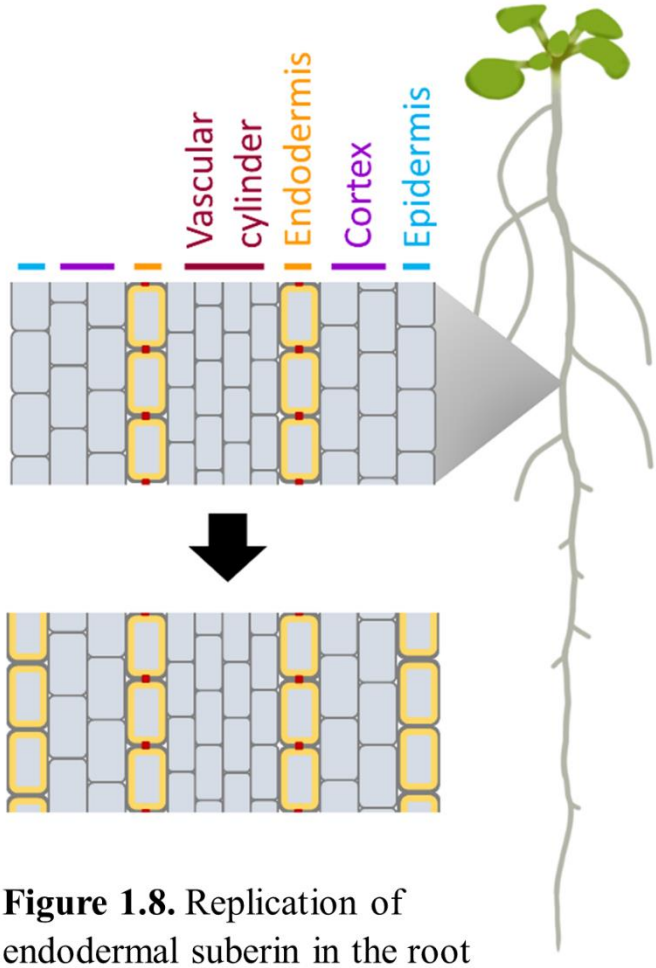

Figure 1.8. Replication of endodermal suberin in the root epidermis of *Arabidopsis thaliana*. yellow: suberin; red: Casparian strip

Chapter 2: Root epidermal expression of R2R3 MYB transcription factors

Each MYB transcription factor was transformed into a vector under the ABCG37/PDR9 promoter. ABCG37/PDR9 is involved in the transport of various compounds, including IBA, auxinic compounds, and coumarins (Ziegler et al., 2017; Fourcroy et al., 2013). Sara Oemke, a previous graduate student in the Medford Lab, confirmed expression of pABCG37/PDR9 in the root epidermis with a DIG inducible circuit. GFP signal was found in the root epidermis and root hairs (Figure 2.1) (Oemke, 2020). Due to confirmed expression of this promoter in the root epidermis, pABCG37/PDR9 was selected for expression of MYB transcription factors in the root epidermis.

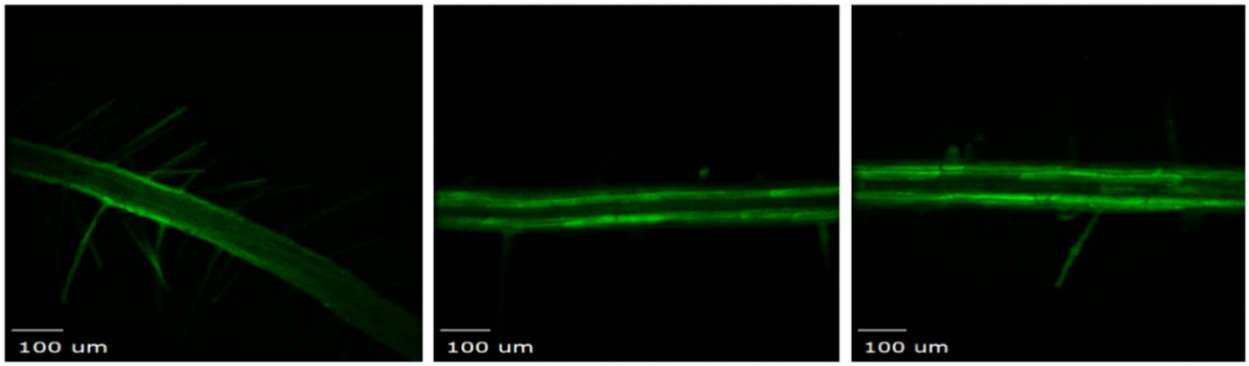

Figure 2.1. Confocal images of the zone of maturation. Plants were treated with 1, 10, and 100 µM digoxin (left to right) for 16 hours (Oemke, 2020).

Amino acids with high phosphorylation scores according to PhosPhAt 4.0 and similarity in sequence to the successful phosphomimic of MYB41 (Ser251) were chosen to mutagenize into aspartic acid (Figure 2.2). The following amino acids were chosen for mutagenesis: MYB49 S273; MYB49 T277; MYB84 Ser256; 107 Ser253. No candidate amino acids were found for MYB53.

Transgenic *Arabidopsis thaliana* plants expressing the MYB genes in the root epidermis were generated. MYB genes cloned from *Arabidopsis* cDNA were ligated into a plant expression

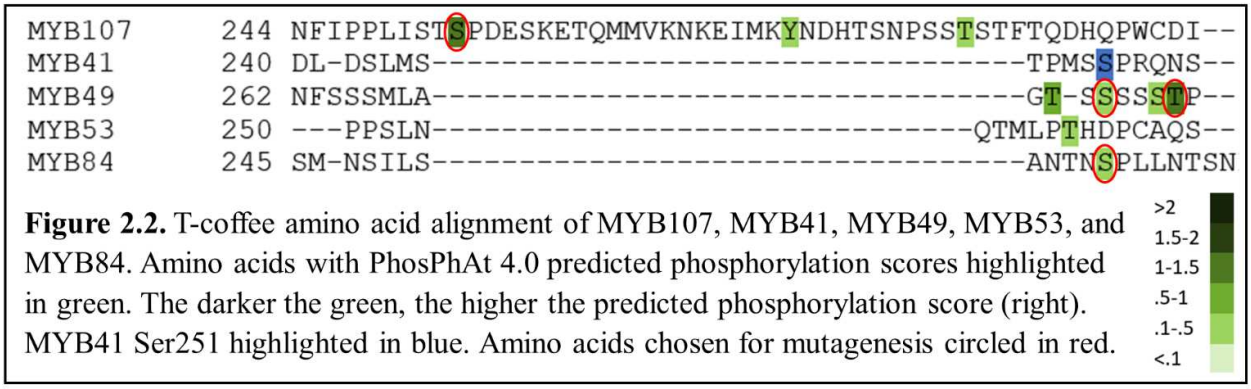

Figure 2.2. T-coffee amino acid alignment of MYB107, MYB41, MYB49, MYB53, and MYB84. Amino acids with PhosPhAt 4.0 predicted phosphorylation scores highlighted in green. The darker the green, the higher the predicted phosphorylation score (right). MYB41 Ser251 highlighted in blue. Amino acids chosen for mutagenesis circled in red.

vector with Kanamycin (Kan) antibiotic resistance under the ABCG37/PDR9 promoter (Figure 2.5). Kan resistance allows for selection of transgenic plants. Constructs were transformed into *Agrobacterium tumefaciens,* and the floral dip method used to transform wildtype *Arabidopsis* (ecotype Columbia [Col-0]) (Figure 2.3), transferring the DNA insertion (T-DNA) into the plant genome (Figure 2.3). Primary transformant (T-0) seed was harvested from dipped Col-0. T-0 plants were grown and self-fertilized to generate T-1 seed. T-1 plants were self-fertilized to generate T-2 seed (Figure 2.4).

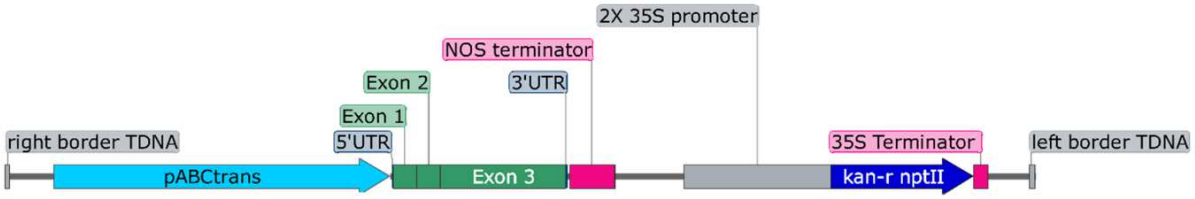

Figure 2.3. Map of transfer DNA (T-DNA) integrated into transgenic plant genome. MYB transcription factor genes (green) under the ABCG37/PDR9 promoter (blue) with the NOS terminator (pink). Kanamycin (dark blue) antibiotic resistance under the 35S promoter (grey) and terminator (pink).

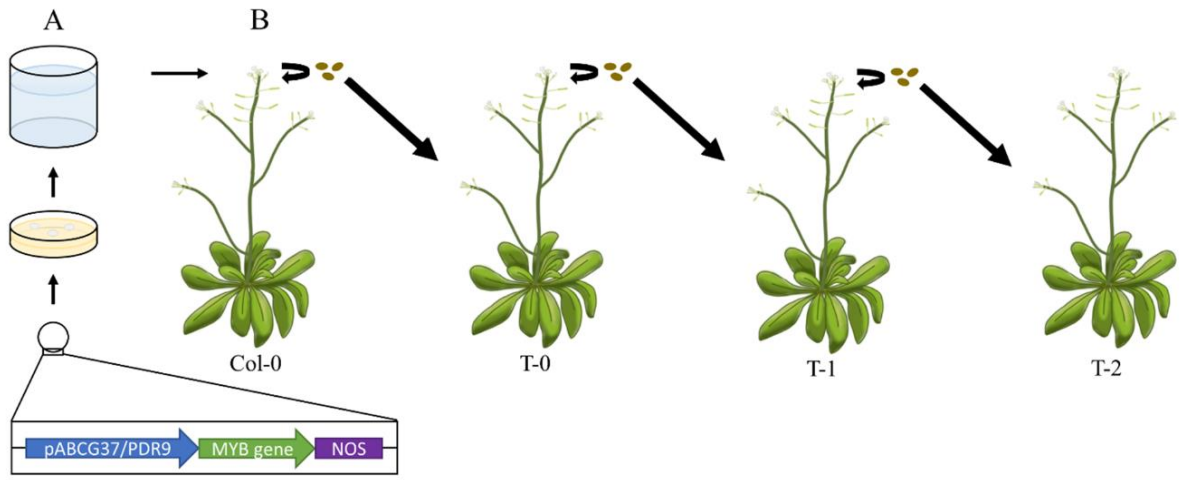

Figure 2.4. Schematic of transgenic plant generation. **A.** Transformation of plant expression vector containing the MYB gene under the root epidermal specific promoter, ABCG37/PDR9, into *Agrobacterium tumefaciens*. *Agrobacterium* containing the vector was added to New Infiltration Media, then the floral dip method used to transform Col-0 plants. **B.** T-0 seed from dipped Col-0 was harvested. T-0 plants were grown and self-fertilized to generate T-1 seed. T-1 plants were self-fertilized to generate T-2 seed.

Methods

Cloning Procedure and Construct Design

Cloning primers for each MYB gene were designed in Snapgene (Table A.1) and ordered from Integrated DNA Technologies (IDT). MYB genes were amplified with Phusion High-Fidelity DNA Polymerase from a cDNA pool synthesized from RNA isolated from *Arabidopsis thaliana.* PCR products were gel purified, ligated into NEB pminiT2.0 vector (MYBs 49, 53, 84, and 107), then transformed into NEB 10-beta *E. coli* using heat shock and plated on Carbenicillin (Carb) -containing LB media. Colonies were PCR verified with the cloning primers, grown overnight in liquid cultures, miniprepped (either by hand or using a QiaCube) and the minipreps sequence verified by Genewiz Sanger Sequencing with the NEB pminiT2.0 sequencing primers.

A pCAMBIA2300-similar plasmid containing a gene fused to mCherry under control of the ABCG37 promoter was digested with NEB BamHI-HF and Eco53kI to remove the gene and mCherry. The backbone containing the ABCG37 promoter was gel purified. MYB53, MYB84, and MYB107 were digested with NEB BamHI-HF and ZraI, then ligated into the TKK670 backbone using T4 DNA ligase. MYB49 was ligated into pminiT2.0 backwards so a forward cloning primer containing a BamHI site (MYB49clone-F_BamHI) and the reverse cloning primer (MYB49clone-R) were used to add a BamHI to the 5' end of MYB49. The PCR product

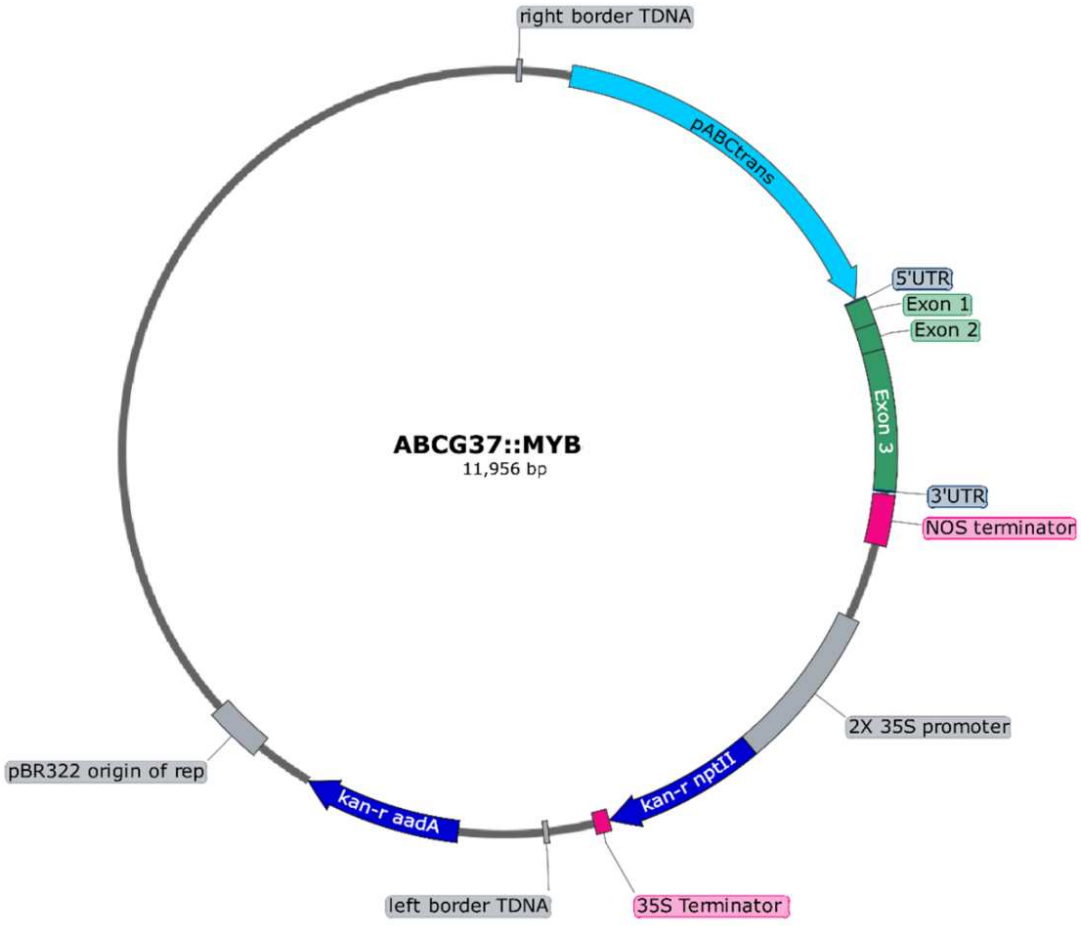

Figure 2.5. Plant expression vector map. Vector includes Kanamycin resistance for selection for vector-containing bacteria. Transfer DNA (T-DNA) contains the MYB transcription factor gene (green) under the ABCG37/PDR9 promoter (blue) with the NOS terminator (pink). Kanamycin resistance within the T-DNA allows for selection of plants the T-DNA integration.

was gel purified, digested with BamHI, gel purified again, then ligated into the TKK670 backbone. The ligations were transformed into DH5 alpha electro-competent cells and plated on Kanamycin (Kan)-containing LB media. Colonies were PCR verified, miniprepped, and verified with internal sequencing primers via Genewiz Sanger Sequencing. MYB102 cloned into pENTR was ordered on Tair (clone U16808).

Mutagenesis

Amino acid sequences of MYB49, MYB53, MYB84, and MYB107 were aligned to MYB41 using T-coffee (Figure 2.2). Amino acids with high phosphorylation scores according to PhosPhAt 4.0 and similarity in sequence to the successful phosphomimic of MYB41 (Ser251) were chosen to mutagenize into aspartic acid. The following amino acids were chosen for mutagenesis: MYB49 S273; MYB49 T277; MYB84 Ser256; 107 Ser253. No candidate amino acids were found for MYB53. Agilent QuikChange II kit or NEB Q5 Site-Directed Mutagenesis kit was used for mutagenesis. Primers were designed using the Agilent primer design or NEB primer design, respectively.

Plant Growth

Seed Preparation

All seed was sterilized and stratified prior to plating. Seeds were sterilized by incubation in 70% ethanol for approximately 2 minutes then replaced with 30% bleach. The seeds were then washed with sterile DI water five times and stratified for at least two days in the dark at 4°C.

Col-0 Grown for Transformation

Wildtype *Arabidopsis thaliana* (ecotype Columbia [Col-0]) seed was plated on full MS and grown under short day conditions. After rosettes reached around 2 cm in diameter, plants were transferred to soil. Plants were transferred to long days to induce flowering and bolts removed to promote increased bolting.

T-0 Plants

T-0 seed from dipped Col-0 was plated on Kan50 Cefo100 full MS plates. After 10 days grown in short day conditions, resistant plants were transferred to vertical plates. After microscopy screening, rescued plants were grown on plates until roots sufficiently grew back. Plants with increased suberin in the epidermis were transferred to soil and moved to long days to promote flowering. T-0 plants were selfed to generate T-1 seed.

T-1 Plants

50 T-1 seeds were plated on Kan50 full MS and grown in a growth chamber in long day conditions. A ratio of 3 Kan-Resistant :1 Kan-Susceptible was expected for one T-DNA insertion and 15 Kan-Resistant :1 Kan-Susceptible for two T-DNA insertions. A chi-squared analysis was performed to test that the observed number of resistant and susceptible plants conformed to the expected ratio for one T-DNA insertions. Five resistant plants for each line were transferred to soil and moved to a long day growth room. These plants were selfed to generate T-2 seed.

T-2 Plants

50 T-2 seeds were plated on Kan50 full MS and grown in a growth chamber in long day conditions. If all 50 T-2 plants were Kan-Resistant, plants were further characterized.

Agrobacterium-Mediated Transformation

TKK670 plasmids containing the MYBs transformed into GV3101 (all native MYBs) or EHA105 (all phosphomimic MYBs) *Agrobacterium tumefaciens* and plated on Rif/Gen/Kan LB (GV3101) or Rif/Kan LB (EHA105). The floral dip method, adapted from Zhang et al. (2006), was used to transform Col-0 plants with multiple inflorescences.

Fluorol Yellow Staining

Fluorol yellow 088 is a lipophilic fluorochrome with absorption at 450nm and emission at 515nm, allowing for visualization under a fluorescent microscope with a GFP filter. Fluorol yellow was made fresh each day of microscopy. Fluorol yellow powder was dissolved in lactic

acid at 1mg/10mLs, vortexed vigorously, then incubated in a heat bath at 50°C. Fluorol yellow was covered in foil, again vortexed vigorously, then filtered with a VWR Sterile Syringe Filter 0.45 μm to remove undissolved fluorol yellow. Roots were removed from plants and placed in 24-well-plates. Approximately 1ml of filtered fluorol yellow was poured into each well containing a root. Forceps were used to ensure entire roots were submerged. The plates were covered with foil to protect from light and then placed in an oven or on top of a heat block at 65-70°C for 30 min. The Fluorol yellow was then removed from each well. The roots were washed with DI water, which was removed and more DI water was added. The plates were then placed on a shaker at 150 rpm for 10 minutes. The DI water was replaced again, then the plates were placed back on the shaker for an additional 10 minutes. The DI water was replaced again and placed on the shaker for another 10 minutes (30 minutes total). The roots were mounted on microscope slides with 50% glycerol.

Microscopy Screening of Primary Transgenics

T-0 seed were grown in short days on Murashige and Skoog (MS) media containing 50 ng/ml kanamycin (Kan) and 100 ng/ml cefotaxime (Cefo). Kan-resistant plants were moved to vertical plates (5 per plate) after approximately 10 days. Kan-resistant plants were grown vertically for approximately 2 weeks, 3 weeks, and 4 weeks. The roots were removed and stained with Fluorol yellow. Rosettes of these plants were moved to rescue MS plates containing 50 ng/mL Kan and 100 ng/ml Cefo. Fluorescent microscopy was then used to compare the roots of transgenic plants to wildtype *Arabidopsis* (ecotype Columbia [Col-0]) to determine whether the epidermis contains higher levels of fluorescence that would indicate deposition of suberin. The Leica DFC450 camera was used to take pictures of roots. Plants found to have suberin in the

epidermis were moved to soil after recovery on rescue plates and moved to a growth room with long day light conditions to promote flowering.

Microscopy Screening of T-2 plants

A Leica CRT5500 microscope and Leica K5 fluorescent camera were used to take fluorescent and brightfield images of T-2 roots. Fluorol yellow was made fresh each day of microscopy screening. Due to this, fluorescence varied each day of microscopy. To account for variability in fluorescence, exposure was adjusted each day of microscopy by ensuring that no background fluorescence was visible in the epidermis of Col-0 with high fluorescence in the endodermis. The same settings were used for each picture taken each day unless noted otherwise in figure legend. Images of T-2 plants were taken at the root-shoot transition, at lateral root junctions, in the zone of maturation (middle of root), and in the zone of elongation.

Preparation of Microscopy Images

Microscopy images were rotated in photoshop. Contrast and brightness were adjusted for brightfield and merged images if needed to improve visualization (original images are available). The same settings were used for the same root pictures and reference Col-0. Image size was adjusted to 300 dots per inch (dpi) Resample: Preserve Details (enlargement). Images were exported as high resolution png files (Resample: Preserve Details), which were imported into Powerpoint to assemble into figures and add arrows and scale bars. Sizing of images was carefully preserved to ensure accurate scale bars. Powerpoint figures were exported as 300dpi png files.

MYB84-8.4 three-week-old root brightfield and fluorescent images were merged in photoshop. Fluorescent image was added as a layer to the brightfield image. The fluorescent image was duplicated, turned black and white, and the fluorescent duplicate and black and white

were merged to create a black and white layer of the fluorescence. The black and white layer was subtracted from the brightfield layer, and the fluorescent layer was changed to Screen to merge the brightfield and fluorescence. Contrast and brightness were adjusted if necessary.

Hormone Treatment

Homozygous T2 transgenics and Col-0 were grown on half MS for two weeks and transferred to half MS (half the amount of MS and half the amount of sucrose) plates containing 1 µM ABA, 2 µM ACC, or 5 µM ACC for 24 hours. Five plants per transgenic line were treated and compared to treated Col-0, untreated Col-0, and untreated transgenics via fluorol yellow staining.

Measurement of Root Length

Root length of MYB84 transgenics was compared to Col-0 to determine whether directed expression of MYB84 has an impact on root length. Thirty transgenic plants and thirty Col-0 were plated on vertical plates. After two weeks, pictures were taken of the roots and later measured in IMAGEJ. The scale was set based on the square markers on the vertical plates (square length = 13mm). The same scale was used for all images due to all pictures taken from the same height relative to the plates. Roots were traced using a stylus pen for touch screens on a touch screen laptop. Three measurements were taken for each root, and the average length used. Student's t-test considering 2 tailed equal variance was performed to compare root length. Error bars: standard error. After pictures were taken, roots were measured from root-shoot transition to root tip. A representative root of the average length for each line was chosen for a visual image of the differences in root length. Contrast and brightness of representative root length images were altered in Photoshop to increase visualization of roots. Image size was adjusted to 300dpi

Resample: Preserve Details (enlargement). Scale bars were added and images were exported as high resolution png files (Resample: Preserve Details).

Measurement of Root Weight

Roots from nine-ten, four-week-old plants grown on vertical plates were removed below the shoot to root transition and pooled into one tube. Fresh weight was taken on an analytical balance, then roots were snap frozen in liquid nitrogen for subsequent qRT-PCR analysis. This was repeated twice for each line to create three pools of approximately ten roots each (three biological replicates). Pools of roots instead of individual root weight was used for a more accurate root weight due to the low sensitivity of such low weights on an analytical balance. Average root weight per pool was calculated in Excel. Student's t-test considering 2 tailed equal variance was performed to compare average root weight per pool. Error bars on graphs represent standard deviation between average root weight for each pool.

qRT-PCR

Three pools of nine-ten roots from four-week-old plants grown for Measurement of Root Weight were snap frozen in liquid nitrogen after weighing for qRT-PCR (three biological replicates). Col-0 grown under the same conditions was used as a control. The TRIzol chloroform method described by Shi and Bressan (2006) was used to isolate RNA from pooled roots (described in Measurement of Root Weight). cDNA was synthesized with Invitrogen SuperScript II Reverse Transcriptase (Catalog number: 18064022) and Oligo (dT) 12-18 primer (Catalog number: 18418012). No template and no enzyme negative controls were performed.

Primers for qPCR were designed with IDT PrimerQuest Tool for Intercalating Dyes (Primers only) (Table A.1). cDNA samples were checked for genomic contamination by performing PCR on samples with primers that span introns in ABCG37 and Vacuole ATP

synthase subunit C genes and running the samples with gel electrophoresis. No genomic DNA was detected. A standard curve was used to check the efficiency of the MYB84 primers used for qPCR. Efficiency was calculated at 104.49% with an R^2 of 0.9989. All other primer pairs were previously calculated to have efficiencies of 96.5% for ACT2, 106.8% for KCS2, 94.7% for FACT, 98.6% for ABCG6, and 101.3% for GELP51 (Berning, 2022).

LightCycler® 480 SYBR Green I Master was used to load Hard-Shell 96-Well PCR plates (HSP9601). Four technical replicates were used for each biological replicate to ensure accurate quantification cycle (Cq) values. 75ng of cDNA was used per well. The reference gene, ACT2, was included on each plate.

Technical replicate Cq values were averaged and outliers were removed when standard deviation >0.3. Biological replicate Cq values were averaged and outliers were removed when standard deviation >0.5 unless removal of two was required to lower the standard deviation below 0.5, in which case all three biological replicates were included**.** Delta Cq (ΔCq) values were calculated by subtracting the average Cq value for the transgenic from the control (Col-0). The equation used to calculate ΔΔCq fold change is 2^(ΔCq gene - ΔCq ACT2). Error bars standard deviation of biological replicates excluding outliers. Student's t-test considering 2 tailed equal or unequal variance was performed to compare biological replicates (excluding outliers) for the transgenic and control (Col-0).

Results and Discussion

Microscopy screening for root epidermal suberin in primary transgenics

Seventeen to thirty independent T-0 lines for each transgenic line were screened for root epidermal suberin by visual inspection of roots stained with fluorol yellow under a Leica fluorescent microscope. A Leica DFC450 Digital Color Microscope camera was used to take

images of fluorol yellow staining for T-0 and T-1 plant roots. Fluorol yellow staining appears as green fluorescence while lack of fluorescence appears blue (Figure 2.6). Therefore roots with fluorol yellow fluorescence in the endodermis only appear to have a blue epidermis (Figure 2.7 A, C), while roots with epidermal fluorescence appear green in the epidermis and endodermis (Figure 2.7 B, D).

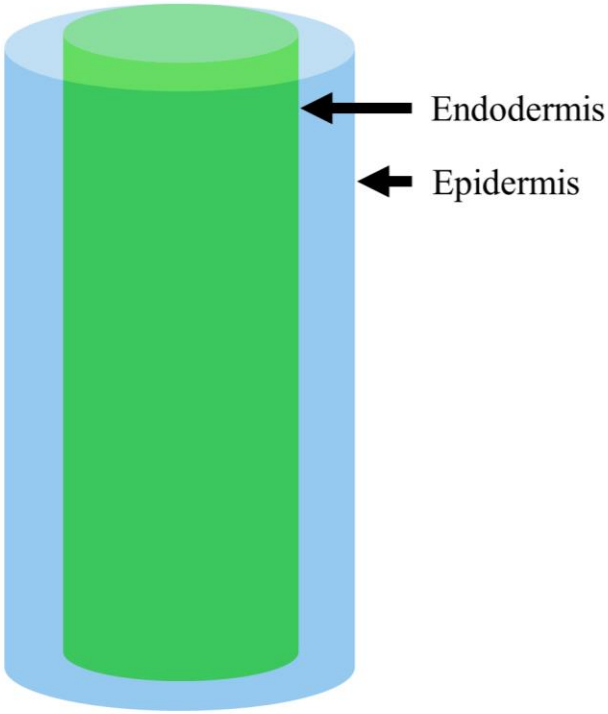

Figure 2.6. Endodermal fluorol yellow staining diagram for DFC450 microscope camera. Fluorol yellow staining appears as green fluorescence. Lack of fluorol yellow staining appears blue. Roots without epidermal suberin appear blue in the epidermis and green in the endodermis due to suberin in the endodermis and not the epidermis.

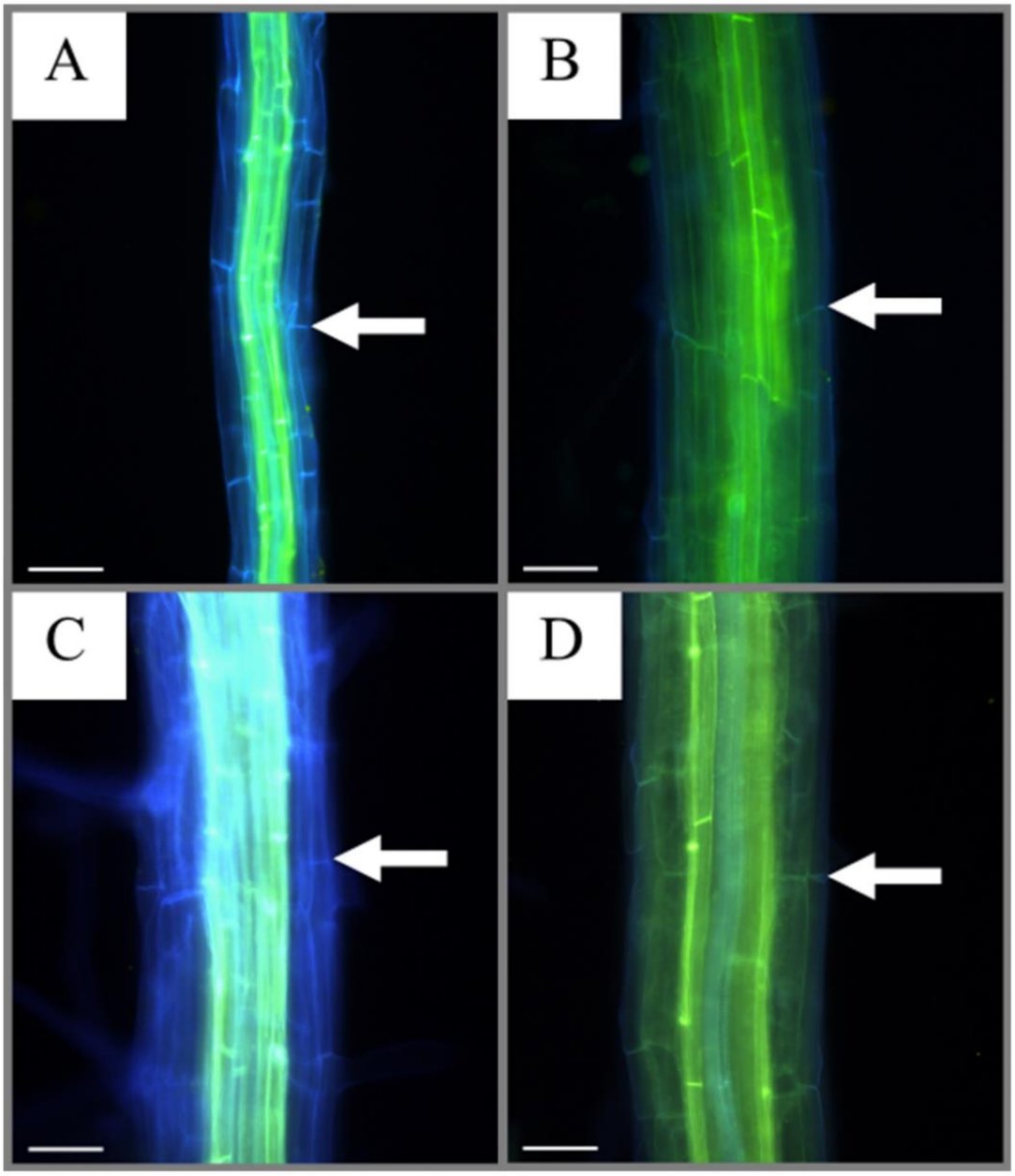

Figure 2.7. Fluorol yellow staining of Col-0 (A, C) compared to MYB84 T-0 (B), and MYB84_S256D T-0 (D). Scale bars: 200 μm.

Table 2.1. Fluorol yellow screening of primary transformants. Percentage of transgenics with no suberin (-), slight suberin (+-), increased suberin (+), or high levels of suberin (++) compared to Col-0. No phosphomimics had higher levels of suberin in T-0 lines than the MYBs.

MYB TRANSCRIPTION FACTOR	NUMBER OF T-0 LINES	-	+-	+	++
MYB49	20	10%	55%	30%	5%
MYB49_S273D	29	44.83%	41.38%	13.79%	0%
MYB49_T277D	30	26.67%	73.33%	0%	0%
MYB49_S273D_T277D	30	30%	50%	20%	0%
MYB53	30	33.33%	40%	26.67%	0%
MYB84	24	29.17%	41.67%	29.17%	0%
MYB84_S256D	30	40%	36.67%	13.33%	0%
MYB102	30	20%	46.67%	26.67%	6.67%
MYB107	17	64.71%	29.41%	5.88%	0%
MYB107_S253D	30	26.67%	73.33%	0%	0%

Only MYB49 and MYB102 had high levels of suberin compared to Col-0 for any T-0 lines. MYB49, MYB102, MYB53, and MYB84 had similar percentages of plants with increased suberin compared to Col-0 (Table 2.1). MYB107 had slight increases in suberin for some transgenics and the highest percentage of plants with no epidermal suberin. None of the phosphomimics had higher levels of suberin visually than the unmutated MYBs, therefore these transgenic lines were not analyzed further. MYB84 and MYB84_S256D microscopy images are provided as examples (Figure 2.7).

T-0 plants with epidermal suberin were rescued on MS media containing 50 ng/mL Kanamycin (Kan MS) and transferred to soil after sufficient root growth. Seed from these plants was harvested and plated on Kan MS to select transgenic plants. These plants contain at least one DNA insertion transferred from *Agrobacterium* into the plant's genome (T-DNA) containing the Kanamycin resistance gene. The ratio of Kan-resistant to susceptible plants is due to the number of T-DNA insertions for the transgenic line. Based on Mendelian genetics, lines with a ratio of 3

resistant to 1 susceptible contain a single T-DNA insertion, while lines with two T-DNA insertion have a ratio of 15:1. Chi-squared analysis was used to determine whether the observed ratio of resistant to susceptible fits with the expected ratio (3:1) (Table 2.2). If the resulting p-value is greater than 0.05, the observed ratio is not significantly different from the expected, supporting a single T-DNA insertion during transformation. If the p-value is less than 0.05, the ratios are significantly different, supporting the more than one T-DNA insertion.

Kan-resistant T-1 plants were transferred to soil and self-fertilized to generate T-2 seed. T-2 seed was plated on Kan MS to choose transgenic lines homozygous for a single T-DNA. If all T-2 plants from a single T-1 line are all Kan-resistant with no susceptible plants (ratio of 1:0) with a single T-DNA insertion for the T-1 line (Table 2.2), this suggests these T-2 plants are homozygous for the T-DNA (Table 2.3). Two homozygous T-2 lines from separate T-0 lines were chosen for each MYB besides MYB107. Only one MYB107 T-2 line was chosen to screen due to the lower levels of suberin during T-0 screening (Table 2.1).

Table 2.2. Kanamycin (Kan) segregation and chi-squared of T-1 transgenic lines. T-1 lines with p-value >0.05 have single T-DNA insertions (grey highlighted).

MYB	*T-0 line*	*T-1 Kan Resistant to Susceptible*	*Chi-squared*	*P-value*
MYB49	2	41:9	1.31	0.2530
MYB49	3	7:3	0.67	0.4142
MYB49	6	37:12	0.01	0.9343
MYB49	7	7:3	0.67	0.4142
MYB49	8	18:7	0.24	0.6242
MYB49	10	33:16	1.53	0.2160
MYB49	16	7:3	0.67	0.4142
MYB49	19	37:13	0.03	0.8703
MYB53	2	37:13	0.03	0.8703
MYB53	22	4:1	0.60	0.4386
MYB53	28	47:1	13.44	0.0002
MYB84	7	45:2	10.79	0.0010
MYB84	8	14:3	1.47	0.2253
MYB84	10	33:16	1.53	0.2160
MYB84	20	43:6	4.25	0.0392
MYB102	9	19:6	0.03	0.8703
MYB102	13	37:12	0.01	0.9343
MYB102	16	11:1	7.11	0.0077
MYB102	17	38:11	0.17	0.6801
MYB107	18	47:2	11.44	0.0007
MYB107	19	19:6	0.03	0.8703

Table 2.3. Kanamycin (Kan) segregation of T-2 transgenic lines. T-1 lines with p-value >0.05 (Table 2.2) have single T-DNA insertions (highlighted in grey). Lines with single T-DNA insertions and T-2 Kan Resistant to Susceptible ratio of 1:0 are homozygous for the T-DNA insertion. T-1 lines are derived from T-0 lines, i.e., 3.1 is progeny from T-0 line 3. T-2 lines highlighted in green were stained for suberin (Table 2.4).

MYB	*T-0 line*	*T-1 line*	*T-2 Kan Resistant to Susceptible*
MYB49	3	3.1	7:3
		3.2	33:17
		3.3	37:13
		3.4	37:13
MYB49	6	6.1	14:11
		6.2	7:3
		6.3	13:4
		6.4	13:4
		6.5	1:0
MYB49	7	7.1	49:1
		7.3	1:0
MYB49	8	8.2	1:0
		8.3	44:1
MYB53	2	2.1	34:11
		2.2	37:12
		2.3	41:9
		2.4	23:1
		2.5	35:16
		2.6	1:0
MYB53	22	22.1	4:1
		22.2	1:0
		22.3	32:9
MYB84	7	7.2	1:0
		7.10	1:0
MYB84	8	8.1	1:0
		8.2	1:0
		8.4	1:0
MYB84	10	10.2	1:0
MYB102	9	9.1	1:0
		9.2	5:2
MYB102	13	13.1	1:0
		13.2	39:11
MYB107	18	18.3	1:0
MYB107	19	19.3	1:0

MYB84 T-1 phenotype

A yellow, stunted phenotype was observed for multiple MYB84 T-1 plants from separate T-0 lines (MYB84-7, MYB84-8, MYB84-10) (Figure 2.9). The observed phenotype was stronger in the MYB84-7 T-1 line (Figure 2.9), whose segregation of Kan-resistant to susceptible is consistent with more than one T-DNA insertion (Table 2.2). Due to the stronger phenotype in this line, multiple MYB84-7 roots were stained with fluorol yellow and viewed under a fluorescent microscope to determine whether this phenotype was related to epidermal suberin. Figure 2.8 proves the presence of root epidermal suberin in MYB84-7 plants. The high levels of root epidermal suberin correlated with the stunted phenotype. This suggests high levels of root epidermal suberin impacts plant growth. This may be due to the suberin preventing nutrient acquisition.

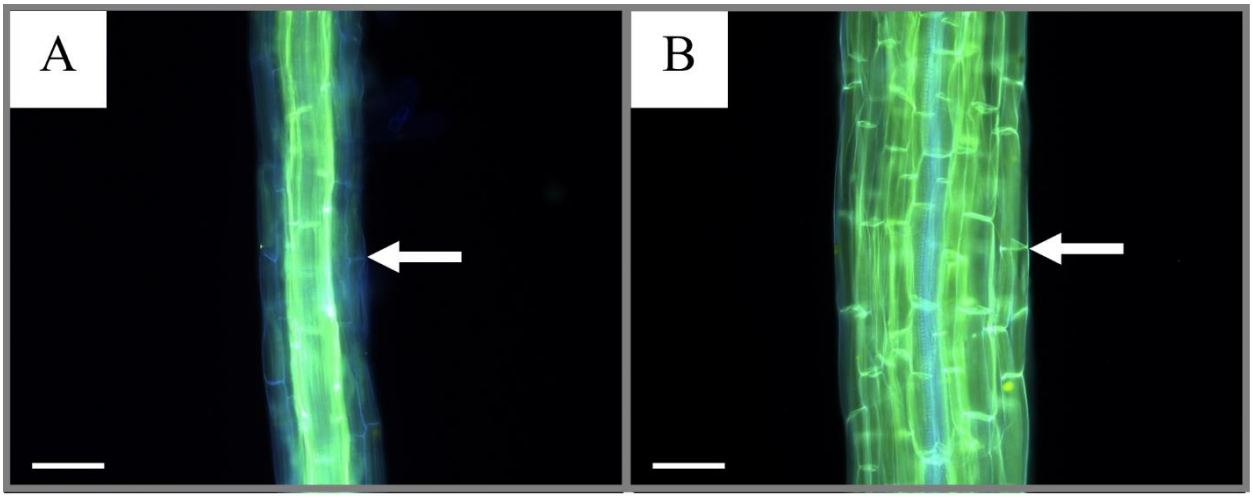

Figure 2.8. Fluorol yellow staining of **A.** Col-0 and **B.** MYB84-7 T-1. Green: fluorol yellow staining Blue: absence of fluorol yellow staining. Scale bars: 200 µm.

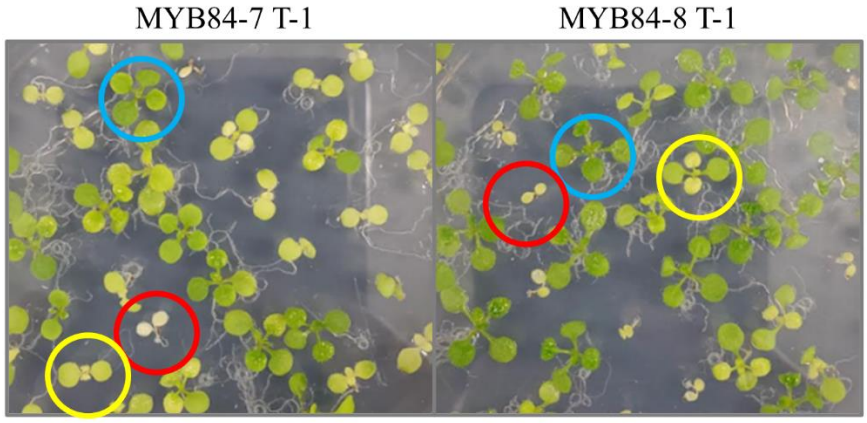

Figure 2.9. Twelve-day-old MYB84 T-1 phenotype. Blue circle: Kanamycin (Kan)-resistant; Red circle: Kan-susceptible; Yellow circle: Kan-resistant and yellow/stunted.

Fluorol yellow staining of T-2 plants

Roots from two independent transformation lines for each MYB, besides one for MYB107, were examined with fluorol yellow staining to determine whether homozygous plants expressing the MYB gene in the root epidermis led to epidermal suberin deposition. Col-0 roots contain suberin in the endodermis and not the epidermis, therefore Col-0 was used as a control to determine whether the transgenics contain epidermal suberin. To confirm the presence or absence of root epidermal fluorol yellow staining, the entire root was screened under a fluorescent microscope. For plants with epidermal suberin, microscopy images were taken at the root-shoot transition zone, at lateral root junctions, within the zone of maturation, and within the zone of elongation of two-week, three-week, and four-week-old plants to confirm epidermal suberin deposition throughout the root at various plant developmental stages (Figure 2.10).

A Leica sCMOS Microscope Camera K5 was used to take images of fluorol yellow fluorescence for T-2 plants (except MYB49-7.3; Figure 2.36). For this camera, fluorol yellow staining appears as green fluorescence, therefore roots without epidermal suberin do not have fluorescence in the epidermis compared to Col-0, only the endodermis (Figure 2.11). Both

MYB84 T-2 transgenic lines showed fluorol yellow fluorescence in the root epidermis (Figures 2.12-35).

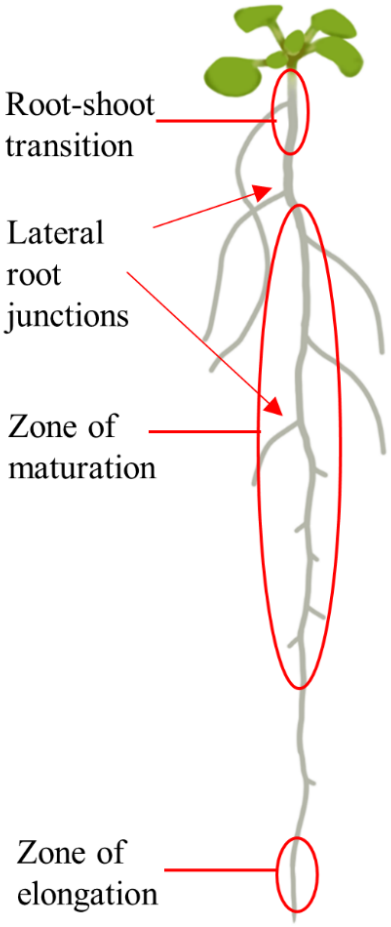

Figure 2.10. Diagram of *Arabidopsis* root. Microscopy images were taken at the root-shoot transition, at lateral root junctions, in the zone of maturation (middle of root), and in the zone of elongation.

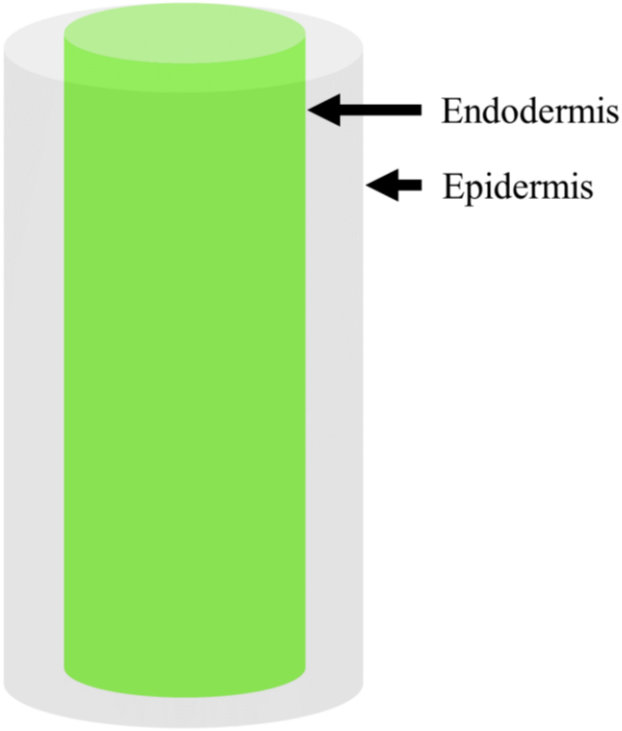

Figure 2.11. Endodermal fluorol yellow staining diagram for Leica sCMOS Microscope Camera K5. Roots without epidermal suberin will only fluoresce in the endodermis when stained with fluorol yellow.

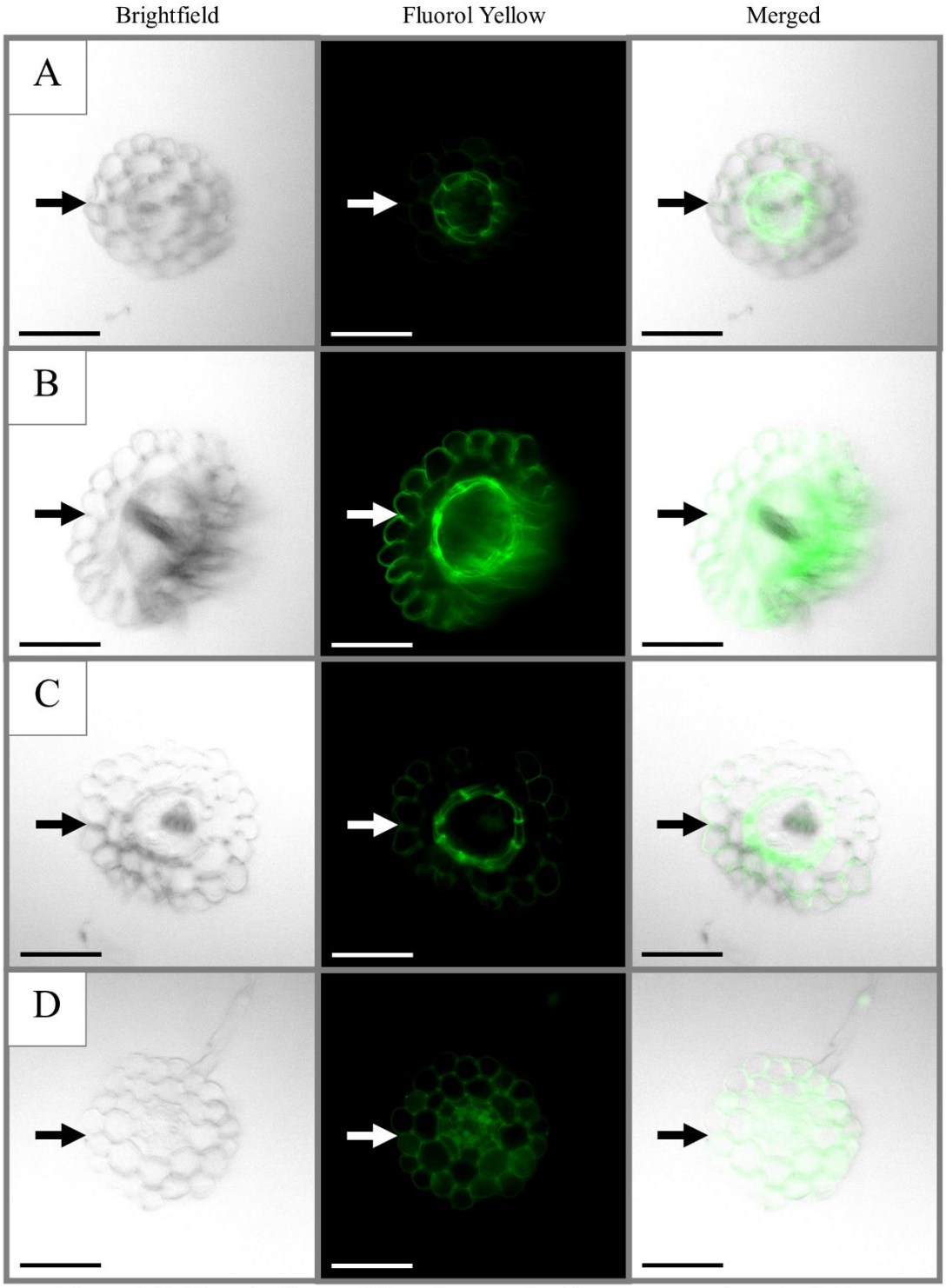

Figure 2.12. Fluorol yellow staining of two-week-old root cross sections. **A.** Col-0 **B.** MYB84-8.4 **C.** MYB84-10.2 **D:** MYB84-10.2. Scale Bars: 100 µm.

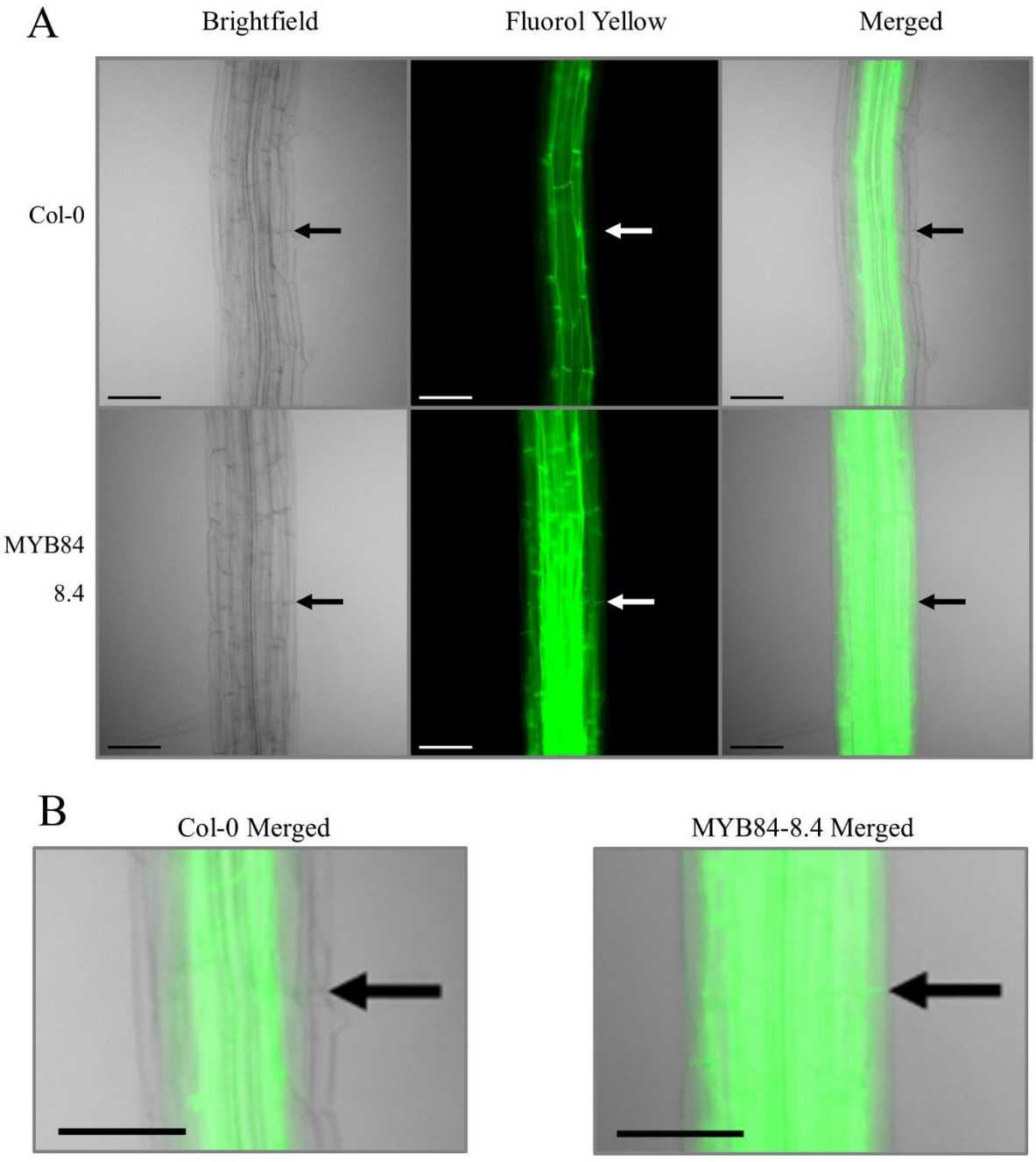

Figure 2.13. Fluorol yellow staining of ABCG37::MYB84-8.4 and reference Col-0 roots in the zone of maturation of two-week-old plants. **A.** Brightfield, fluorol yellow, and merged. Fluorol yellow stains for suberin and associated waxes. Arrows indicate the root epidermis. **B.** Close up of merged Col-0 and MYB84-8.4 images in **A.** Scale bars: 100 µm.

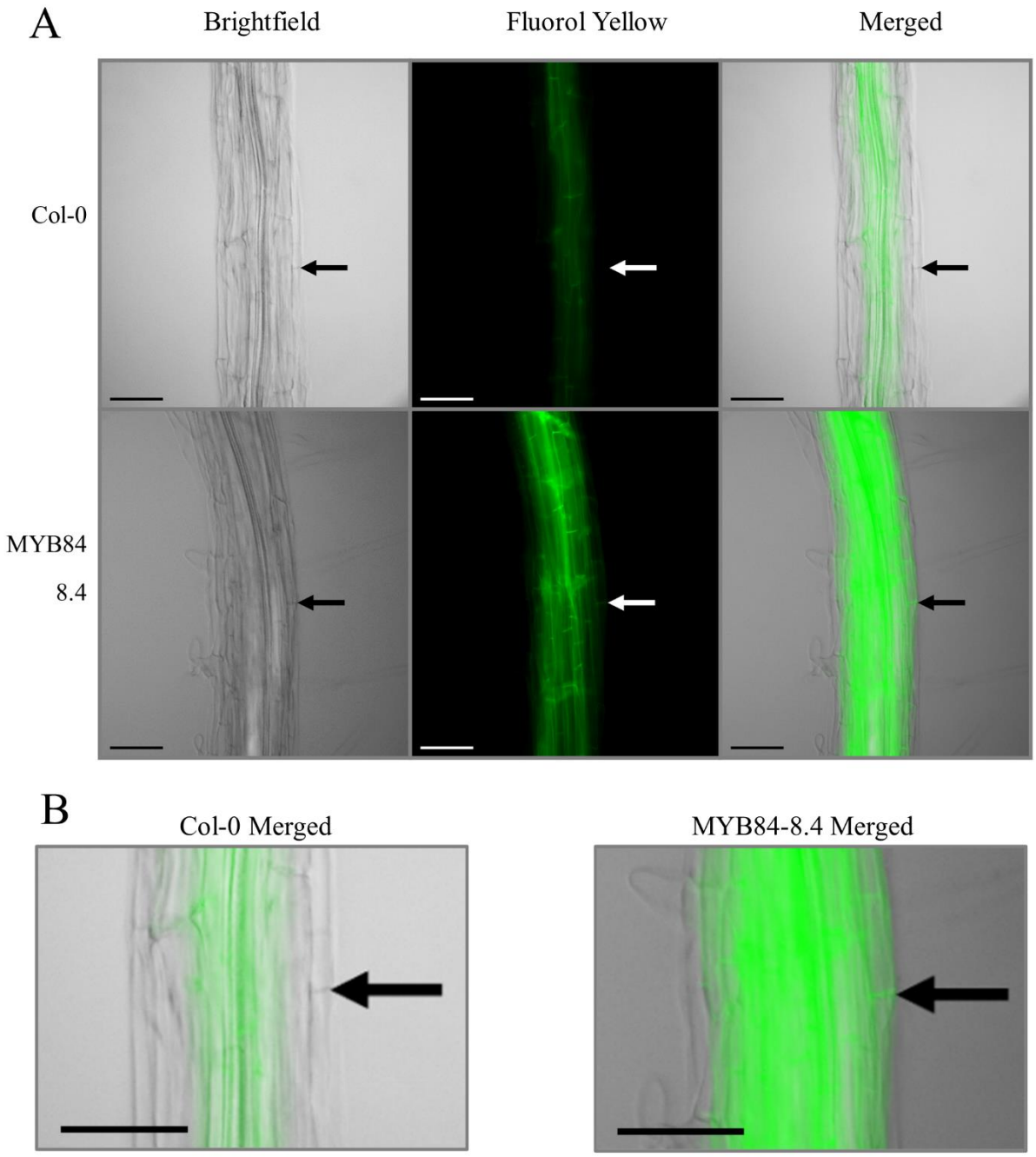

Figure 2.14. Fluorol yellow staining of ABCG37::MYB84-8.4 and reference Col-0 roots in the zone of maturation of three-week-old plants. **A.** Brightfield, fluorol yellow, and merged. Fluorol yellow stains for suberin and associated waxes. Arrows indicate the root epidermis. **B.** Close up of merged Col-0 and MYB84-8.4 images in **A.** Scale bars: 100 µm.

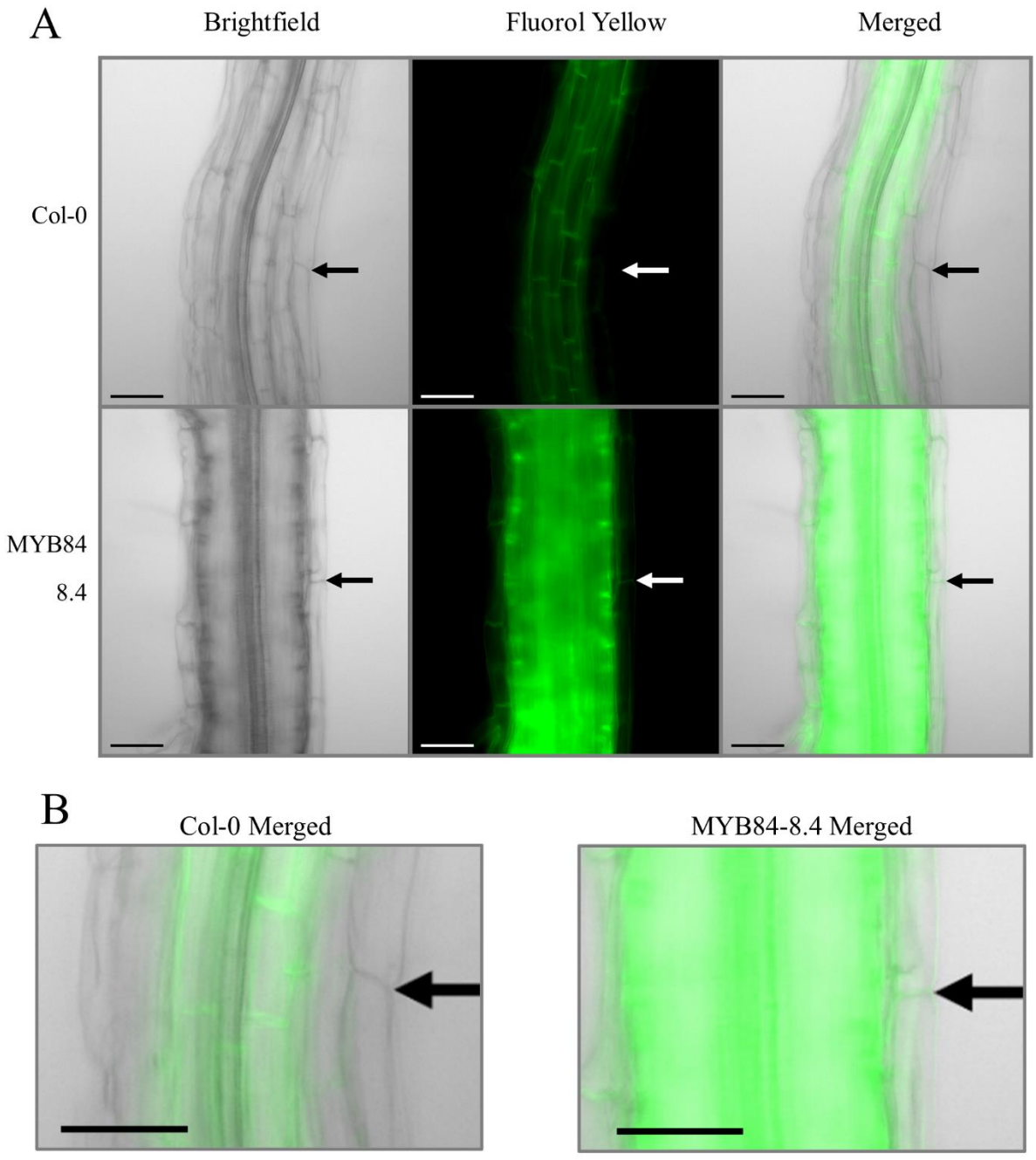

Figure 2.15. Fluorol yellow staining of ABCG37::MYB84-8.4 and reference Col-0 roots in the zone of maturation of four-week-old plants. **A.** Brightfield, fluorol yellow, and merged. Fluorol yellow stains for suberin and associated waxes. Arrows indicate the root epidermis. **B.** Close up of merged Col-0 and MYB84-8.4 images in **A.** Scale bars: 100 µm.

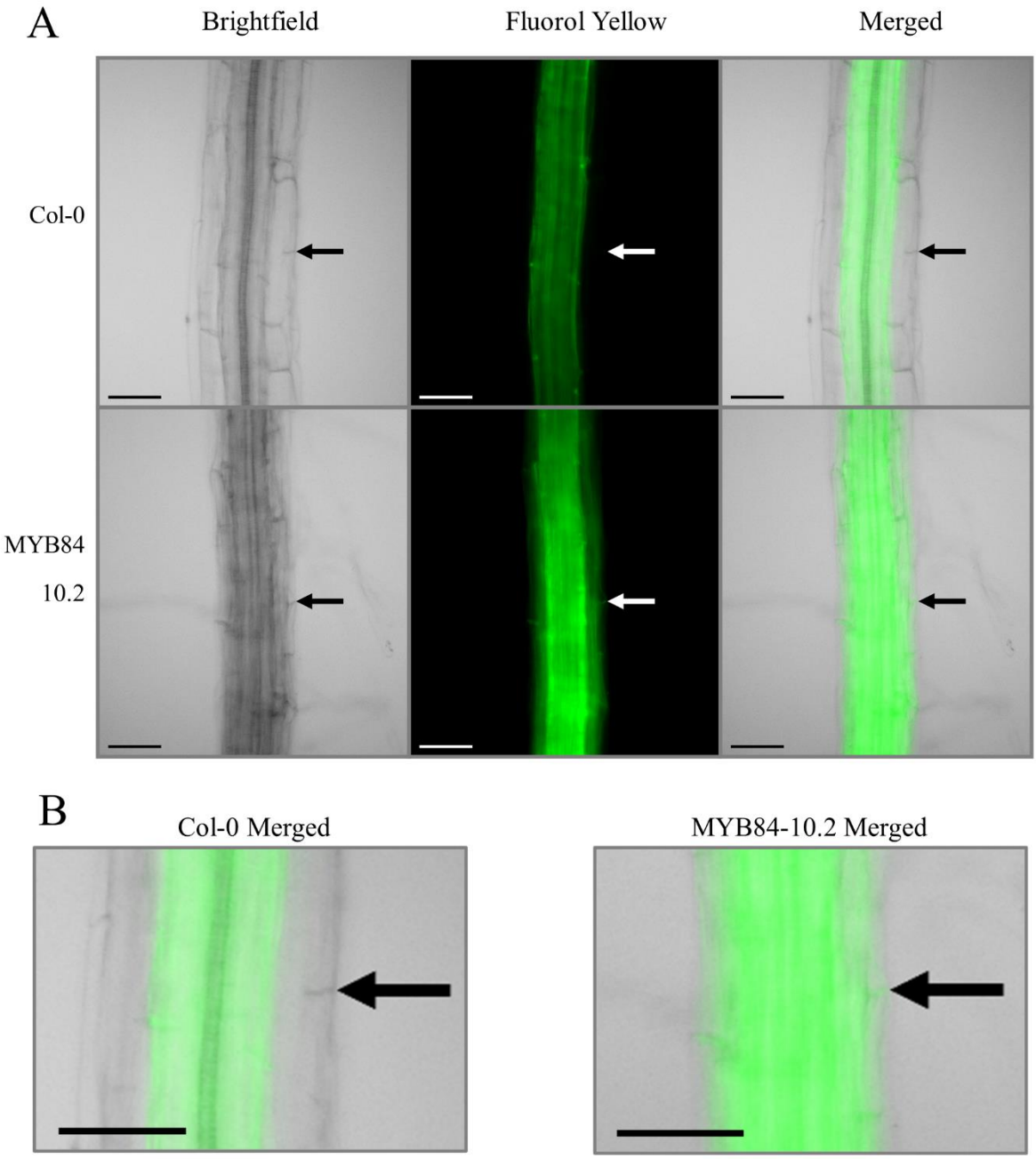

Figure 2.16. Fluorol yellow staining of ABCG37::MYB84-10.2 and reference Col-0 roots in the zone of maturation of two-week-old plants. **A.** Brightfield, fluorol yellow, and merged. Fluorol yellow stains for suberin and associated waxes. Arrows indicate the root epidermis. **B.** Close up of merged Col-0 and MYB84-8.4 images in **A.** Scale bars: 100 µm.

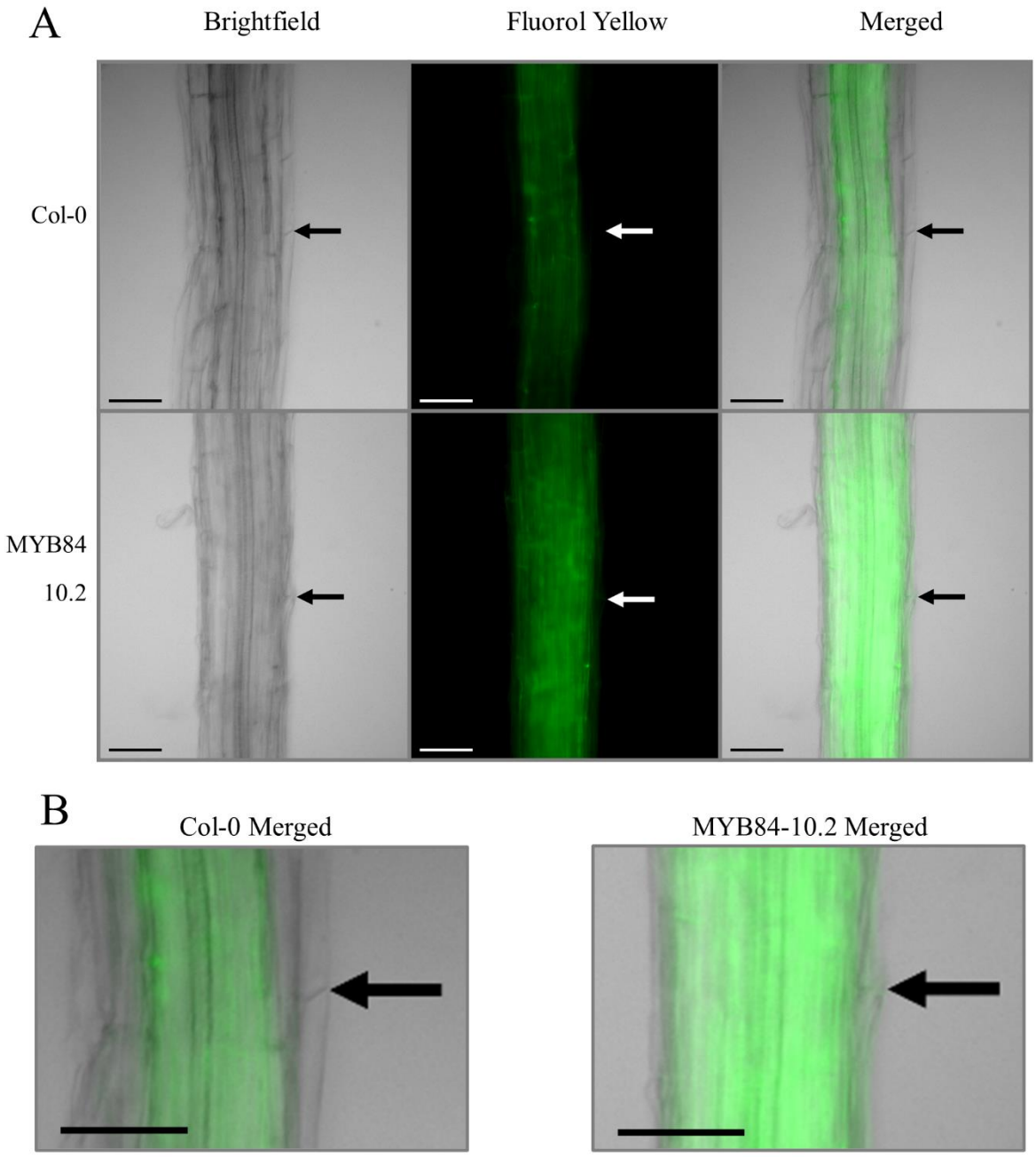

Figure 2.17. Fluorol yellow staining of ABCG37::MYB84-10.2 and reference Col-0 roots in the zone of maturation of three-week-old plants. **A.** Brightfield, fluorol yellow, and merged. Fluorol yellow stains for suberin and associated waxes. Arrows indicate the root epidermis. **B.** Close up of merged Col-0 and MYB84-8.4 images in **A.** Scale bars: 100 µm.

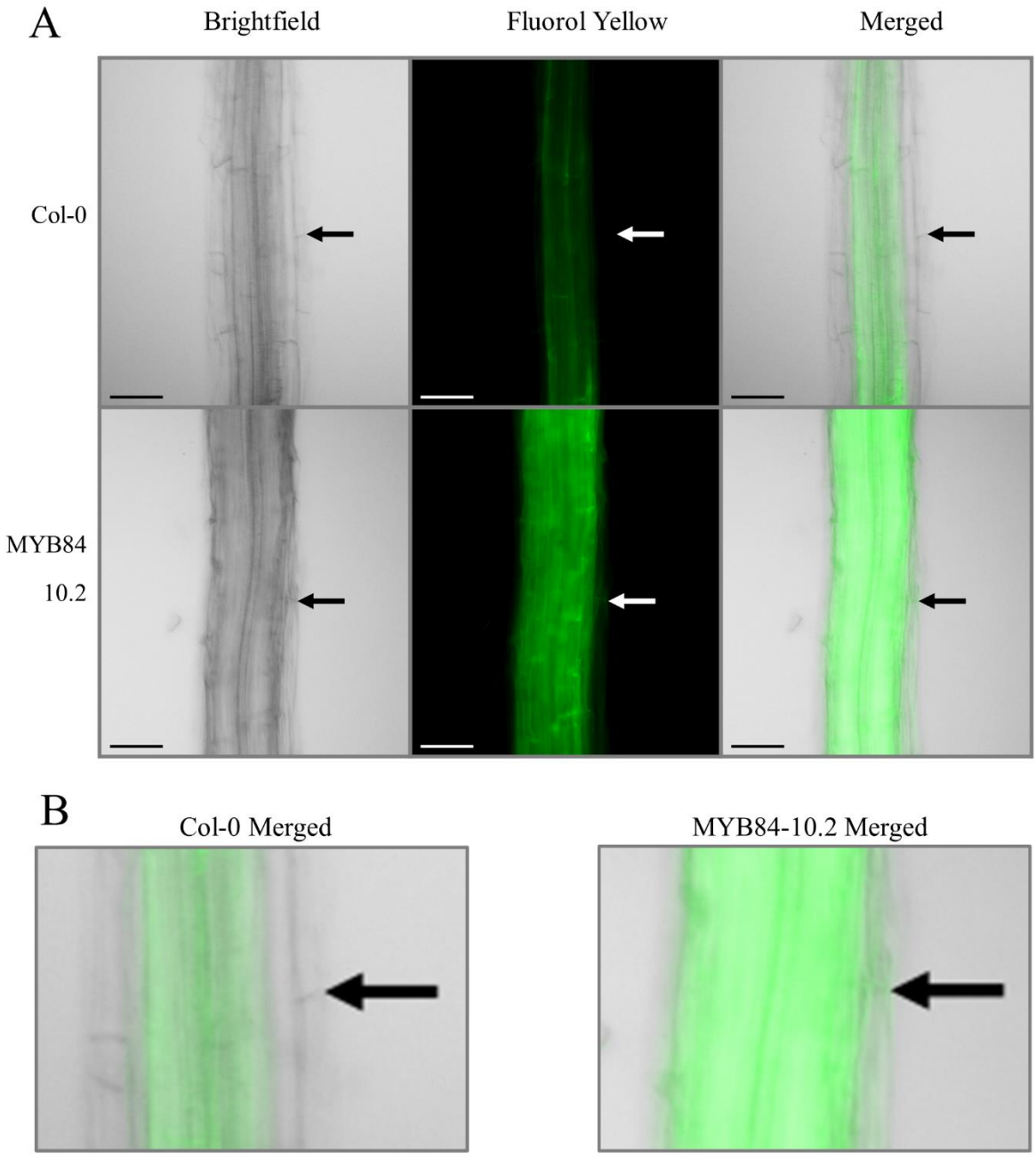

Figure 2.18. Fluorol yellow staining of ABCG37::MYB84-10.2 and reference Col-0 roots in the zone of maturation of four-week-old plants. **A.** Brightfield, fluorol yellow, and merged. Fluorol yellow stains for suberin and associated waxes. Arrows indicate the root epidermis. **B.** Close up of merged Col-0 and MYB84-8.4 images in **A.** Scale bars: 100 µm.

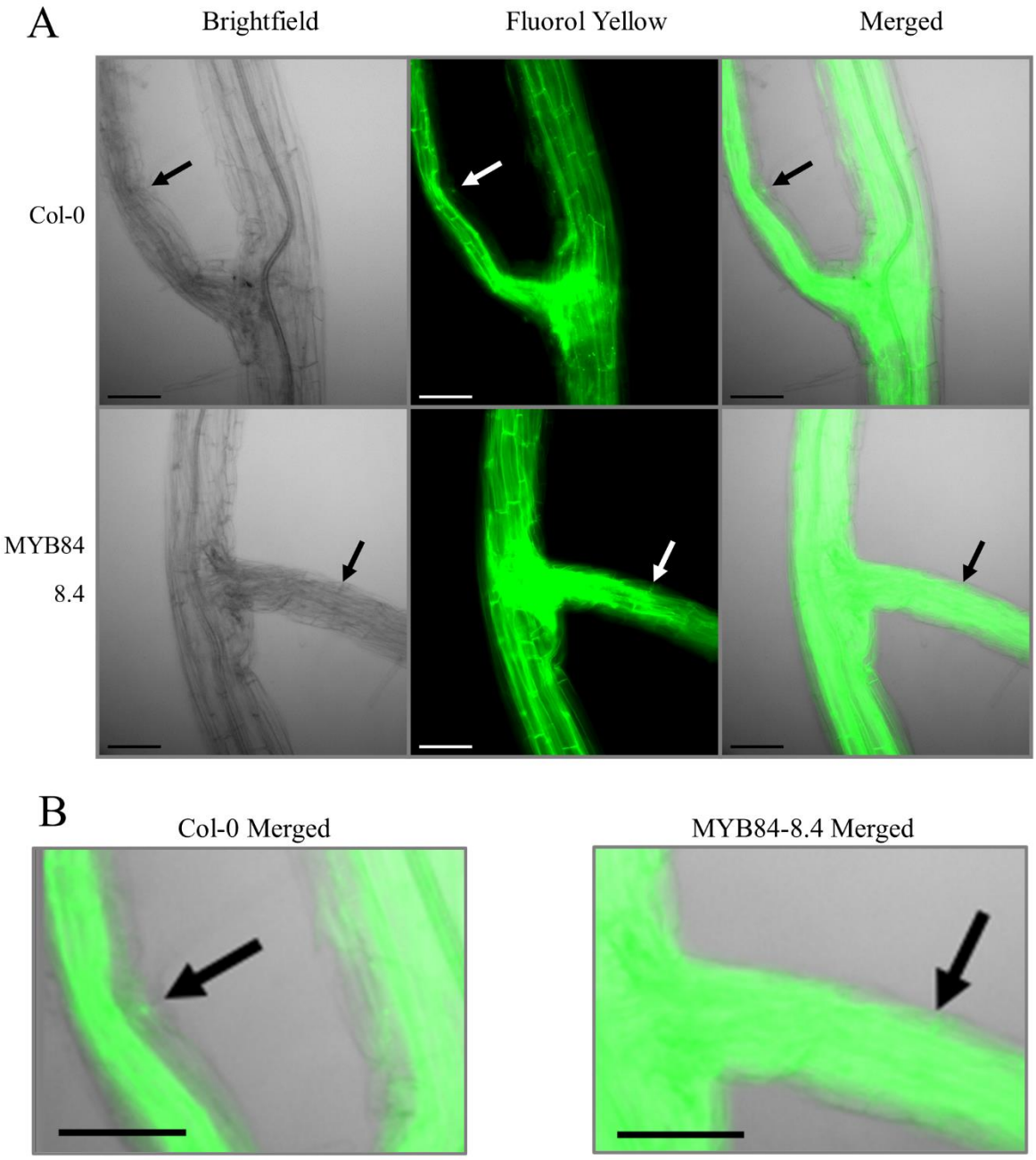

Figure 2.19. Fluorol yellow staining of ABCG37::MYB84-8.4 and reference Col-0 roots at lateral root junctions of two-week-old plants. **A.** Brightfield, fluorol yellow, and merged. Fluorol yellow stains for suberin and associated waxes. Arrows indicate the root epidermis. **B.** Close up of merged Col-0 and MYB84-8.4 images in **A.** Scale bars: 100 µm.

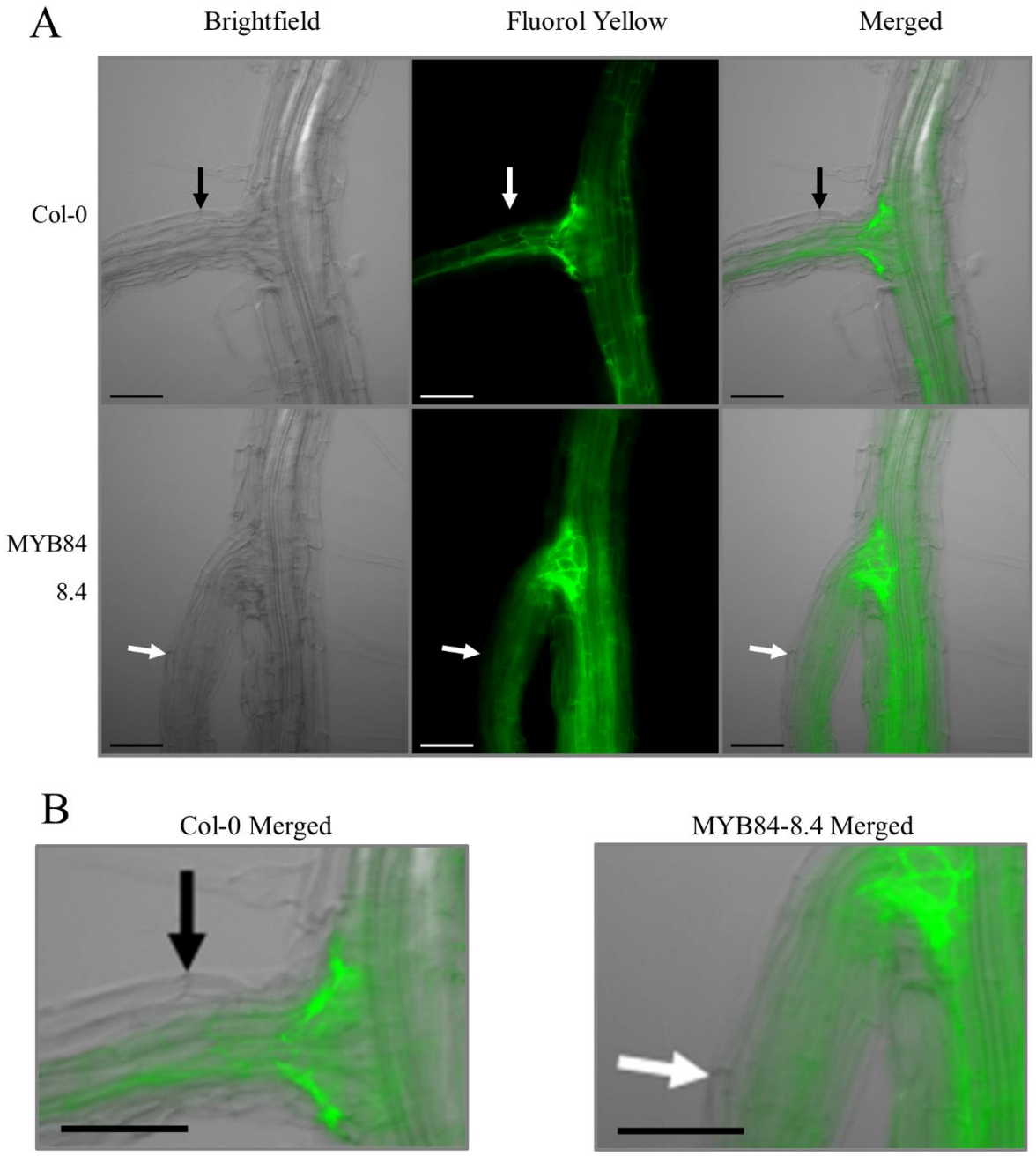

Figure 2.20. Fluorol yellow staining of ABCG37::MYB84-8.4 and reference Col-0 roots at lateral root junctions of three-week-old plants. **A.** Brightfield, fluorol yellow, and merged. Fluorol yellow stains for suberin and associated waxes. Arrows indicate the root epidermis. **B.** Close up of merged Col-0 and MYB84-8.4 images in **A.** Scale bars: 100 µm.

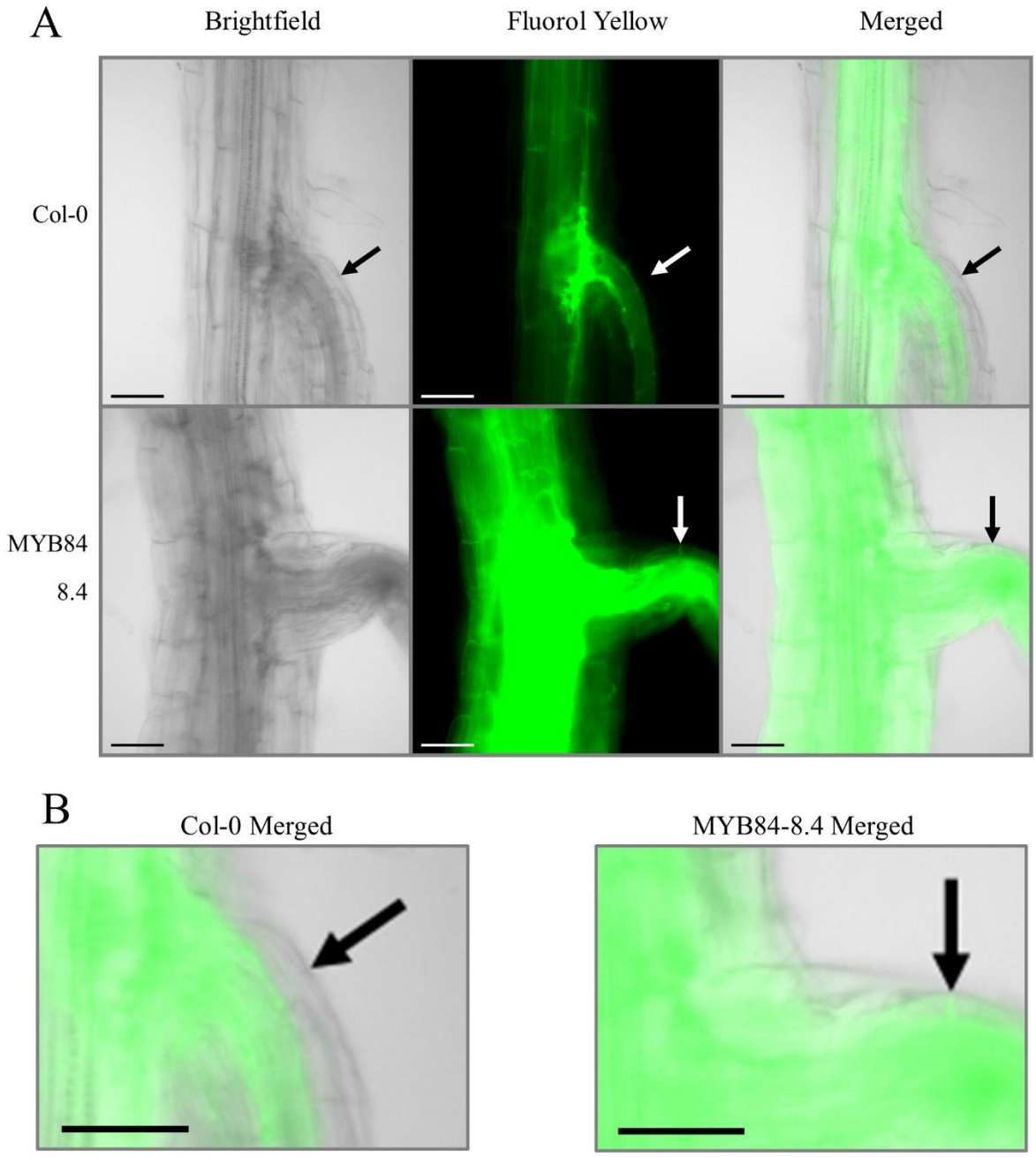

Figure 2.21. Fluorol yellow staining of ABCG37::MYB84-8.4 and reference Col-0 roots at lateral root junctions of four-week-old plants. **A.** Brightfield, fluorol yellow, and merged. Fluorol yellow stains for suberin and associated waxes. Arrows indicate the root epidermis. **B.** Close up of merged Col-0 and MYB84-8.4 images in **A.** Scale bars: 100 µm.

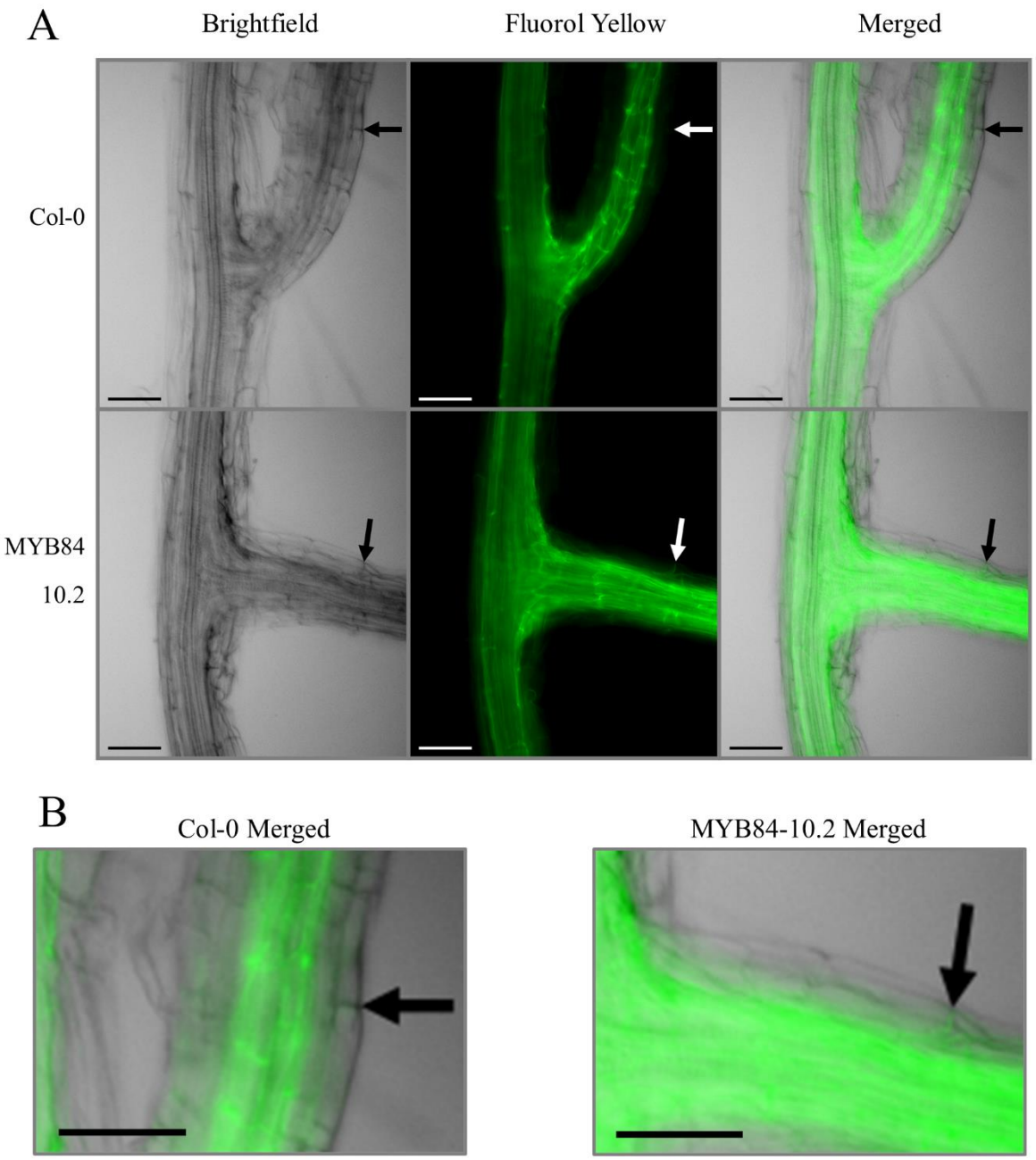

Figure 2.22. Fluorol yellow staining of ABCG37::MYB84-10.2 and reference Col-0 roots at lateral root junctions of two-week-old plants. **A.** Brightfield, fluorol yellow, and merged. Fluorol yellow stains for suberin and associated waxes. Arrows indicate the root epidermis. **B.** Close up of merged Col-0 and MYB84-8.4 images in **A.** Scale bars: 100 µm.

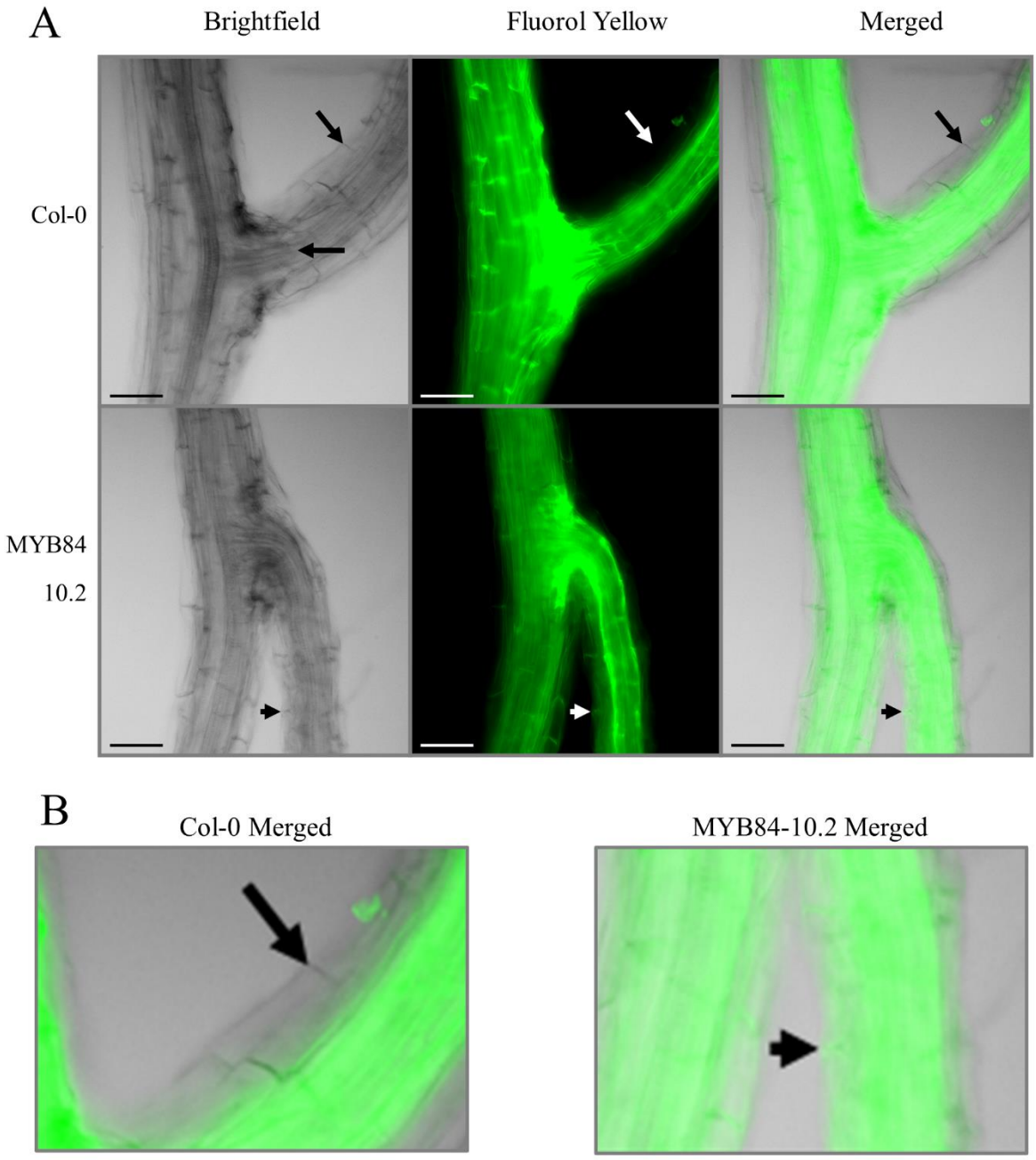

Figure 2.23. Fluorol yellow staining of ABCG37::MYB84-10.2 and reference Col-0 roots at lateral root junctions of three-week-old plants. **A.** Brightfield, fluorol yellow, and merged. Fluorol yellow stains for suberin and associated waxes. Arrows indicate the root epidermis. **B.** Close up of merged Col-0 and MYB84-8.4 images in **A.** Scale bars: 100 µm.

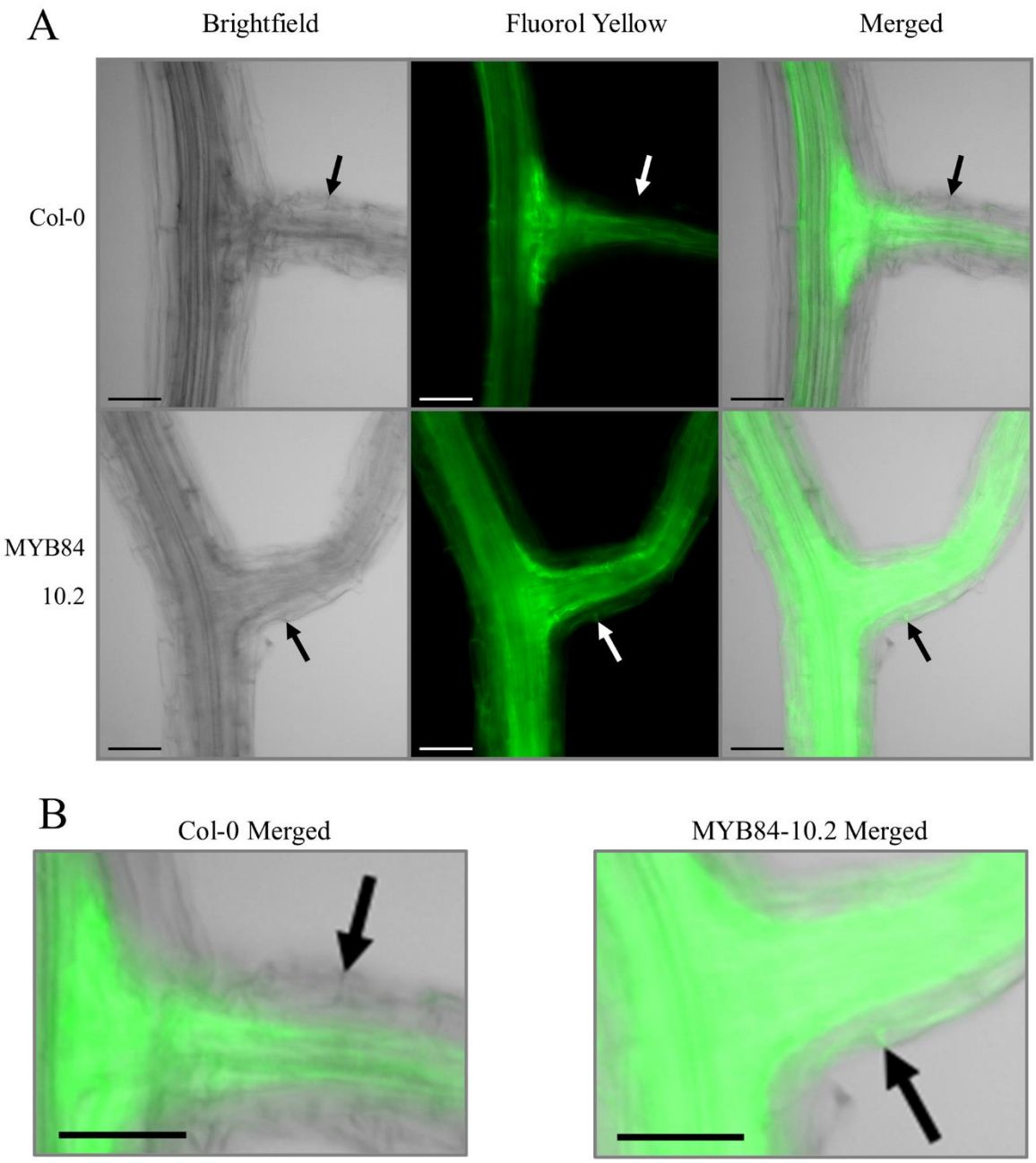

Figure 2.24. Fluorol yellow staining of ABCG37::MYB84-10.2 and reference Col-0 roots at lateral root junctions of four-week-old plants. **A.** Brightfield, fluorol yellow, and merged. Fluorol yellow stains for suberin and associated waxes. Arrows indicate the root epidermis. **B.** Close up of merged Col-0 and MYB84-8.4 images in **A.** Scale bars: 100 µm.

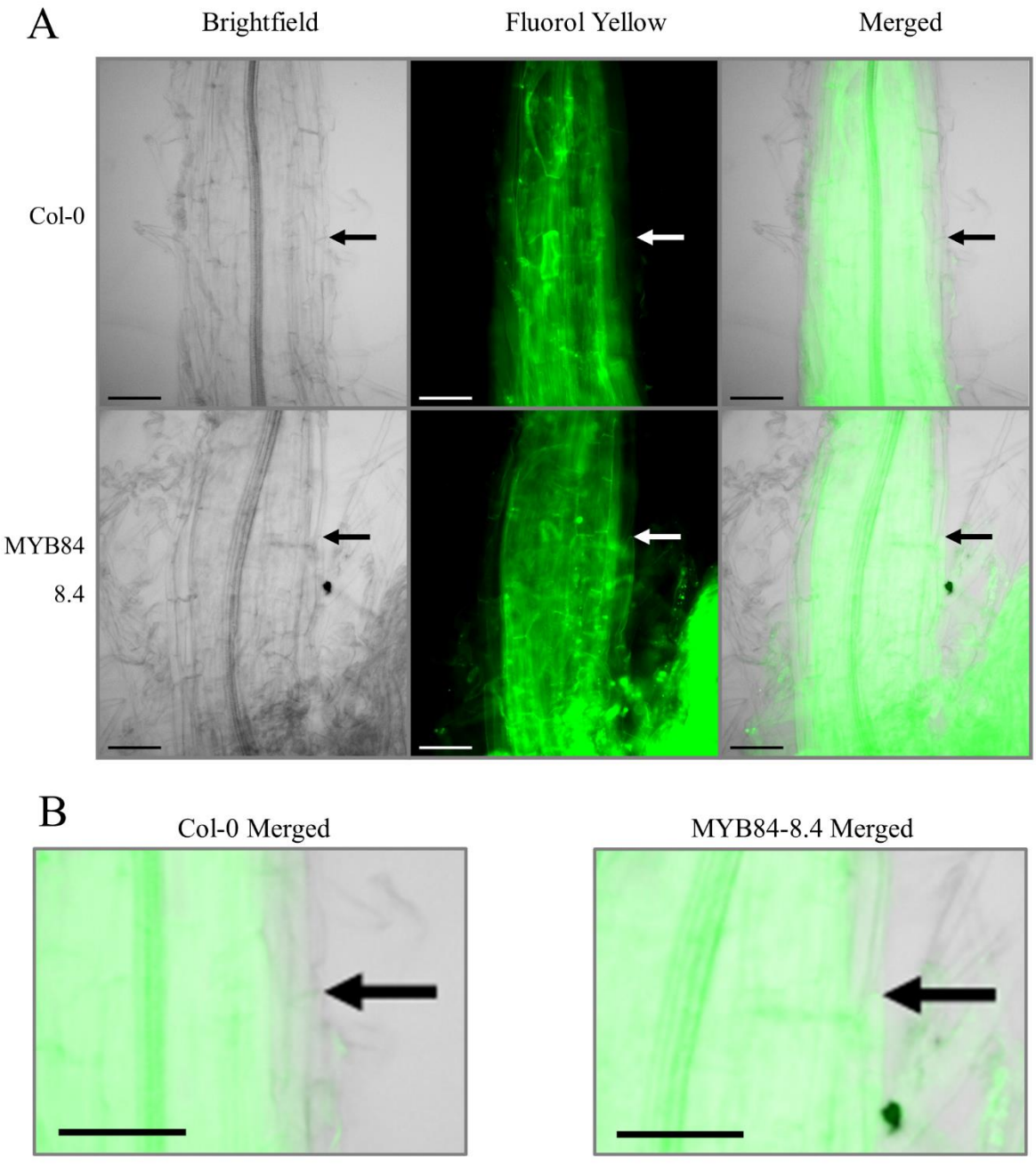

Figure 2.25. Fluorol yellow staining of ABCG37::MYB84-8.4 and reference Col-0 roots at root-shoot transitions of two-week-old plants. **A.** Brightfield, fluorol yellow, and merged. Fluorol yellow stains for suberin and associated waxes. Arrows indicate the root epidermis. **B.** Close up of merged Col-0 and MYB84-8.4 images in **A.** Scale bars: 100 µm.

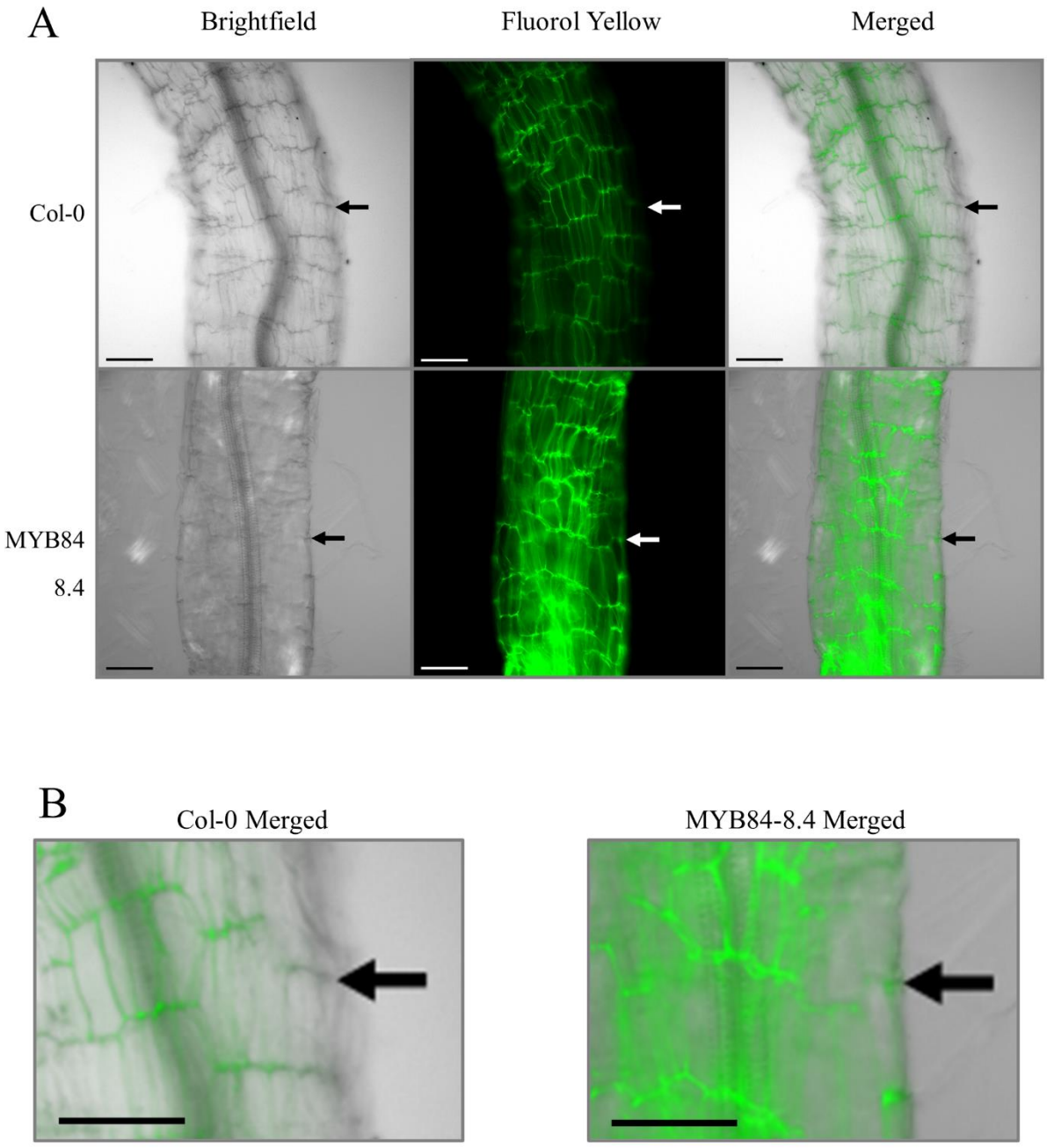

Figure 2.26. Fluorol yellow staining of ABCG37::MYB84-8.4 and reference Col-0 roots at root-shoot transitions of three-week-old plants. **A.** Brightfield, fluorol yellow, and merged. Fluorol yellow stains for suberin and associated waxes. Arrows indicate the root epidermis. **B.** Close up of merged Col-0 and MYB84-8.4 images in **A.** Scale bars: 100 µm.

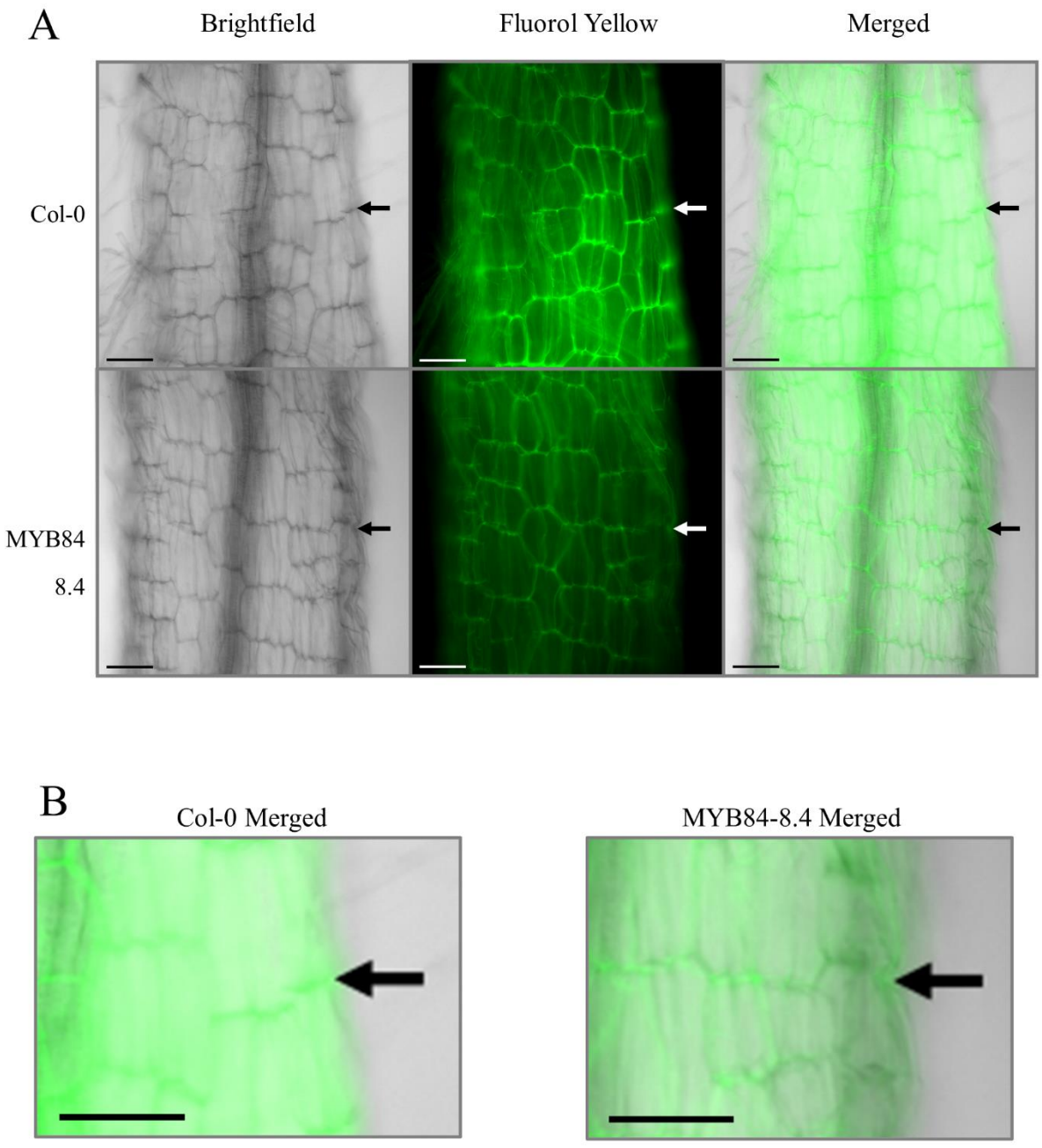

Figure 2.27. Fluorol yellow staining of ABCG37::MYB84-8.4 and reference Col-0 roots at root-shoot transitions of four-week-old plants. **A.** Brightfield, fluorol yellow, and merged. Fluorol yellow stains for suberin and associated waxes. Arrows indicate the root epidermis. **B.** Close up of merged Col-0 and MYB84-8.4 images in **A.** Scale bars: 100 µm.

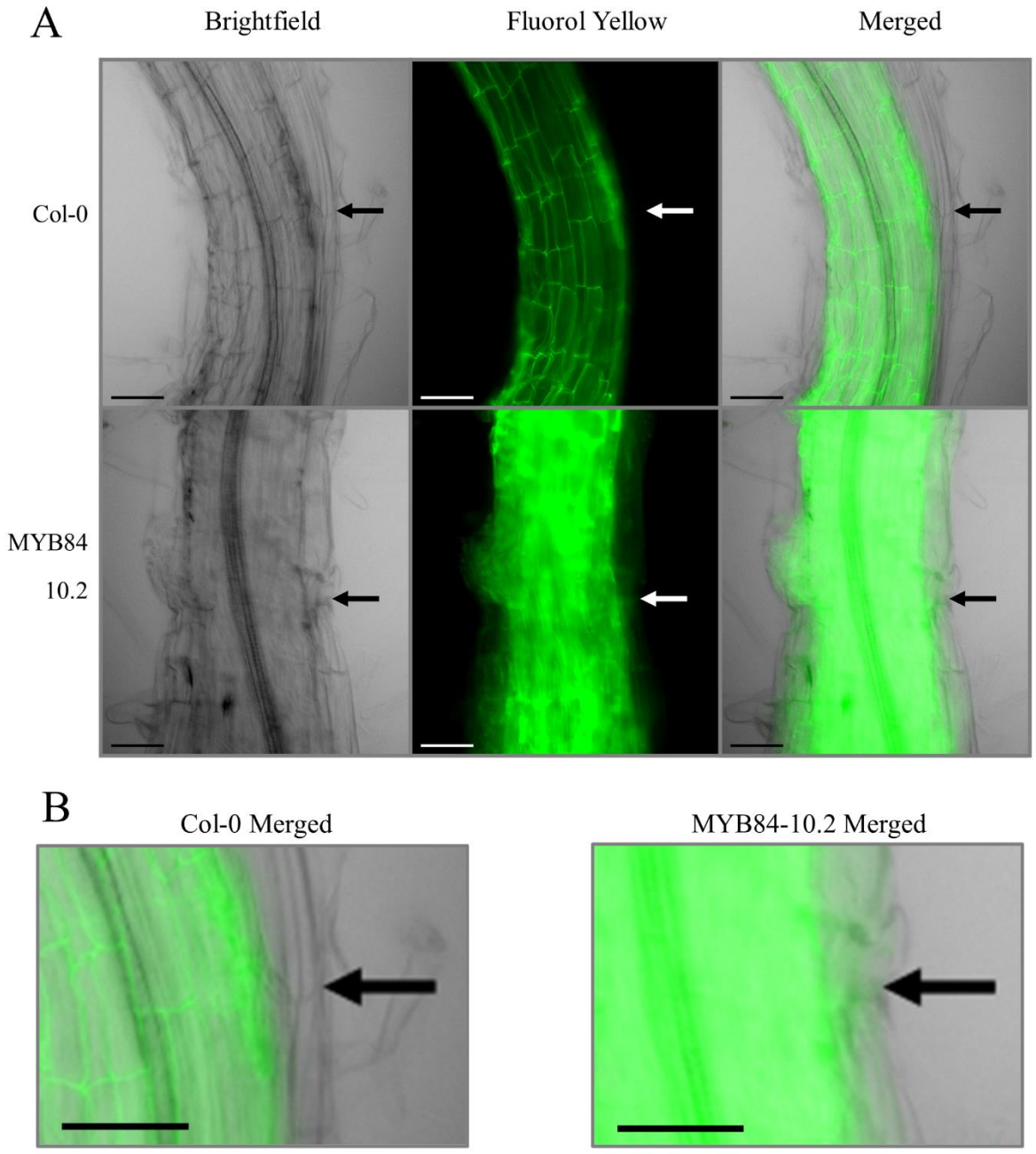

Figure 2.28. Fluorol yellow staining of ABCG37::MYB84-10.2 and reference Col-0 roots at root-shoot transitions of two-week-old plants. **A.** Brightfield, fluorol yellow, and merged. Fluorol yellow stains for suberin and associated waxes. Arrows indicate the root epidermis. **B.** Close up of merged Col-0 and MYB84-8.4 images in **A.** Scale bars: 100 µm.

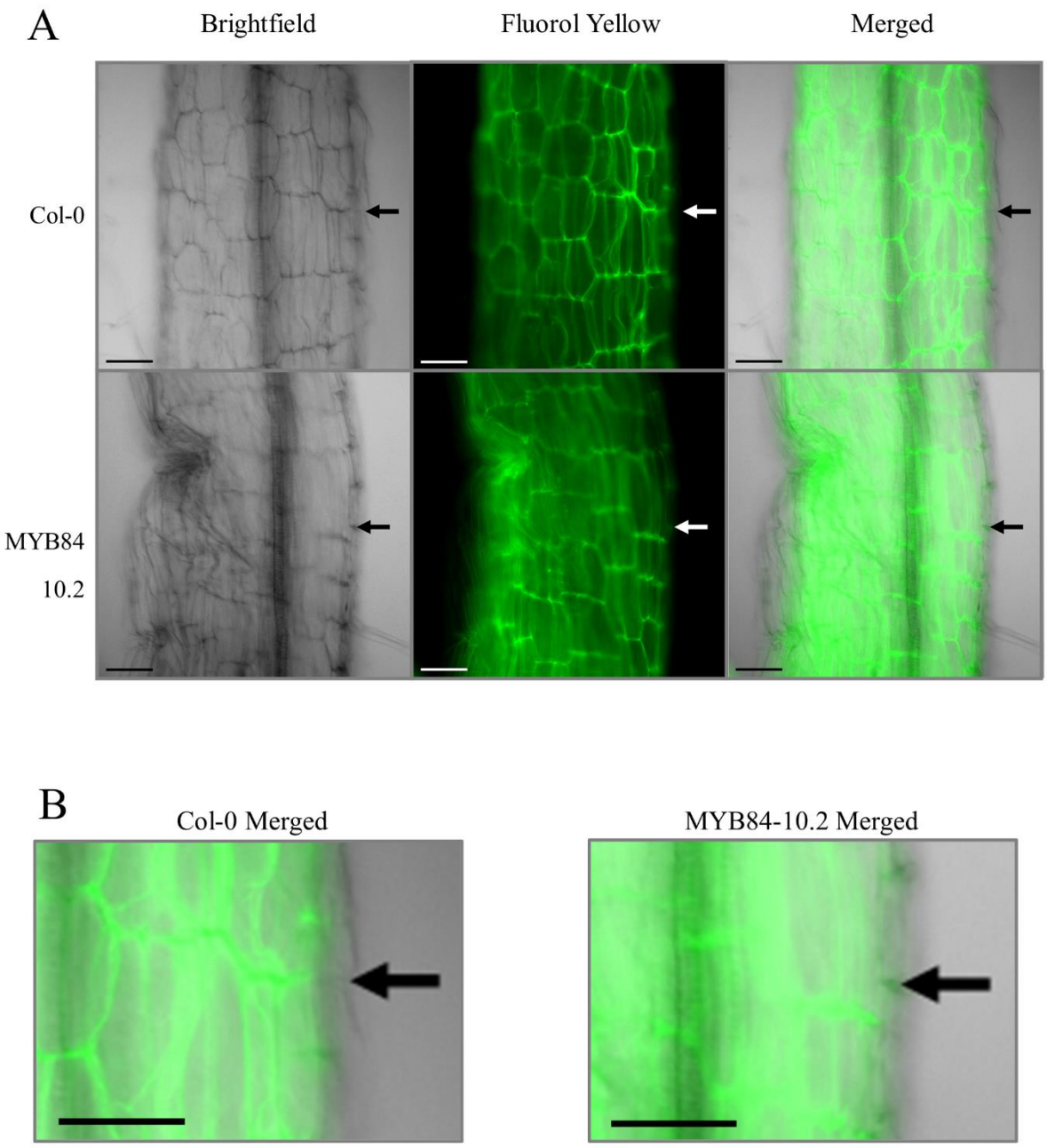

Figure 2.29. Fluorol yellow staining of ABCG37::MYB84-10.2 and reference Col-0 roots at root-shoot transitions of three-week-old plants. **A.** Brightfield, fluorol yellow, and merged. Fluorol yellow stains for suberin and associated waxes. Arrows indicate the root epidermis. **B.** Close up of merged Col-0 and MYB84-8.4 images in **A.** Scale bars: 100 µm.

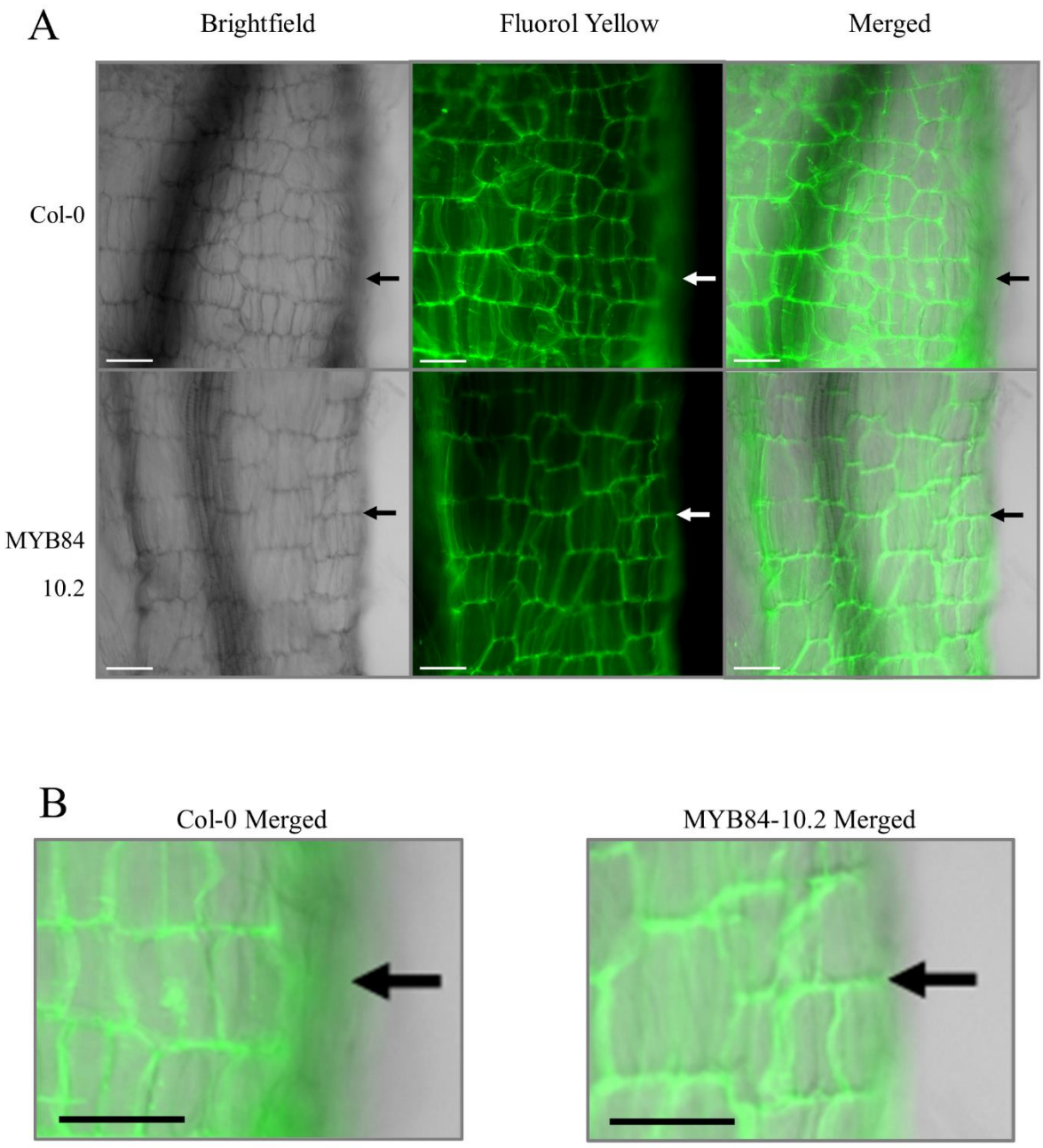

Figure 2.30. Fluorol yellow staining of ABCG37::MYB84-10.2 and reference Col-0 roots at root-shoot transitions of four-week-old plants. **A.** Brightfield, fluorol yellow, and merged. Fluorol yellow stains for suberin and associated waxes. Arrows indicate the root epidermis. **B.** Close up of merged Col-0 and MYB84-8.4 images in **A.** Scale bars: 100 µm.

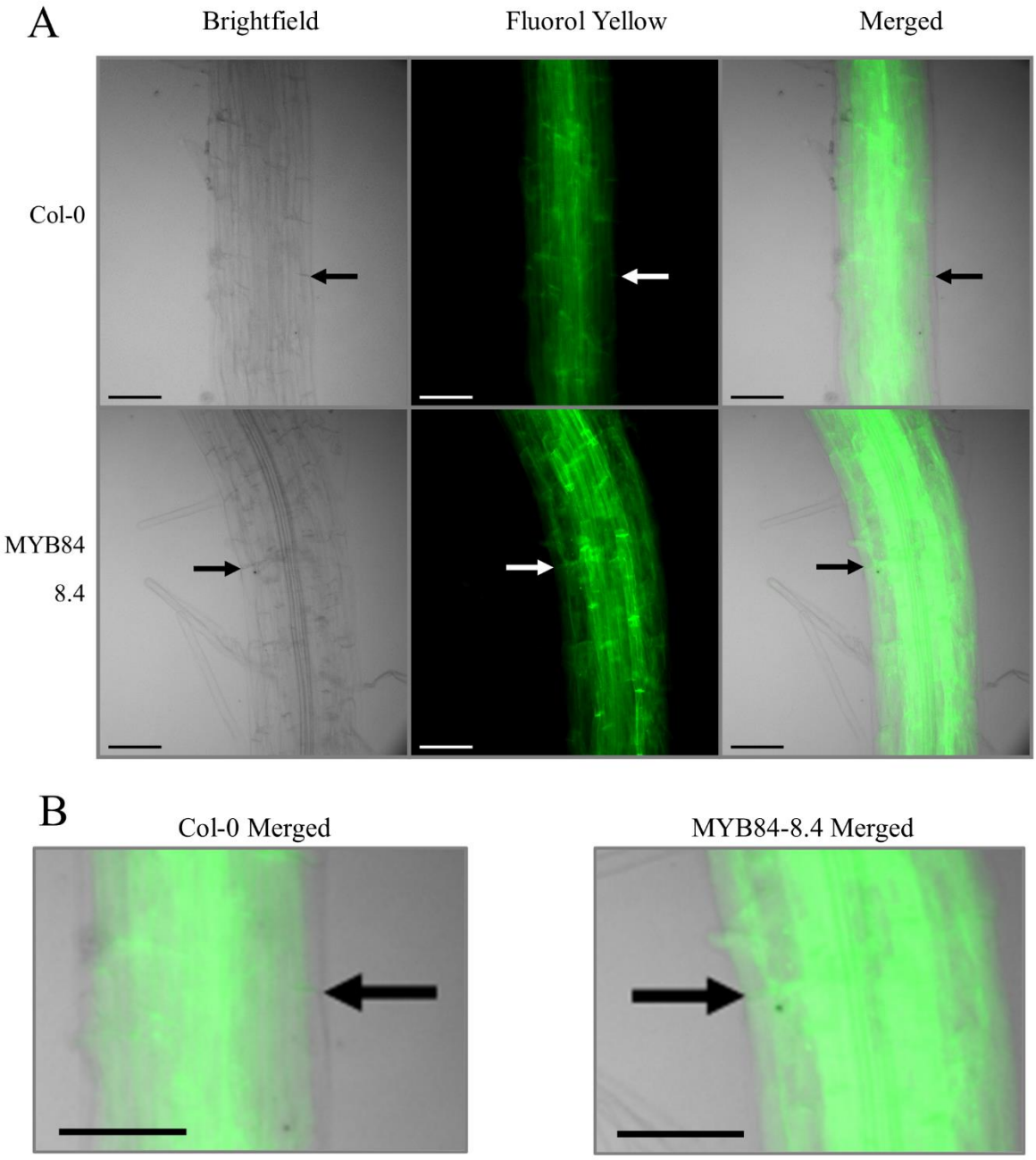

Figure 2.31. Fluorol yellow staining of ABCG37::MYB84-8.4 and reference Col-0 roots in the zone of elongation of two-week-old plants. **A.** Brightfield, fluorol yellow, and merged. Fluorol yellow stains for suberin and associated waxes. Arrows indicate the root epidermis. **B.** Close up of merged Col-0 and MYB84-8.4 images in **A.** Scale bars: 100 µm.

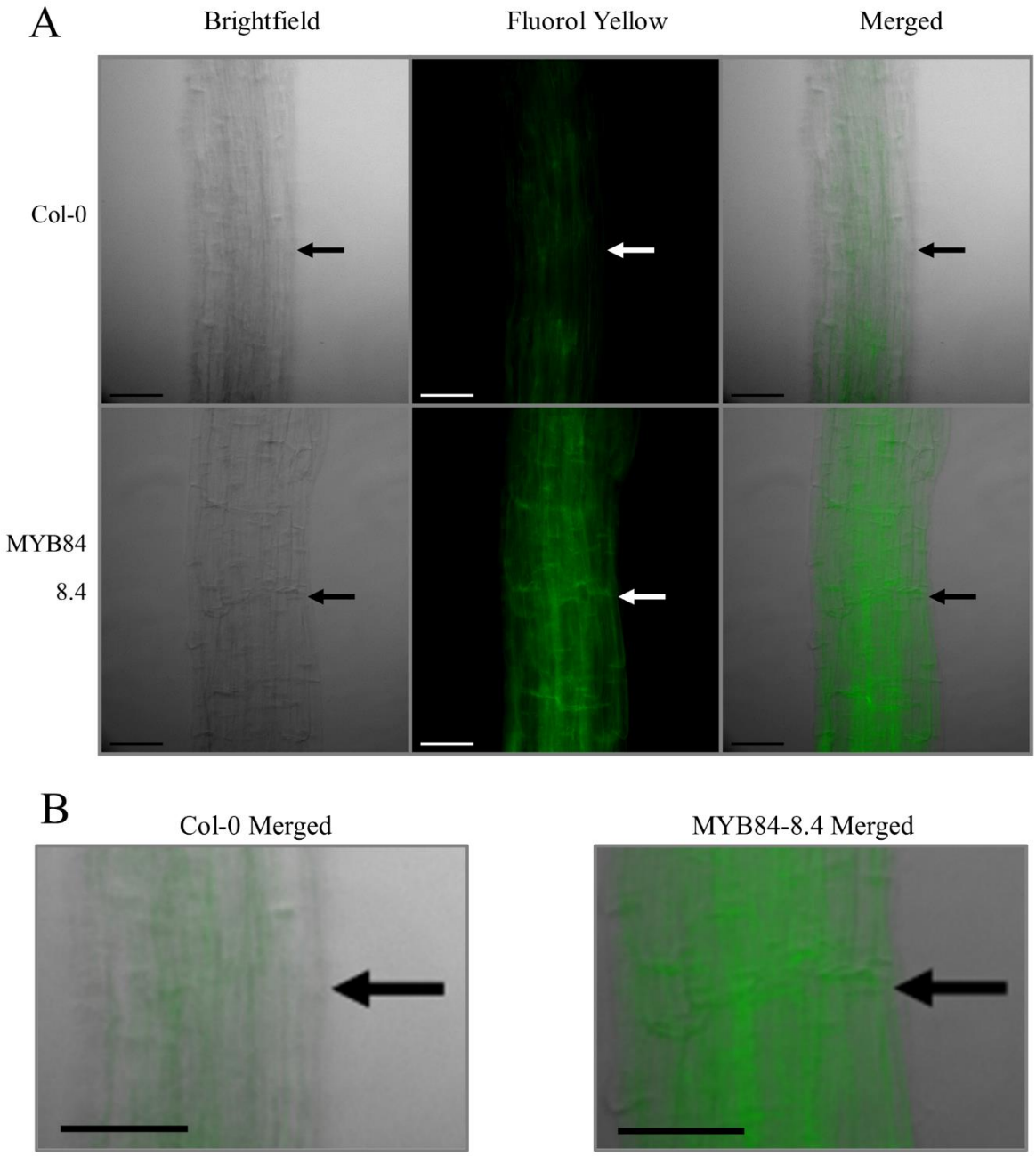

Figure 2.32. Fluorol yellow staining of ABCG37::MYB84-8.4 and reference Col-0 roots in the zone of elongation of three-week-old plants. **A.** Brightfield, fluorol yellow, and merged. Fluorol yellow stains for suberin and associated waxes. Arrows indicate the root epidermis. **B.** Close up of merged Col-0 and MYB84-8.4 images in **A.** Scale bars: 100 μm.

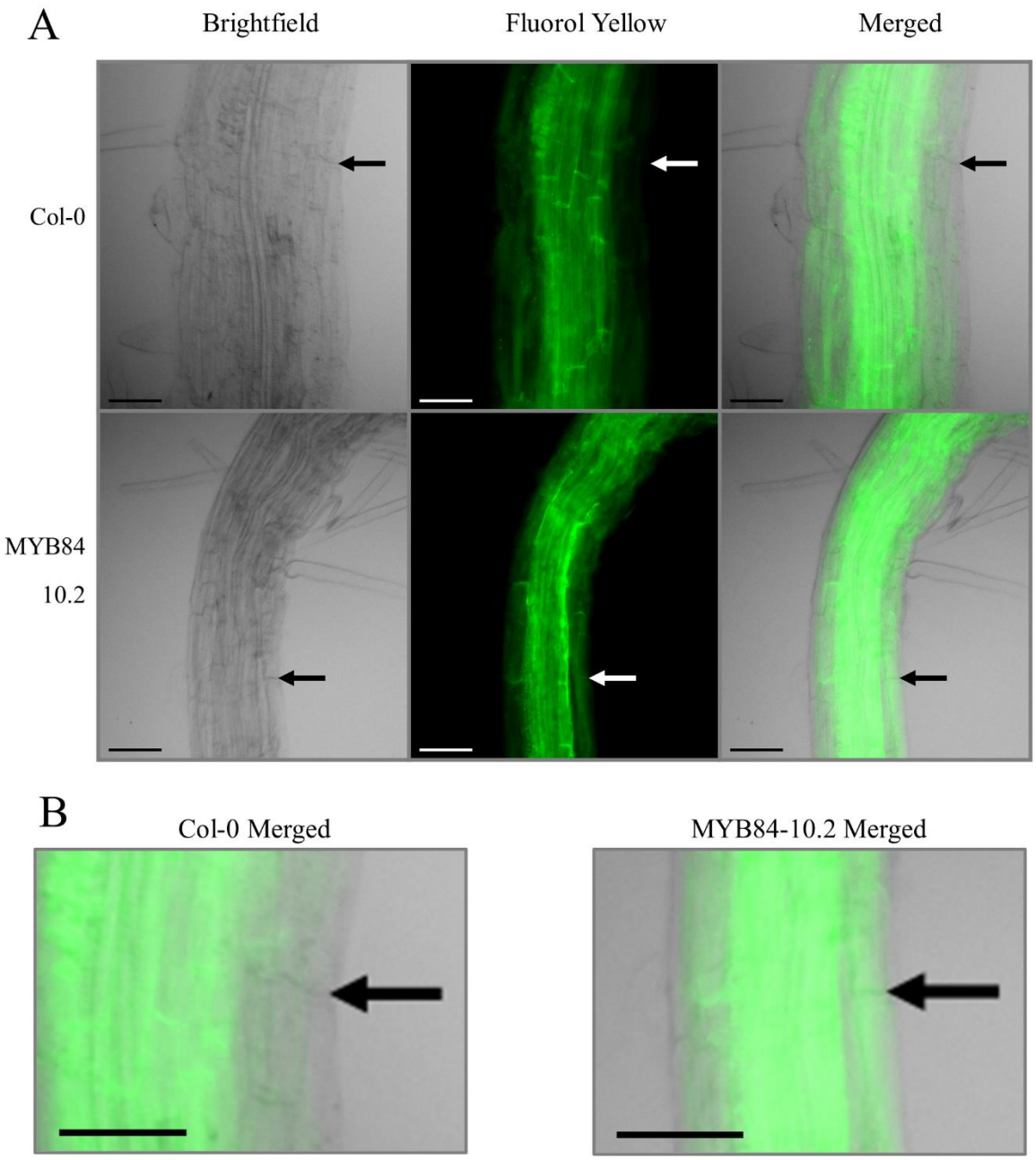

Figure 2.33. Fluorol yellow staining of ABCG37::MYB84-10.2 and reference Col-0 roots in the zone of elongation of two-week-old plants. **A.** Brightfield, fluorol yellow, and merged. Fluorol yellow stains for suberin and associated waxes. Arrows indicate the root epidermis. **B.** Close up of merged Col-0 and MYB84-8.4 images in **A.** Scale bars: 100 µm.

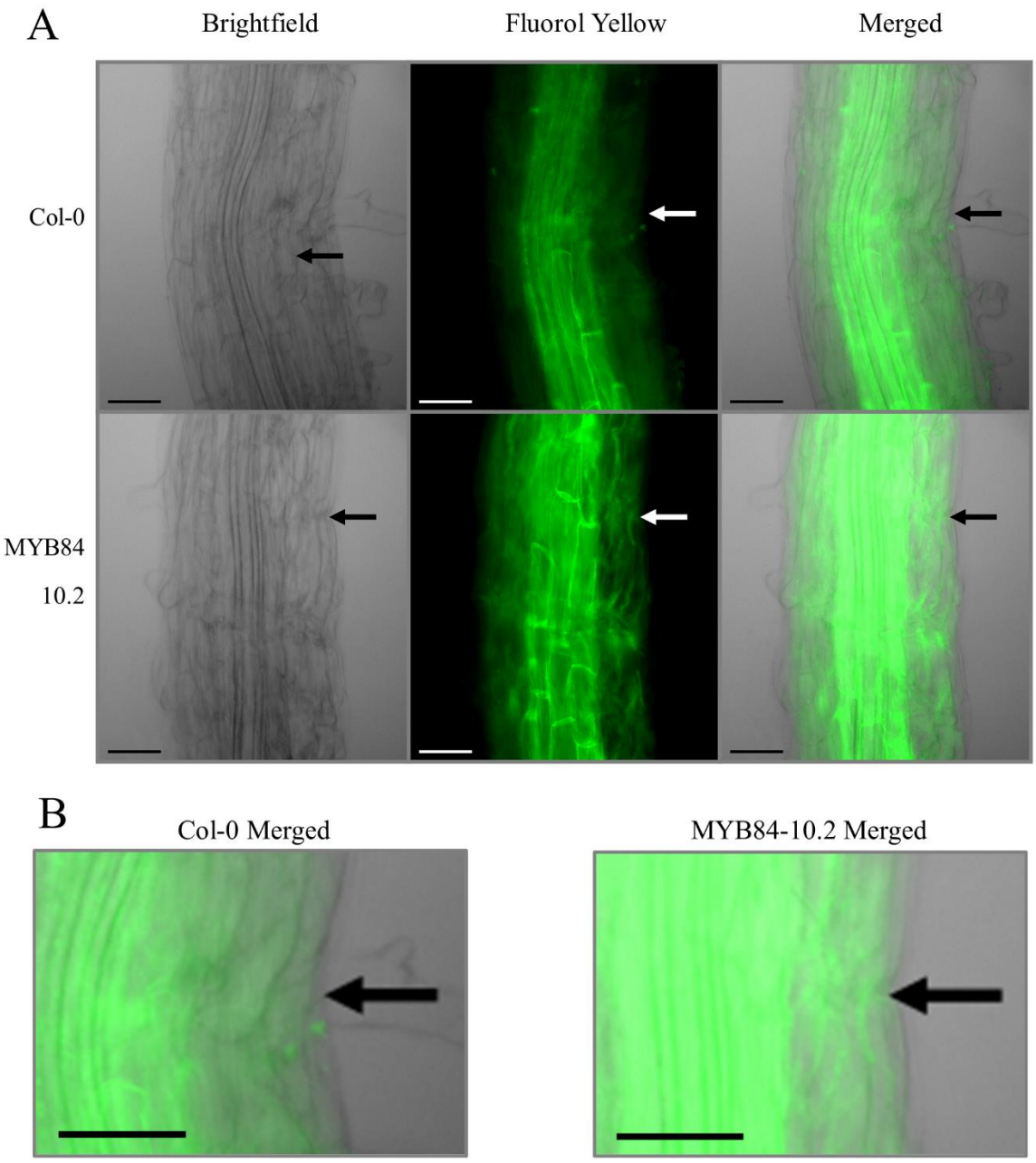

Figure 2.34. Fluorol yellow staining of ABCG37::MYB84-10.2 and reference Col-0 roots in the zone of elongation of three-week-old plants. **A.** Brightfield, fluorol yellow, and merged. Fluorol yellow stains for suberin and associated waxes. Arrows indicate the root epidermis. **B.** Close up of merged Col-0 and MYB84-8.4 images in **A.** Scale bars: 100 µm.

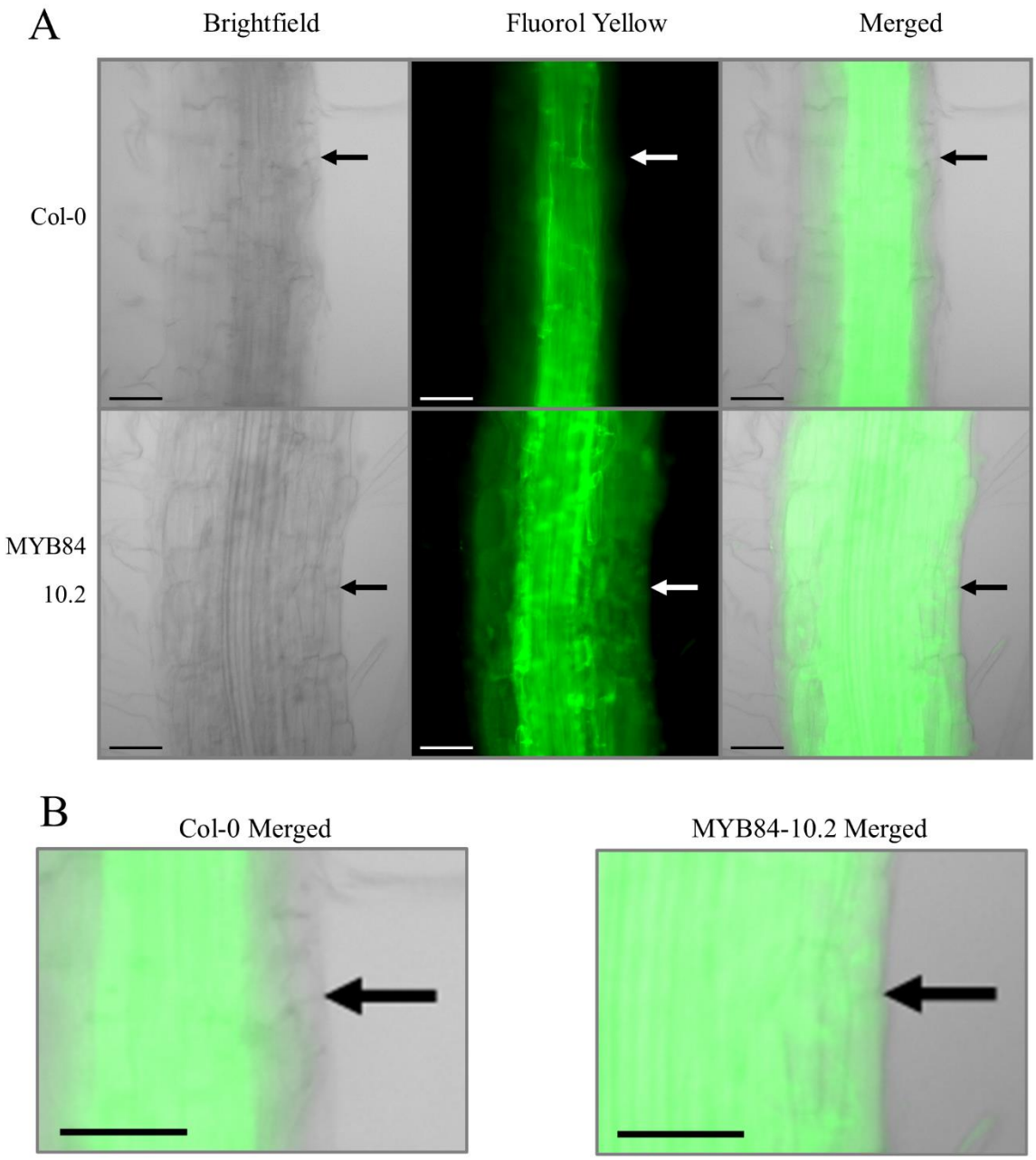

Figure 2.35. Fluorol yellow staining of ABCG37::MYB84-8.4 and reference Col-0 roots in the zone of elongation of four-week-old plants. **A.** Brightfield, fluorol yellow, and merged. Fluorol yellow stains for suberin and associated waxes. Arrows indicate the root epidermis. **B.** Close up of merged Col-0 and MYB84-8.4 images in **A.** Scale bars: 100 µm.

Increased fluorol yellow staining in the root epidermis of MYB84-8.4 homozygous T-2 plants compared to Col-0 indicates the presence of epidermal suberin deposition. Increased epidermal fluorol yellow staining was observed in the zone of maturation (Figures 2.13-18), in lateral roots (Figures 2.19-24), and in the zone of elongation (Figures 2.31-35) for two-week, three-week, and four-week-old plants. Two-week-old and three-week-old MYB84-8.4 have increased suberin near the root to shoot transition (Figure 2.25-26; Figure 2.28-29). During secondary growth, the endodermis is replaced by periderm at the root-shoot transition, a suberized tissue (Ranathunge and Schreiber, 2011). In four-week-old roots, both Col-0 and MYB84-8.4 have fluorol yellow staining in the periderm due to peridermal suberin (Figure 2.27; Figure 2.30). There is not a visually apparent increase in peridermal suberin for MYB84, suggesting that MYB84 does not impact suberization in the periderm. MYB84 has been previously implicated in the regulation of periderm formation (Wei et al. 2020). The lack of increased peridermal suberin suggests that increasing expression of MYB84 does not impact the periderm. An alternative explanation is my fluorol yellow staining does not provide quantitative data.

The endodermal suberin appears brighter in MYB84 T-2 plants compared to Col-0 (Figures 2.13-24). When visualized in the longitudinal plane, I hypothesized that the epidermal suberin in front of and behind the endodermis led to visually higher fluorescence due to the stacked layers of fluorol yellow staining. Cross sections of two-week-old Col-0, MYB84-8.4, and MYB84-10.2 roots is consistent with this hypothesis (Figure 2.12).

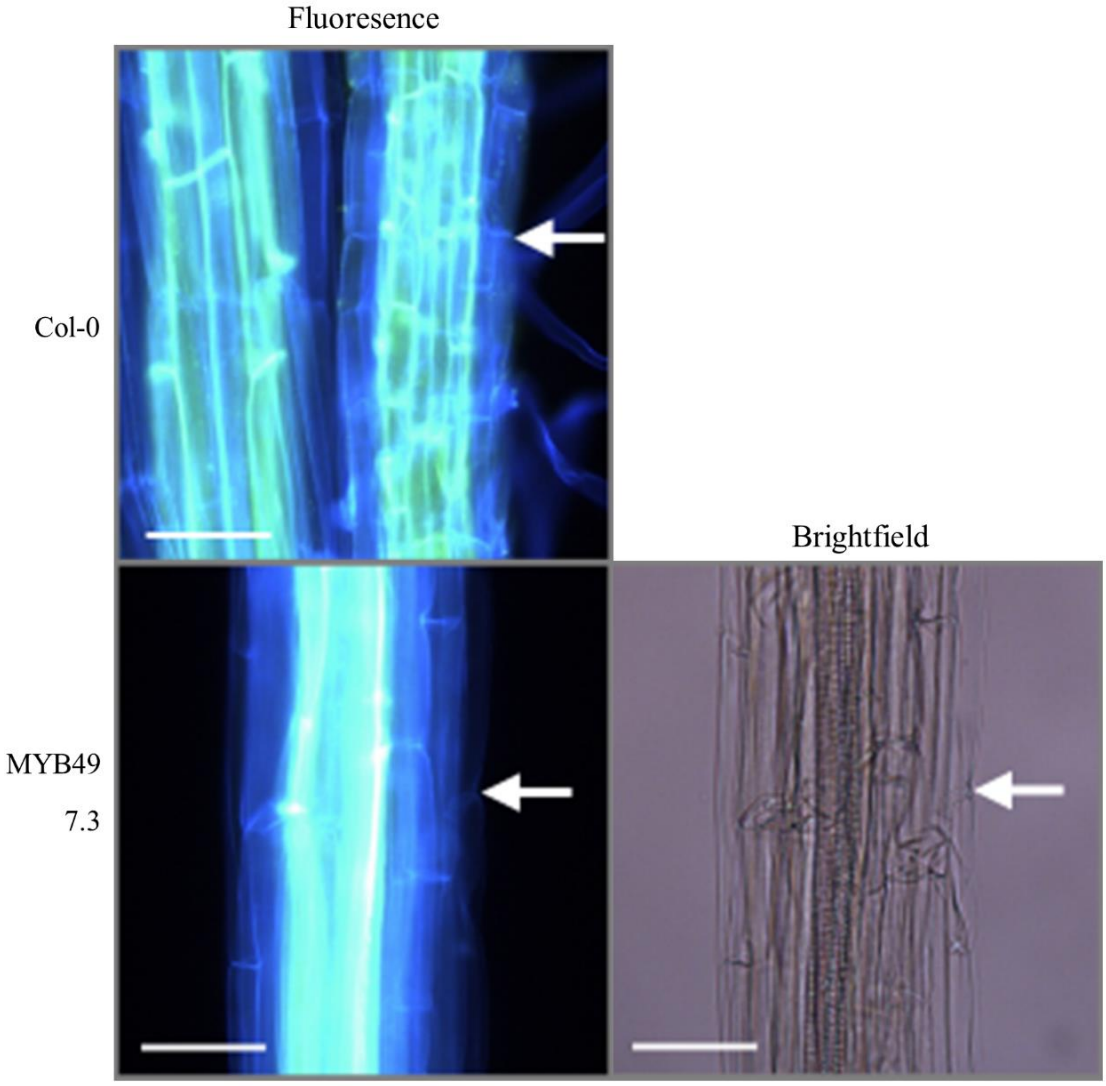

Figure 2.36. Fluorol yellow staining of ABCG37::MYB49-7.3 and reference Col-0 roots in the zone of maturation of two-week-old plants. Fluorol yellow stains for suberin and associated waxes. Arrows indicate the root epidermis. Scale bars: 200 µm. DFC450 camera used.

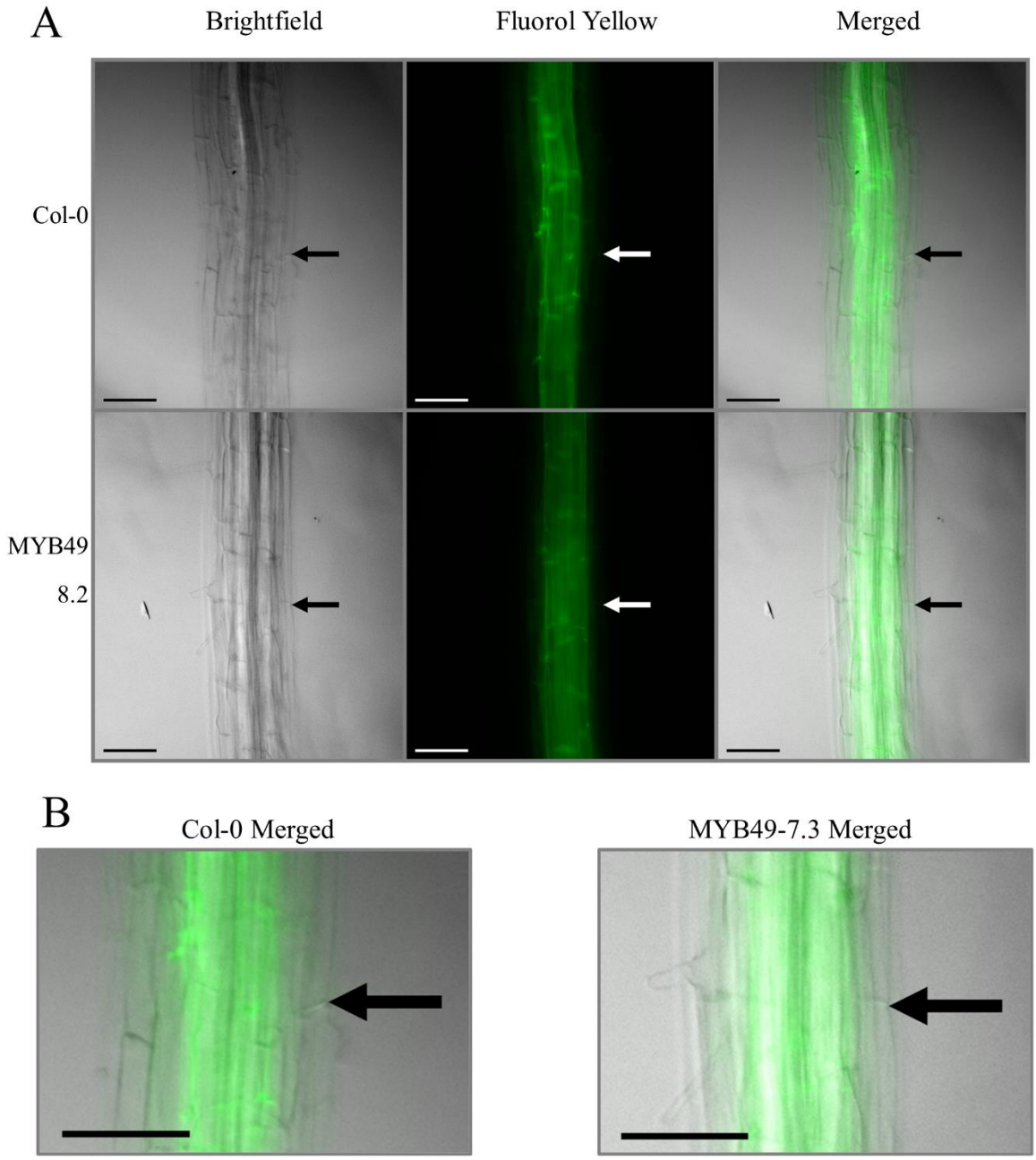

Figure 2.37. Fluorol yellow staining of ABCG37::MYB49-8.2 and reference Col-0 roots in the zone of maturation of two-week-old plants. **A.** Brightfield, fluorol yellow, and merged. Fluorol yellow stains for suberin and associated waxes. Arrows indicate the root epidermis. **B.** Close up of merged Col-0 and MYB84-8.4 images in **A.** Scale bars: 100 µm.

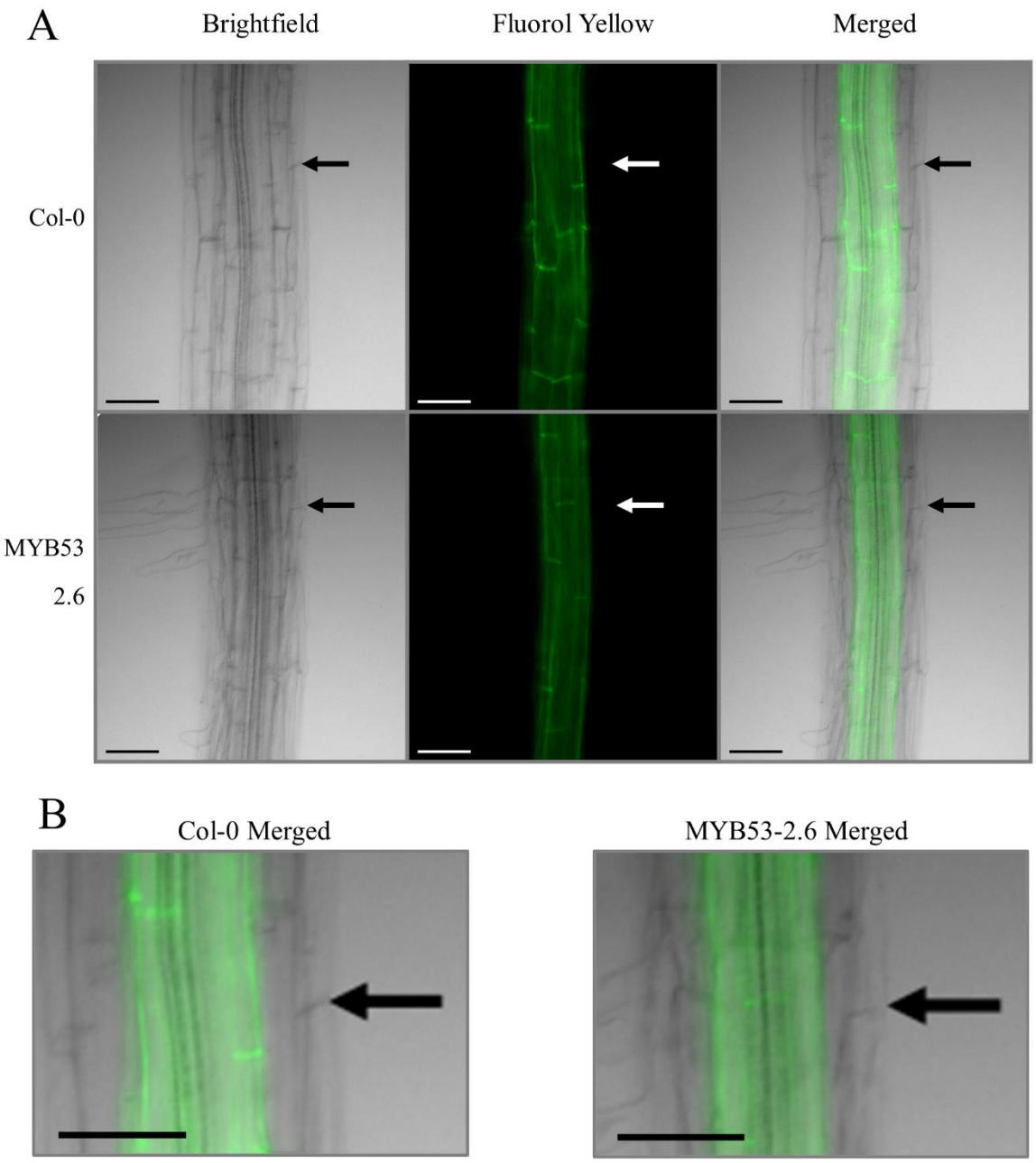

Figure 2.38. Fluorol yellow staining of ABCG37::MYB53-2.6 and reference Col-0 roots in the zone of maturation of two-week-old plants. **A.** Brightfield, fluorol yellow, and merged. Fluorol yellow stains for suberin and associated waxes. Arrows indicate the root epidermis. **B.** Close up of merged Col-0 and MYB84-8.4 images in **A.** Scale bars: 100 µm.

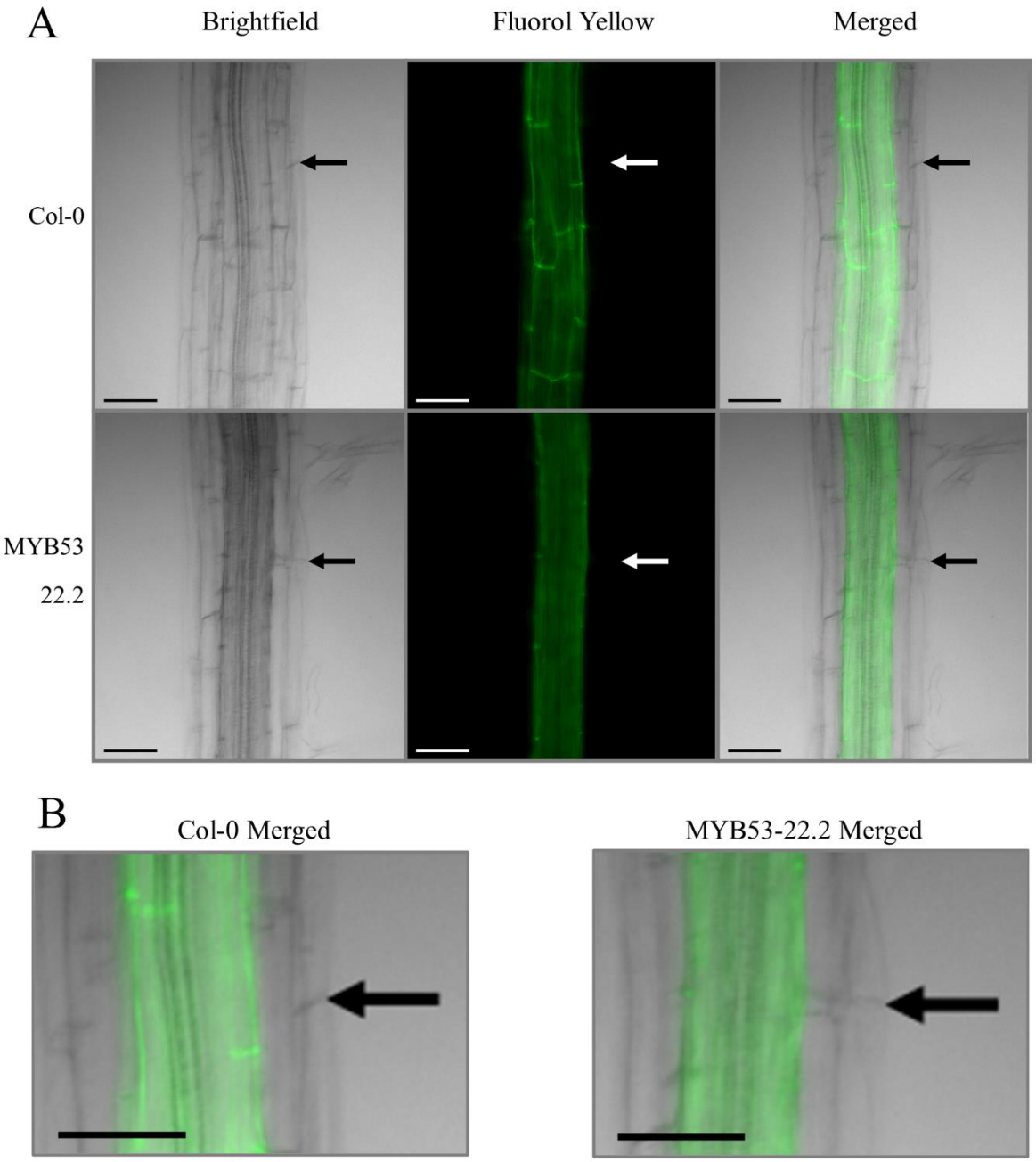

Figure 2.39. Fluorol yellow staining of ABCG37::MYB53-2.22 and reference Col-0 roots in the zone of maturation of two-week-old plants. **A.** Brightfield, fluorol yellow, and merged. Fluorol yellow stains for suberin and associated waxes. Arrows indicate the root epidermis. **B.** Close up of merged Col-0 and MYB84-8.4 images in **A.** Scale bars: 100 µm.

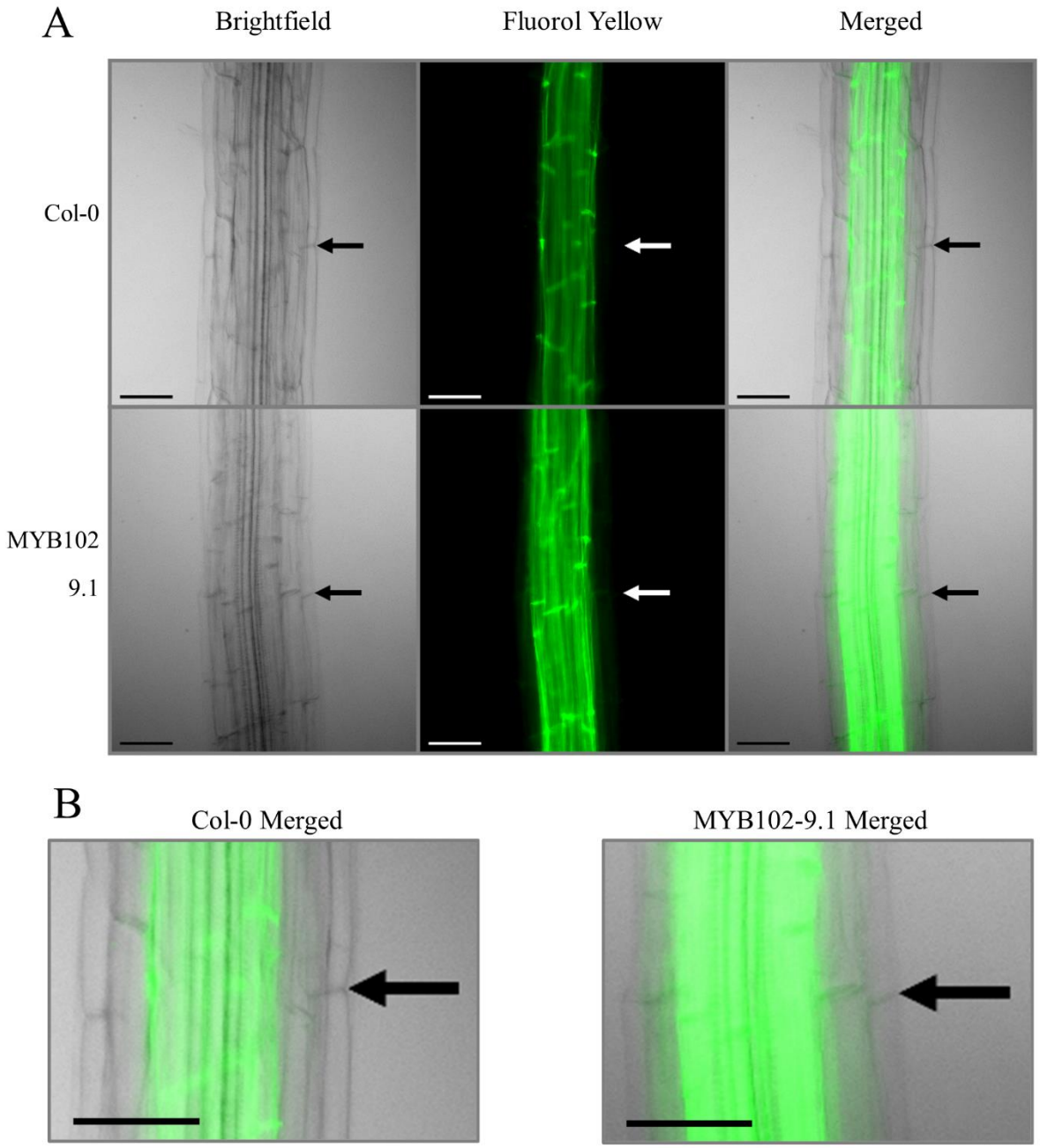

Figure 2.40. Fluorol yellow staining of ABCG37::MYB102-9.1 and reference Col-0 roots in the zone of maturation of two-week-old plants. **A.** Brightfield, fluorol yellow, and merged. Fluorol yellow stains for suberin and associated waxes. Arrows indicate the root epidermis. **B.** Close up of merged Col-0 and MYB84-8.4 images in **A.** Scale bars: 100 µm.

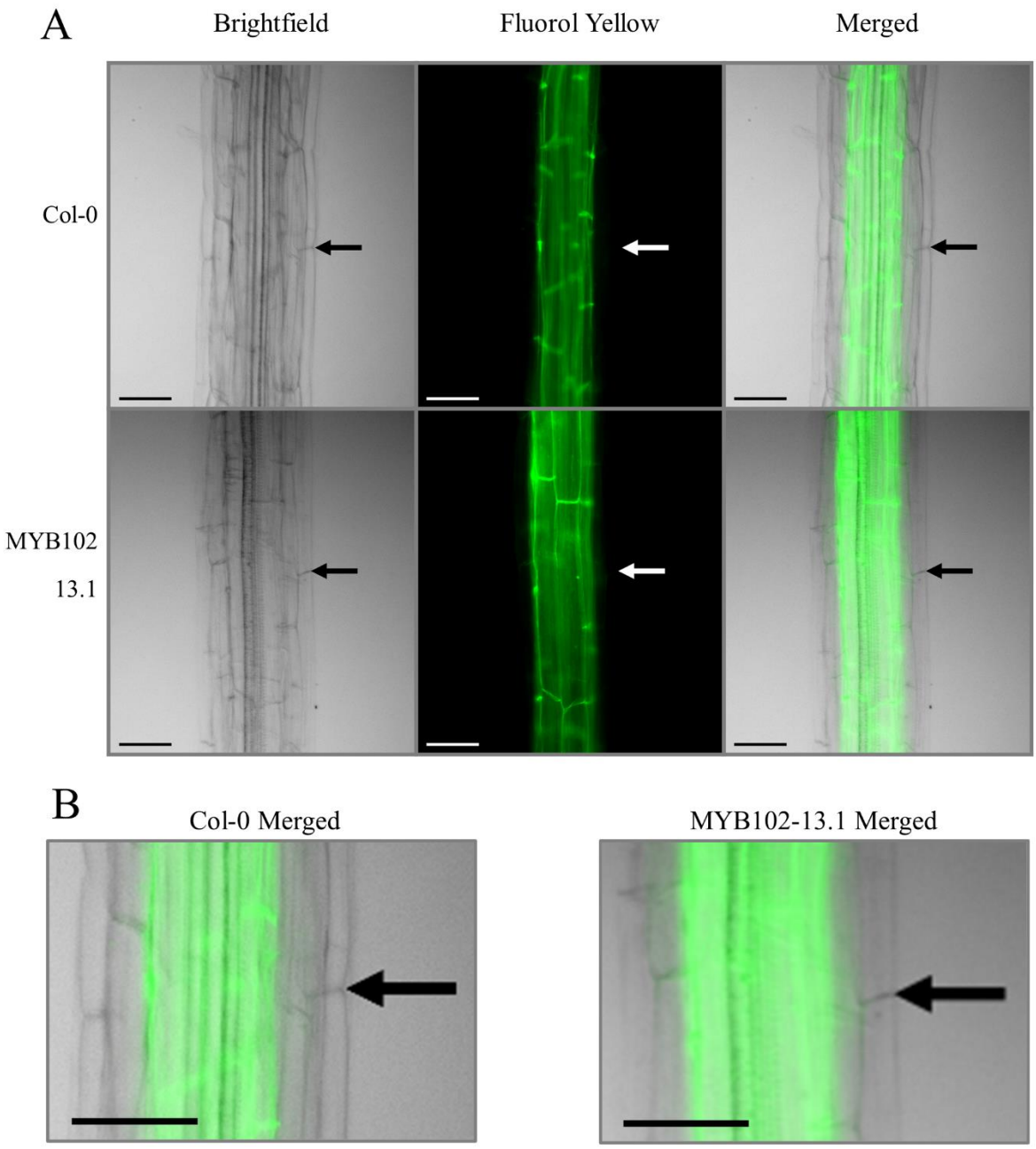

Figure 2.41. Fluorol yellow staining of ABCG37::MYB102-13.1 and reference Col-0 roots in the zone of maturation of two-week-old plants. **A.** Brightfield, fluorol yellow, and merged. Fluorol yellow stains for suberin and associated waxes. Arrows indicate the root epidermis. **B.** Close up of merged Col-0 and MYB84-8.4 images in **A.** Scale bars: 100 µm.

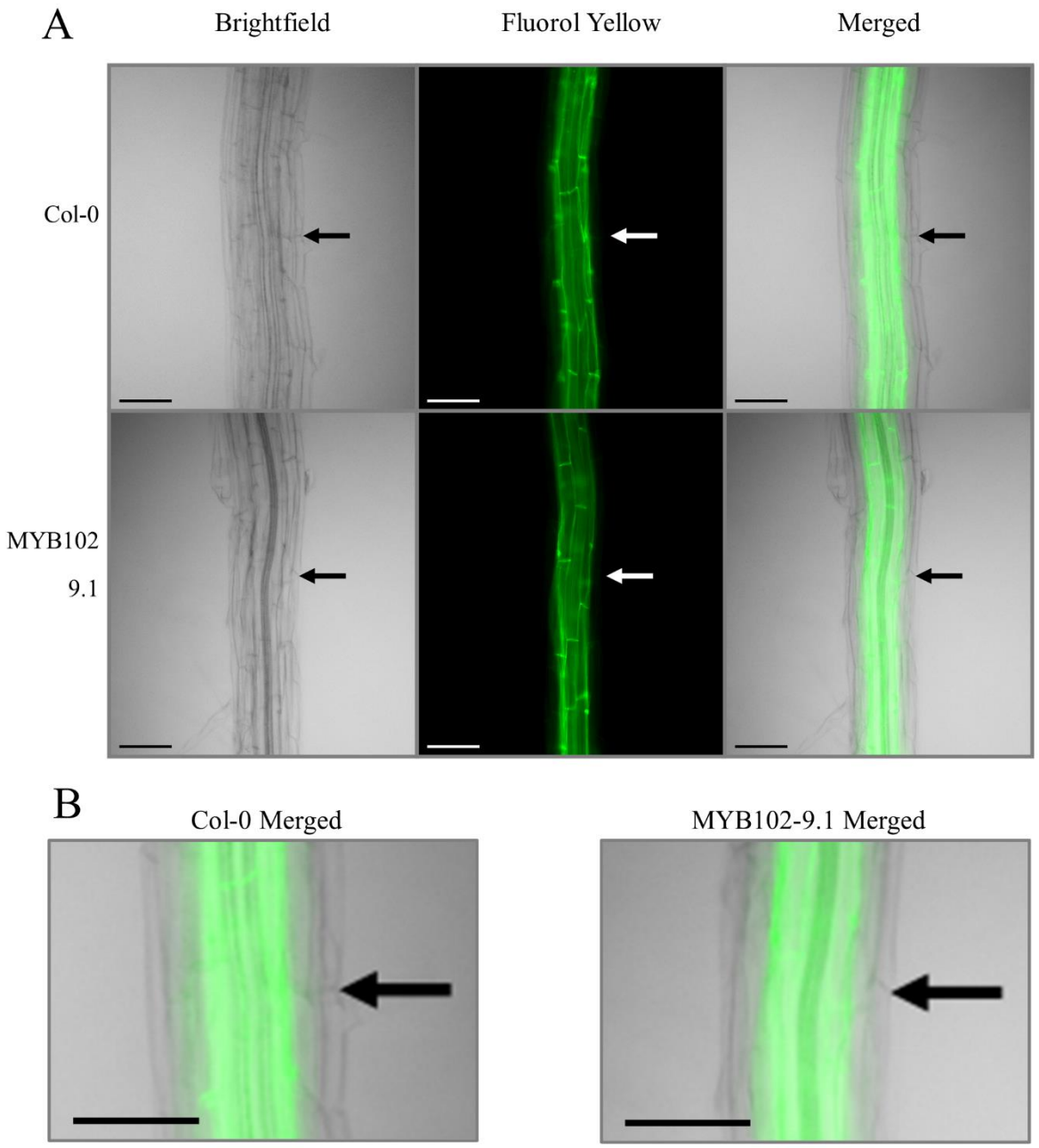

Figure 2.42. Fluorol yellow staining of ABCG37::MYB107-19.3 and reference Col-0 roots in the zone of maturation of two-week-old plants. **A.** Brightfield, fluorol yellow, and merged. Fluorol yellow stains for suberin and associated waxes. Arrows indicate the root epidermis. **B.** Close up of merged Col-0 and MYB84-8.4 images in **A.** Scale bars: 100 µm.

MYB49, MYB53, MYB102, and MYB107 homozygous T-2 lines did not have visual increases in suberin compared to Col-0, therefore only images of two-week old plants were taken (Figures 2.36-42). MYB49 and MYB102 had the highest levels of suberin in primary transformants (Table 2.1); however, the two T-2 lines screened for each did not have increased suberin compared to Col-0 (Table 2.4). This may be due to silencing or transcriptional repression at the T-2 generation since T-2 lines with epidermal suberin have stunted growth. Alternatively, the appearance of epidermal suberin in T-0 plants may have been false positives due to the use of a color camera (Leica DFC450) instead of fluorescent camera as used for T-2 plants (Leica sCMOS K5).

Table 2.4. Fluorol yellow screening of homozygous T-2 plants. Percentage of transgenics with no suberin (-), slight suberin (+-), increased suberin (+), or high levels of suberin (++) compared to Col-0.

MYB	*T-2 lines*	*T-2 FY staining*
MYB49	7.3	-
	8.2	-
MYB53	2.6	-
	22.2	-
MYB84	8.4	++
	10.2	++
MYB102	9.1	-
	13.1	-
MYB107	19.3	-

Only MYB84 lines had fluorol yellow staining in the epidermis compared to Col-0, indicating the presence of epidermal suberin (Table 2.4). MYB84 T-2 lines (Table 2.4) had higher levels of suberin in relation to T-0 (Table 2.1). This suggests that higher levels of MYB84 result in higher levels of suberin since the homozygous plants have two copies of the T-DNA. This is further supported by the MYB84-7.3 line (Figure 2.8), which has more than one T-DNA

insertion. Plants from this line had higher levels of suberin than either MYB84 single insertion line (8.4 and 10.2).

Reduced root growth in MYB84 T-2 plants

MYB84 T-2 two-week and four-week-old plants have visually shorter roots compared to Col-0 (Figure 2.43; Figure 2.44). Two-week-old MYB84 T-2 root lengths were analyzed and found to be significantly shorter than Col-0 of the same age (Figure 2.45; Figure 2.46). On average MYB84 roots were 22.9mm (MYB84-8.4) and 21mm (MYB84-10.2) shorter than Col-0 (59.9mm and 61.2mm, respectively).

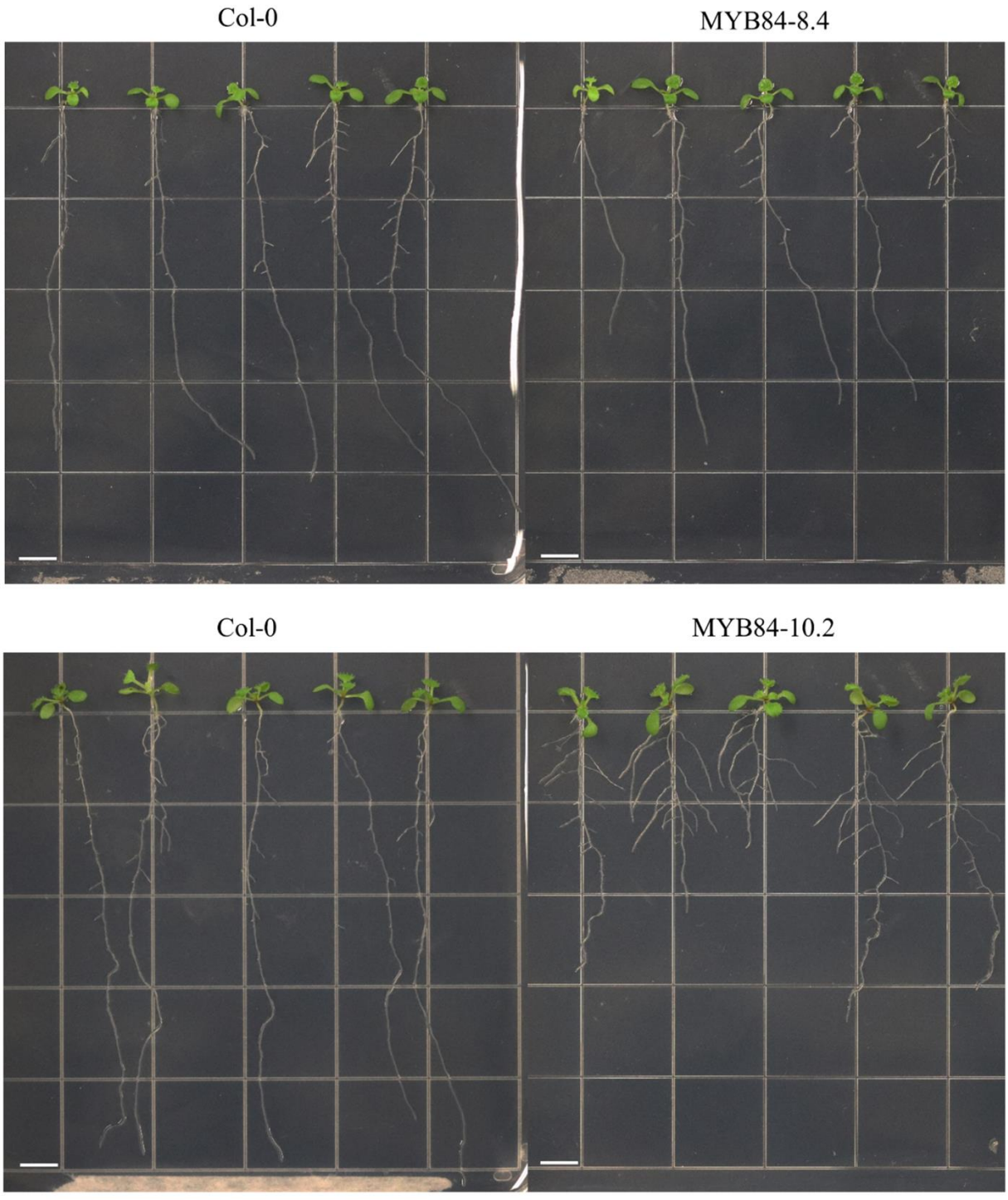

Figure 2.43. Two-week-old Col-0 and MYB84-8.4 or MYB84-10.2 plants. Scale bar: 5mm

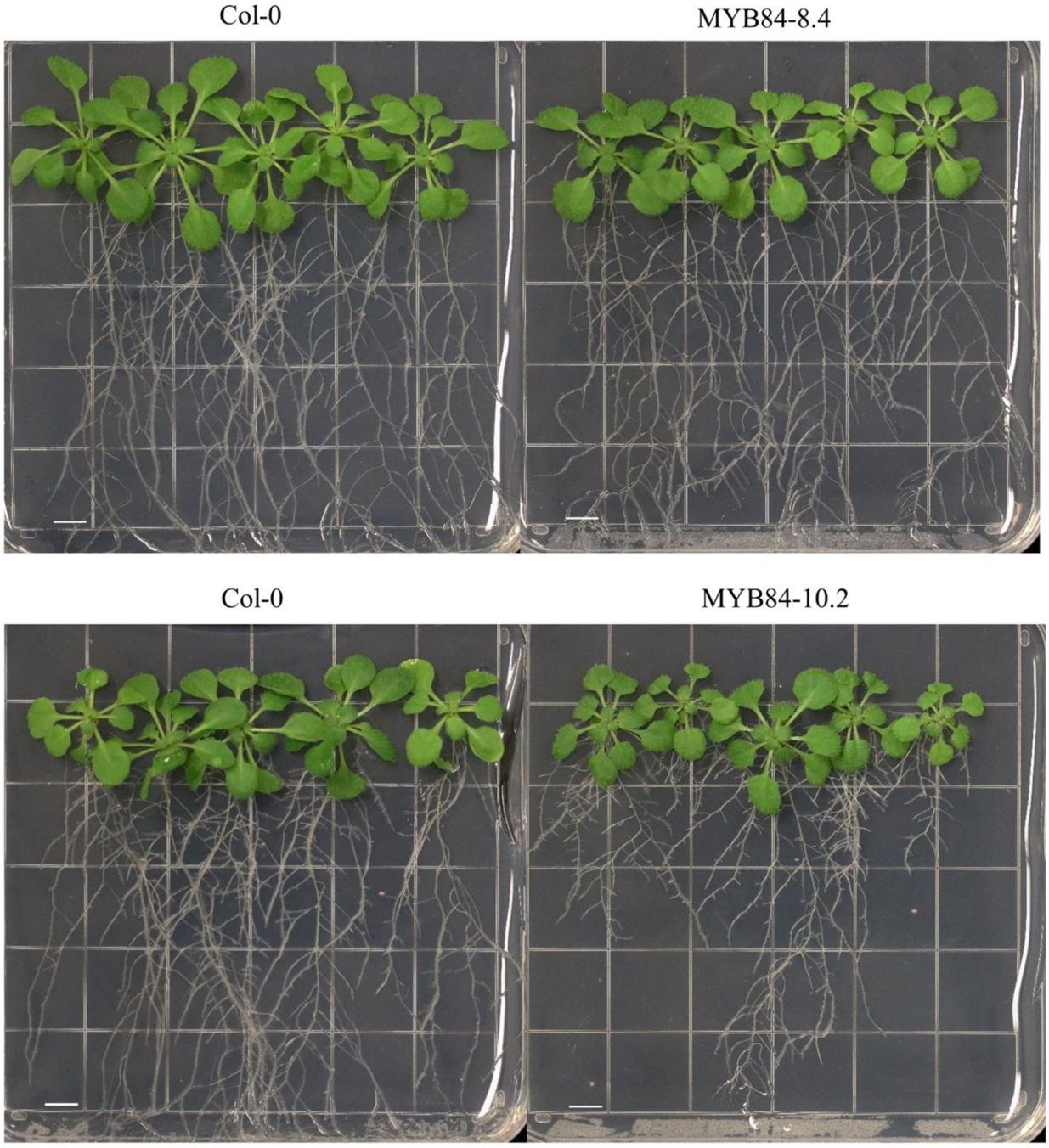

Figure 2.44. Four-week-old Col-0 and MYB84-8.4 or MYB84-10.2 plants. Scale bar: 5mm

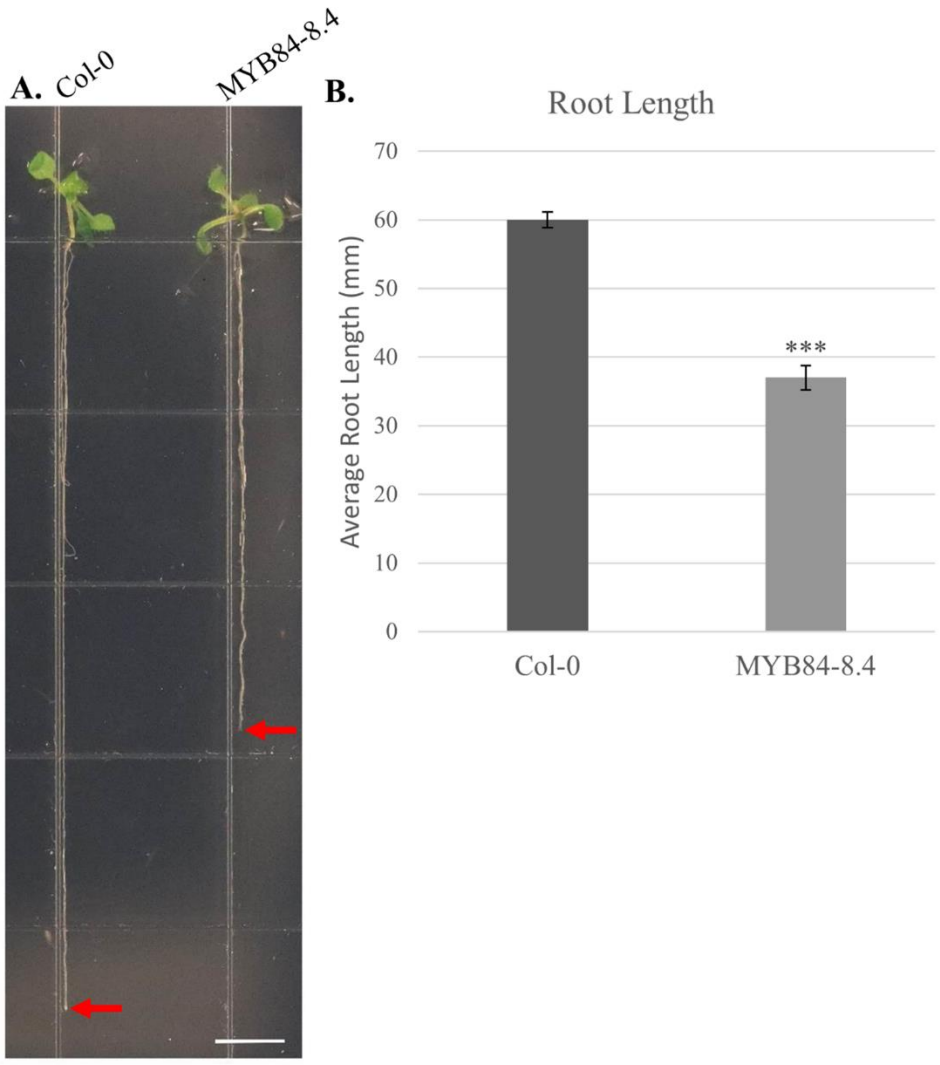

Figure 2.45. A. Two-week-old representative Col-0 and MYB84-8.4 of average root length. Arrows point to root tips. Scale bar: 5mm **B.** Average root length of two-week-old Col-0 (59.99mm) and MYB84-8.4 (37.02mm). n=30. Error bars: standard error. ***Student's t-test significance of 9.09×10^{-16}

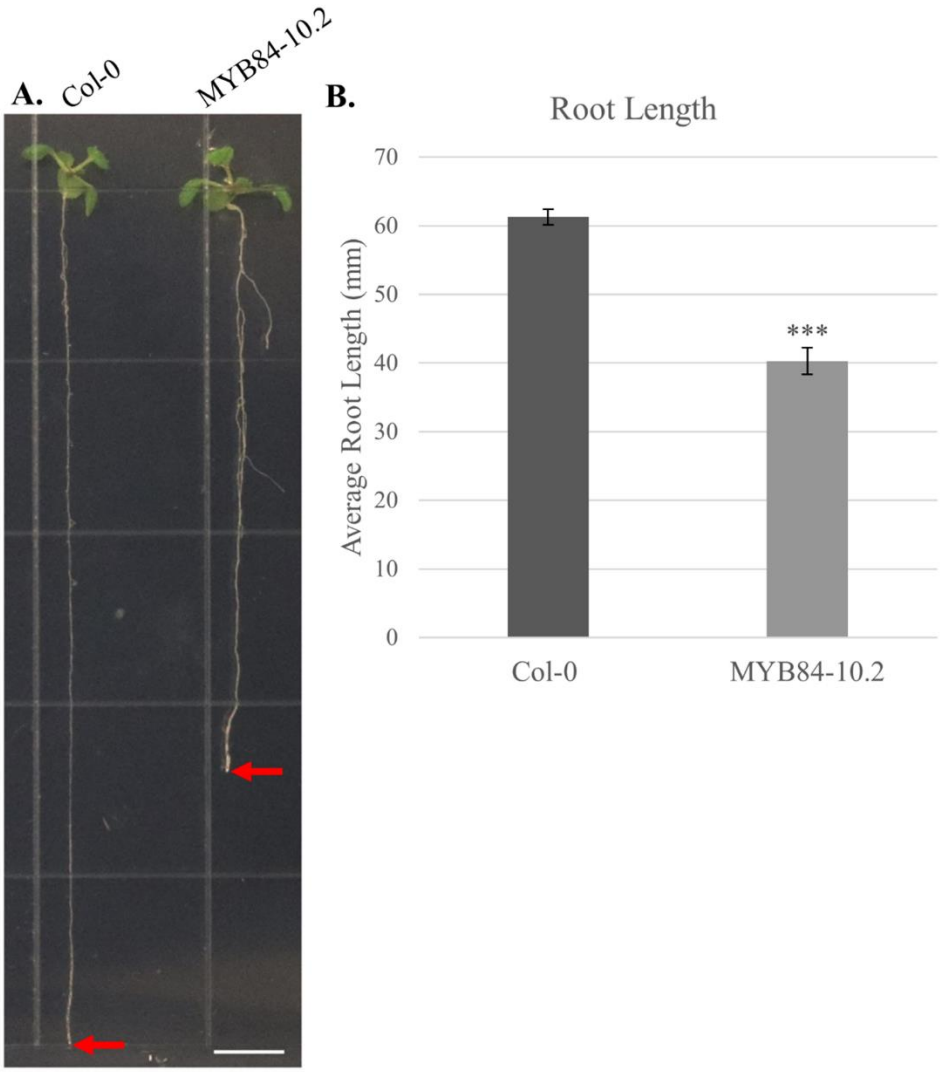

Figure 2.46. A. Two-week-old representative Col-0 and MYB84-10.2 of average root length. Arrows point to root tips. Scale bar: 5mm **B.** Average root length of two-week-old Col-0 (61.25mm) and MYB84-10.2 (40.27mm). n=30. Error bars: standard error. ***Student's t-test significance of 3.23×10^{-13}

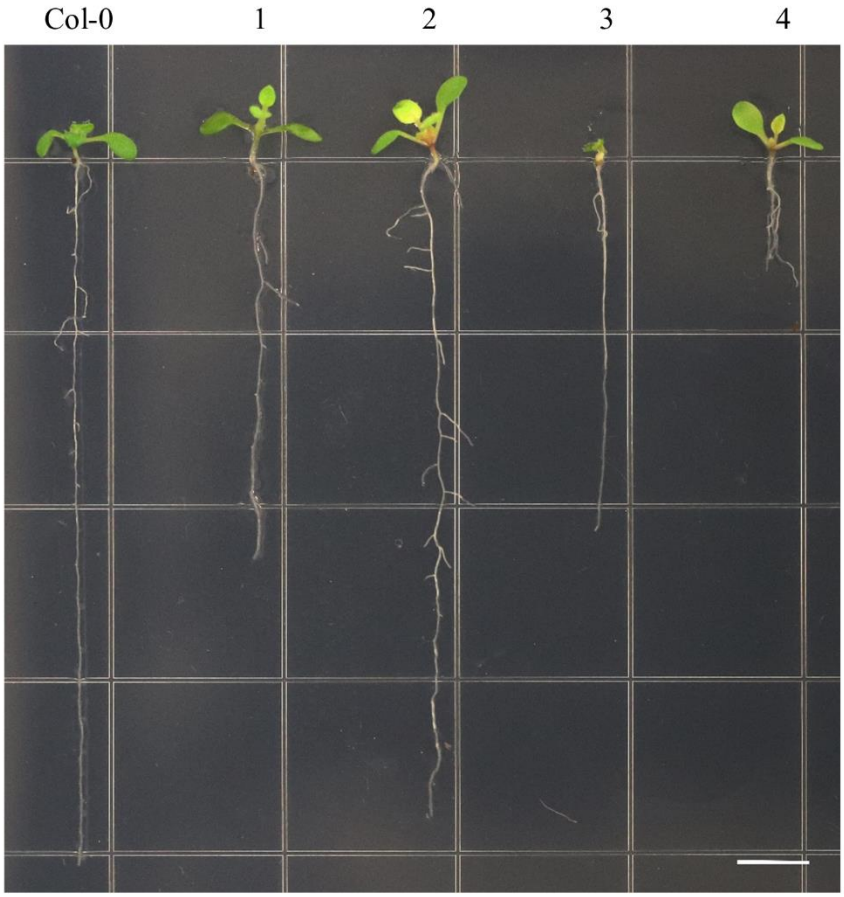

Figure 2.47. Two-week-old representative Col-0 and MYB84-7.10 (**1**) of average root length. **2-4.** MYB84-7.10 with various phenotypes. Scale bar: 5mm

MYB84-7.10 T-2 plants varied in root length. The root length appeared to correlate with suberin levels in these plants. Plant #4 (Figure 2.47) had very high levels of suberin, similar to T-1 plants with the same stunted/yellow phenotype (Figure 2.8). The altered root length and suberin levels in MYB84-7.10 plants suggests that the MYB84 transgene may have been silenced in some plants. The number of T-DNA insertions is greater than one; however, the exact number was not determined. The range of phenotypes may be due to the location and/or number of T-DNA insertions. Alternatively, some T-DNAs may be repressed (transcriptionally or translationally) or silenced.

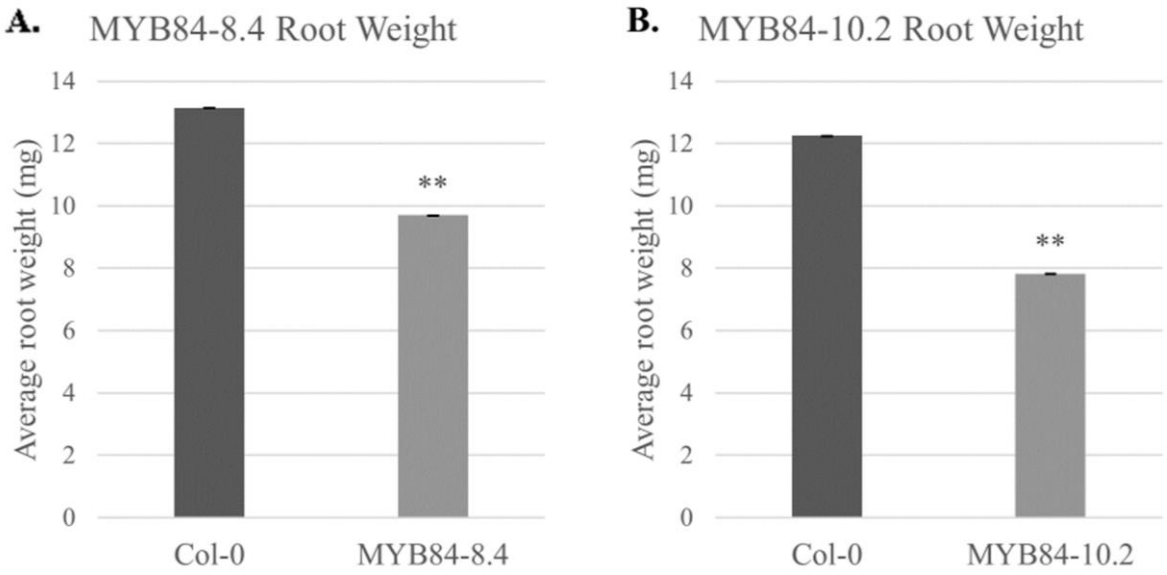

Figure 2.48. Average root weight of four-week-old Col-0 **A.** and MYB84-8.4 (n=30) **B.** and MYB84-10.2 (n=29). **Student's t-test significance <.005 based on the average weight per root of three pools of nine-ten roots. Error bars: standard deviation.

Both MYB84 homozygous T-2 lines had significantly lower weight per root compared to Col-0 (Figure 2.48). The reduced root length and weight in homozygous MYB84 T-2 plants suggests that epidermal suberin reduces root growth. This may be due to the epidermal suberin reducing nutrient acquisition. The increased suberin in the short MYB84-7.10 T-2 plants is consistent with this. The MYB84-7 plants contain more than one T-DNA insertion. Those with the highest levels of suberin were the most severely stunted and yellow.

While two-week-old MYB84-8.4 roots were shorter in comparison to Col-0 than MYB84-10.2 (22.97 mm and 20.99 mm, respectively), the difference in root weight for four-week-old MYB84-8.4 is lower than that of MYB84-10.2 compared to Col-0 (3.45 mg and 4.42 mg, respectively) (Table 2.5).

Table 2.5. Average length and weight for MYB84 roots. Root length in mm; root weight in mg.

	Average root length	*Difference in root length*	*Average root weight*	*Difference in root weight*
Col-0	59.99	22.97	13.15	3.45
MYB84-8.4	37.02		9.70	
Col-0	61.25	20.99	12.25	4.42
MYB84-10.2	40.27		7.82	

MYB84 responses to hormone treatment

The hormones abscisic acid (ABA) and ethylene regulate the deposition and degradation of endodermal suberin, respectively (see Hormonal responses section page 21). If treatment with ABA or the ethylene precursor ACC affects the epidermal suberin in MYB84 transgenics, this suggests that MYB84 is regulated by the respective signaling pathway.

Two-week-old MYB84-8.4 plants treated with 2 µM ACC for 24 hours appeared to have degradation of epidermal suberin when visually inspected under a fluorescent microscope, suggesting that MYB84 is regulated by the ethylene signaling pathway. MYB84-8.4 plants treated with ABA did not have a change in epidermal suberin, suggesting that MYB84 isn't regulated by the ABA signaling pathway. While degradation in epidermal suberin after treatment with ACC was visually apparent under the microscope, images were difficult to capture.

ACC treatment was repeated with 2 µM and 5 µM ACC for 24 hours for MYB84-8.4 and MYB84-10.2 plants to confirm degradation of epidermal suberin. Repeating the ACC treatment did not result in any visual differences in epidermal or endodermal fluorescence for either MYB84 transgenic or Col-0. Due to no difference in endodermal suberin for Col-0 when treated with ACC, the ACC may not have been effective. Because treatment with ABA did not result in a difference in epidermal suberin for MYB84-8.4 plants, ABA treatment was not repeated.

Without the appearance of degraded endodermal suberin in Col-0, the efficacy of the ACC cannot be confirmed, therefore whether the ACC treatment had an effect on MYB84 transgenics cannot be determined.

Gene expression in MYB84 T-2 plants

The expression levels of four genes in the suberin biosynthetic pathway were evaluated via qRT-PCR. KCS2, FACT, ABCG6, and GELP51 were chosen to provide insight into each step of suberin biosynthesis: aliphatic monomer synthesis, aromatic monomer synthesis, monomer transport, and polymerization, respectively. KCS2 is involved the elongation of C_{20} acyl chain suberin precursors (Franke et al. 2009; Lee et al. 2009). Fatty alcohol:caffeoyl-CoA caffeoyl transferase (FACT), a transferase in the BAHD family, is responsible for synthesis of the suberin aromatic monomer alkyl caffeate (Kosma et al., 2012). The ATP-Binding Cassette (ABCG) transporter ABCG6 is involved in the transport of suberin monomers through the plasma membrane (Nomberg et al., 2022). GELP51, a GDSL-type-esterase/lipase protein, is involved in suberin polymerization (Ursache et al., 2021).

Both MYB84 transgenic plants had high levels of MYB84 transcripts, confirming expression of the transgene. While MYB84-8.2 had higher levels of all suberin biosynthetic transcripts than Col-0, none were significantly higher. MYB84-10.2 had significantly higher expression of KCS2 and ABCG6 but not FACT or GELP51. This indicates that MYB84 activates transcription of these genes. KCS2 is involved in the synthesis aliphatic monomers. The increased transcription of KCS2 suggests that MYB84 is involved in the synthesis of aliphatic suberin. This may indicate that MYB84 suberin contains more aliphatic suberin in relation to aromatic suberin since FACT expression was not significantly higher; however, this is not supported by MYB84-8.4. ABCG6 is involved in the transport of suberin monomers. The

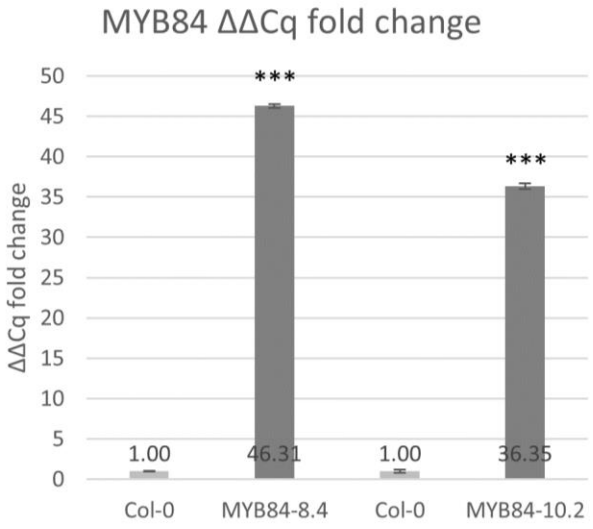
MYB84 ΔΔCq fold change
ΔΔCq fold change
50
45
40
35
30
25
20
15
10
5
0
***
***
1.00
46.31
1.00
36.35
Col-0
MYB84-8.4
Col-0
MYB84-10.2

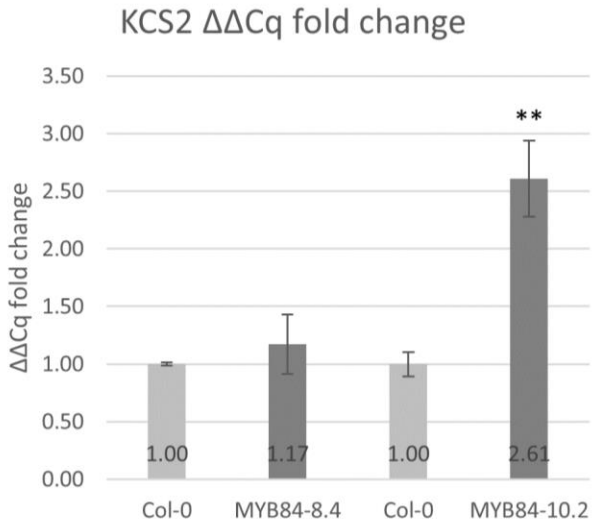
KCS2 ΔΔCq fold change
ΔΔCq fold change
3.50
3.00
2.50
2.00
1.50
1.00
0.50
0.00
**
1.00
1.17
1.00
2.61
Col-0
MYB84-8.4
Col-0
MYB84-10.2

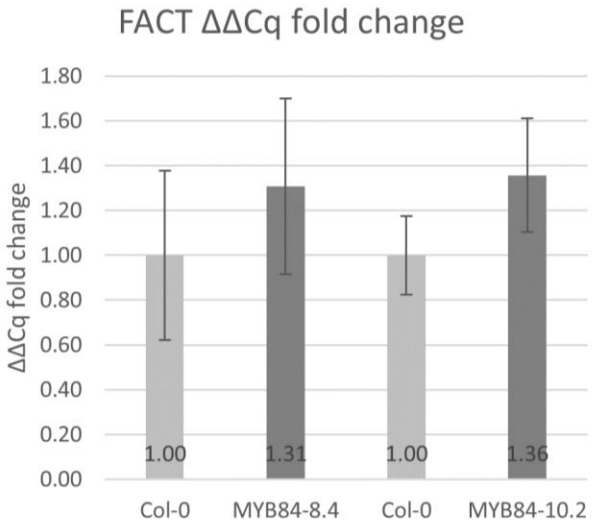
FACT ΔΔCq fold change
ΔΔCq fold change
1.80
1.60
1.40
1.20
1.00
0.80
0.60
0.40
0.20
0.00
1.00
1.31
1.00
1.36
Col-0
MYB84-8.4
Col-0
MYB84-10.2

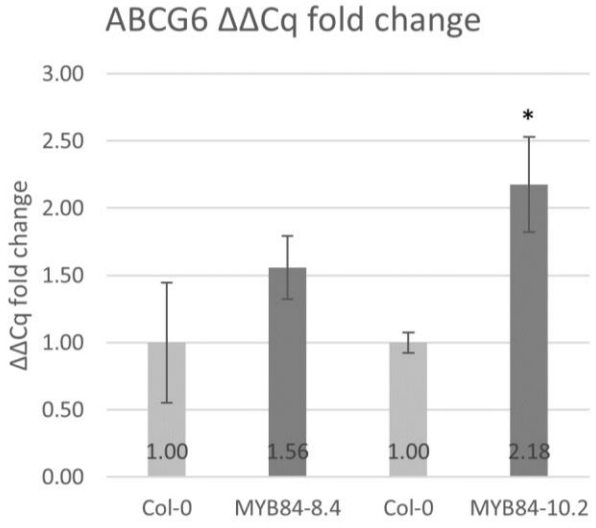
ABCG6 ΔΔCq fold change
ΔΔCq fold change
3.00
2.50
2.00
1.50
1.00
0.50
0.00
*
1.00
1.56
1.00
2.18
Col-0
MYB84-8.4
Col-0
MYB84-10.2

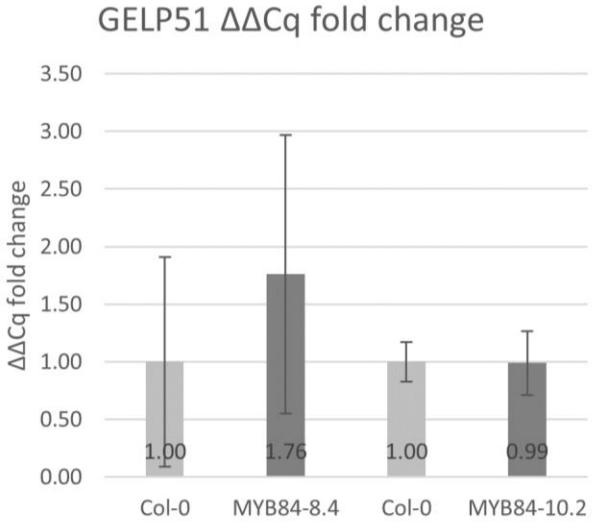
GELP51 ΔΔCq fold change
ΔΔCq fold change
3.50
3.00
2.50
2.00
1.50
1.00
0.50
0.00
1.00
1.76
1.00
0.99
Col-0
MYB84-8.4
Col-0
MYB84-10.2

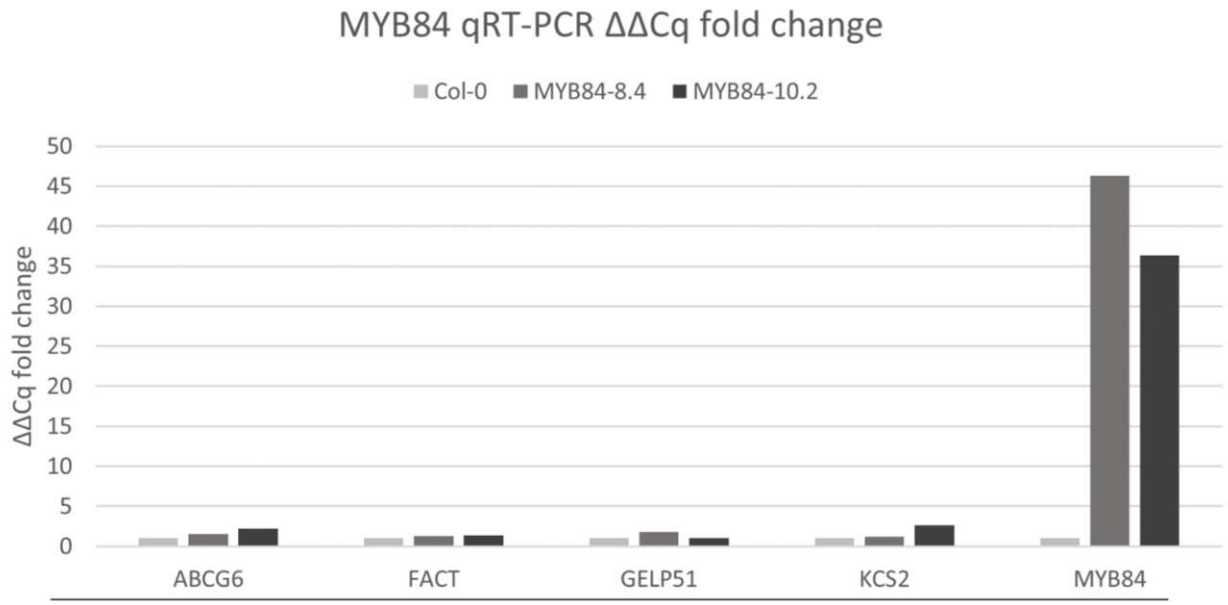

Figure 2.49. qRT-PCR ΔΔCq fold change. Error bars: standard deviation for biological replicates (n=2-3). *Student's t-test significance 0.02727021 ** Student's t-test significance 0.00463673 *** Student's t-test significance <0.001

increased expression in MYB84-10.2 plants along with KCS2 supports the role of ABCG6 in transport of aliphatic suberin.

MYB84-10.2 had higher fold-changes for suberin biosynthetic genes than MYB84-8.4. The higher fold changes for MYB84-10.2 KCS2 and ABCG6 could indicate the T-DNA for this line was inserted into a more active area of chromatin than MYB84-8.4; however, higher levels of MYB84 expression in MYB84-8.4 than MYB84-10.2 does not support this.

While two-week-old MYB84-10.2 roots were not shorter than MYB84-8.4 in comparison to Col-0 grown at the same time (Figure 2.43), four-week-old MYB84-10.2 roots appeared shorter compared to Col-0 than MYB84-8.4 (Figure 2.44). This, along with the higher levels of suberin biosynthetic gene expression in MYB84-10.2 four-week-old plants, suggests that the MYB84 transgene is developmentally regulated. This may be due to the location of the T-DNA insertion; the MYB84-10 T-DNA insertion may be located in an area of chromatin that is expressed more highly in four-week-old roots than two-week-old roots.

Conclusions and Future Directions

MYB84 expression under a root epidermal-specific promoter with continuous expression leads to root epidermal suberin. This suggests MYB84 is either already phosphorylated in the root or it does not rely on phosphorylation for activation. Since MYB84 is usually expressed in the root periderm, either is reasonable. MYB107 T-0 and T-2 plants did not have epidermal suberin. MYB107 is involved in suberin deposition in the seed coat and may need to be post translationally modified for activation in the root. Mutating Ser253 into aspartic acid didn't lead to epidermal suberin, so a different amino acid may need to be phosphorylated, or MYB107 may need to be modified in another way. Determining more structural information about MYB107 may indicate which, if any, amino acids need to be phosphorylated for activation. Alphafold could provide more structural information without the cost of other methods such as x-ray crystallography by predicting the 3D structure of the protein (Jumper & Hassabis, 2022). This would also be beneficial for the other MYBs to increase information about their structures and functions, and the possible differences and similarities between these transcription factors.

MYB49 and MYB102 had the highest levels of suberin in primary transformants (Table 2.1); however, the two T-2 lines screened for each did not have increased suberin compared to Col-0 (Table 2.3). This may be due to silencing at the T-2 generation or repression of the MYB transgene. Alternatively, the appearance of higher levels of suberin in the MYB49 and MYB102 plants may have been due to the camera used. The Leica DFC450 Digital Color Microscope camera is not a fluorescent camera. Use of this camera for screening T-0 plants may have led to the appearance of epidermal suberin where there was none. MYB53 also appeared to have some epidermal suberin in T-0 plants, similar to MYB84 (Table 2.1), but none in T-2 plants. The appearance of epidermal suberin in the T-0 generation may have been due to the camera used, or the transgene may have been silenced or repressed at the T-2 generation.

Lack of epidermal suberin in MYB49, MYB53, MYB102, and MYB107 may have been due to a lack of activity in the root epidermis. Like MYB41, these MYBs may require phosphorylation for activation. None of the phosphomimics had visually different levels of epidermal suberin compared to the unaltered MYBs. This supports that the MYBs do not require phosphorylation at the sites chosen for mutagenesis. Alternatively, aspartic acid may not be chemically or structurally similar enough to the phosphorylated amino acids chosen for mutagenesis to lead to activation of the transcription factor.

Treatment with ABA did not lead to differences in root epidermal suberin in MYB84 transgenics, suggesting MYB84 is not regulated by this pathway. Root epidermal suberin appeared to be degraded in initial ACC treatment, suggesting that MYB84 is regulated by the ethylene signaling pathway; however, this was not seen in repeated experiments. In repeated ACC treatments, no endodermal suberin degradation was observed in Col-0 treated with ACC, suggesting that the ACC did not have an impact or degradation was not high enough for visual observation. Repeating ACC treatment with new ACC would ensure that the lack of endodermal suberin degradation in Col-0 was not due to ineffective ACC.

Epidermal suberin deposition affects root growth. This may be due to the epidermal suberin preventing the entry of nutrients into the root. This is consistent with the plants with the highest levels of suberin in the MYB84 line with multiple T-DNA insertions as they had a severely stunted/yellow phenotype.

Significantly higher expression of KCS2 and ABCG6 but not FACT or GELP51 in MYB84-10.2 plants could suggest that MYB84 is involved in the synthesis of aliphatic suberin and not aromatic suberin. Further analysis of the MYB84 transgenics would provide further insight into MYB84's role in regulating suberin biosynthesis. Analysis of the epidermal suberin

with gas chromatography mass spectrometry (GC-MS) could provide information on the composition of this suberin and whether it contains more aliphatic suberin in relation to aromatic suberin as suggested by the increase in KCS2 expression. Since the endodermis should be similar in suberin composition in the transgenics and Col-0, the ratios of suberin monomers should be similar. If there is not a difference in the ratios of suberin monomers for Col-0 and the MYB84 transgenics, this could suggest the epidermal suberin in the transgenics is similar in composition to the endodermis. qRT-PCR for MYB84 and more genes in the suberin biosynthetic pathway for various ages of plants could provide information on how expression of these genes changes throughout time. This could provide information on the developmental regulation of the transgenes. RNA-seq would be preferrable to qRT-PCR to look at a wider range of transcripts and may provide insight on interactions between proteins.

Determining the DNA that MYB84 binds to through chromatin immunoprecipitation (ChIP) would be also helpful in determining which genes MYB84 directly activates. Co-immunoprecipitation (Co-IP) would be helpful in identifying proteins MYB84 interacts with.

Due to suberin's previously demonstrated protective barrier properties, the root epidermal suberin in MYB84 transgenics may provide a similar role. Testing the epidermal barrier would provide insight into whether the epidermal suberin provides a protective barrier for the plant. Measurement of salt accumulation through inductively coupled plasma mass spectrometry (ICP-MS) in MYB84 plant shoots after treatment with NaCl would show whether the salt is able to pass through the root epidermal suberin into above ground organs. Additionally, salt treatment could show whether the MYB84 transgenics show salt-tolerance by analysis of plant phenotype and growth compared to Col-0 with the same treatment. If salt treatment leads to a more severe

impact on Col-0, this could indicate the epidermal suberin could provide a barrier beneficial for protection against salt stress, and possibly other stresses as well.

The composition of suberin is important in the properties it provides. This suggest the composition of epidermal suberin is important for providing protective qualities. Fine tuning the epidermal barrier by adjusting the amount and composition of root epidermal suberin would allow for optimization of the suberin barrier. Another Master's student in the Medford lab, Nick Berning, recently found MYB92 root epidermal expression to also result in root epidermal suberin. Combining MYB84, MYB92, and MYB41 all together and in other combinations (MYB84 and MYB92; MYB84 and MYB41; MYB92 and MYB41) may allow for fine tuning of the epidermal suberin to provide a more protective barrier.

Use of a different promoter without continuous epidermal expression may allow for a better method to fine tune the barrier, such as use of an inducible promoter. A promoter that induces MYB expression in response to inputs such as higher salinity could provide a barrier when the plant needs protection without hindering growth under more favorable conditions.

Overall, this research supports MYB84 as a regulator of suberin biosynthesis. Ectopic expression of MYB84 in *Arabidopsis* led to suberization of the intended plant tissue. This provides more information about the regulation of suberin deposition. This may be used to modify the root epidermis of plants to create a protective barrier by providing an additional layer of regulation for the materials that enter and exit the plant.

References

Alassimone, J., Naseer, S., & Geldner, N. (2010). A developmental framework for endodermal differentiation and polarity. *Proceedings of the National Academy of Sciences*, *107*(11), 5214–5219. https://doi.org/10.1073/pnas.0910772107

Andersen, T. G., Naseer, S., Ursache, R., Wybouw, B., Smet, W., De Rybel, B., Vermeer, J. E. M., & Geldner, N. (2018). Diffusible cytokinin repression establishes symmetry and passage cells in the endodermis. *Nature*, *555*(7697), 529–533. https://doi.org/10.1038/nature25976

Atkinson, N. J., & Urwin, P. E. (2012). The interaction of plant biotic and abiotic stresses: From genes to the field. *Journal of Experimental Botany*, *63*(10), 3523–3543. https://doi.org/10.1093/jxb/ers100

Babel, W., & Ackermann, J.-U. (Eds.). (2001). *Biopolyesters*. Springer.

Batsale M, Bahammou D, Fouillen L, Mongrand S, Joubès J, Domergue F. (2021). Biosynthesis and Functions of Very-Long-Chain Fatty Acids in the Responses of Plants to Abiotic and Biotic Stresses. *Cells, 10*(6):1284. doi: 10.3390/cells10061284

Barberon, M. (2017). The endodermis as a checkpoint for nutrients. *New Phytologist*, *213*(4), 1604–1610. https://doi.org/10.1111/nph.14140

Barberon, M., & Geldner, N. (2014). Radial Transport of Nutrients: The Plant Root as a Polarized Epithelium1. *Plant Physiology*, *166*(2), 528–537. https://doi.org/10.1104/pp.114.246124

Barberon, M., Vermeer, J. E. M., De Bellis, D., Wang, P., Naseer, S., Andersen, T. G., Humbel, B. M., Nawrath, C., Takano, J., Salt, D. E., & Geldner, N. (2016). Adaptation of Root Function by

Nutrient-Induced Plasticity of Endodermal Differentiation. *Cell*, *164*(3), 447–459. https://doi.org/10.1016/j.cell.2015.12.021

Baxter, I., Hosmani, P. S., Rus, A., Lahner, B., Borevitz, J. O., Muthukumar, B., Mickelbart, M. V., Schreiber, L., Franke, R. B., & Salt, D. E. (2009). Root Suberin Forms an Extracellular Barrier That Affects Water Relations and Mineral Nutrition in Arabidopsis. *PLoS Genetics*, *5*(5), e1000492. https://doi.org/10.1371/journal.pgen.1000492

Beisson, F., Li, Y., Bonaventure, G., Pollard, M., & Ohlrogge, J. B. (2007a). The Acyltransferase GPAT5 Is Required for the Synthesis of Suberin in Seed Coat and Root of Arabidopsis. *The Plant Cell*, *19*(1), 351–368. https://doi.org/10.1105/tpc.106.048033

Beisson, F., Li, Y., Bonaventure, G., Pollard, M., & Ohlrogge, J. B. (2007b). The Acyltransferase GPAT5 Is Required for the Synthesis of Suberin in Seed Coat and Root of *Arabidopsis*. *The Plant Cell*, *19*(1), 351–368. https://doi.org/10.1105/tpc.106.048033

Beisson, F., Li-Beisson, Y., & Pollard, M. (2012). Solving the puzzles of cutin and suberin polymer biosynthesis. *Current Opinion in Plant Biology*, *15*(3), 329–337. https://doi.org/10.1016/j.pbi.2012.03.003

Berning, N. (2022). *Ectopic expression of R2R3-MYB transcription factors to control suberin biosynthesis* [Master of Science thesis]. Colorado State University.

Bouain, N., Krouk, G., Lacombe, B., & Rouached, H. (2019). Getting to the Root of Plant Mineral Nutrition: Combinatorial Nutrient Stresses Reveal Emergent Properties. *Trends in Plant Science*, *24*(6), 542–552. https://doi.org/10.1016/j.tplants.2019.03.008

Calvo-Polanco, M., Ribeyre, Z., Dauzat, M., Reyt, G., Hidalgo-Shrestha, C., Diehl, P., Frenger, M., Simonneau, T., Muller, B., Salt, D. E., Franke, R. B., Maurel, C., & Boursiac, Y. (2021). Physiological roles of Casparian strips and suberin in the transport of water and solutes. *New Phytologist*, *232*(6), 2295–2307. https://doi.org/10.1111/nph.17765

Cheng, H., Inyang, A., Li, C.-D., Fei, J., Zhou, Y.-W., & Wang, Y.-S. (2020a). Salt tolerance and exclusion in the mangrove plant Avicennia marina in relation to root apoplastic barriers. *Ecotoxicology (London, England)*, *29*(6), 676–683. https://doi.org/10.1007/s10646-020-02203-6

Cheng, H., Inyang, A., Li, C.-D., Fei, J., Zhou, Y.-W., & Wang, Y.-S. (2020b). Salt tolerance and exclusion in the mangrove plant Avicennia marina in relation to root apoplastic barriers. *Ecotoxicology*, *29*(6), 676–683. https://doi.org/10.1007/s10646-020-02203-6

Compagnon, V., Diehl, P., Benveniste, I., Meyer, D., Schaller, H., Schreiber, L., Franke, R., & Pinot, F. (2009). CYP86B1 Is Required for Very Long Chain ω-Hydroxyacid and α,ω-Dicarboxylic Acid Synthesis in Root and Seed Suberin Polyester. *Plant Physiology*, *150*(4), 1831–1843. https://doi.org/10.1104/pp.109.141408

Conditions Leading to High CO2 (>5 kPa) in Waterlogged–Flooded Soils and Possible Effects on Root Growth and Metabolism | Annals of Botany | Oxford Academic. (n.d.). Retrieved November 14, 2021, from https://academic.oup.com/aob/article/98/1/9/239989?login=true

Correia, V. G., Bento, A., Pais, J., Rodrigues, R., Haliński, Ł. P., Frydrych, M., Greenhalgh, A., Stepnowski, P., Vollrath, F., King, A. W. T., & Silva Pereira, C. (2020). The molecular structure and multifunctionality of the cryptic plant polymer suberin. *Materials Today Bio*, *5*, 100039. https://doi.org/10.1016/j.mtbio.2019.100039

de Silva, N. D. G., Murmu, J., Chabot, D., Hubbard, K., Ryser, P., Molina, I., & Rowland, O. (2021). Root Suberin Plays Important Roles in Reducing Water Loss and Sodium Uptake in Arabidopsis thaliana. *Metabolites*, *11*(11), 735. https://doi.org/10.3390/metabo11110735

De Vos, M., Denekamp, M., Dicke, M., Vuylsteke, M., Van Loon, L., Smeekens, S. C., & Pieterse, C. (2006). The Arabidopsis thaliana Transcription Factor AtMYB102 Functions in Defense Against The Insect Herbivore Pieris rapae. *Plant Signaling & Behavior*, *1*(6), 305–311. https://doi.org/10.4161/psb.1.6.3512

DeBolt, S., Scheible, W.-R., Schrick, K., Auer, M., Beisson, F., Bischoff, V., Bouvier-Navé, P., Carroll, A., Hematy, K., Li, Y., Milne, J., Nair, M., Schaller, H., Zemla, M., & Somerville, C. (2009). Mutations in UDP-Glucose:Sterol Glucosyltransferase in Arabidopsis Cause Transparent Testa Phenotype and Suberization Defect in Seeds. *Plant Physiology*, *151*(1), 78–87. https://doi.org/10.1104/pp.109.140582

Deeken, R., Saupe, S., Klinkenberg, J., Riedel, M., Leide, J., Hedrich, R., & Mueller, T. D. (2016). The Nonspecific Lipid Transfer Protein AtLtpI-4 Is Involved in Suberin Formation of Arabidopsis thaliana Crown Galls. *Plant Physiology*, *172*(3), 1911–1927. https://doi.org/10.1104/pp.16.01486

Denekamp, M., & Smeekens, S. C. (2003). Integration of Wounding and Osmotic Stress Signals Determines the Expression of the AtMYB102 Transcription Factor Gene. *Plant Physiology*, *132*(3), 1415–1423. https://doi.org/10.1104/pp.102.019273

Differential deposition of suberin phenolic and aliphatic domains and their roles in resistance to infection during potato tuber (Solanum tuberosum L.) wound-healing | Elsevier Enhanced Reader. (n.d.). https://doi.org/10.1006/pmpp.1998.0179

Doblas, V. G., Geldner, N., & Barberon, M. (2017). The endodermis, a tightly controlled barrier for nutrients. *Current Opinion in Plant Biology*, *39*, 136–143. https://doi.org/10.1016/j.pbi.2017.06.010

Domergue, F., Vishwanath, S. J., Joubès, J., Ono, J., Lee, J. A., Bourdon, M., Alhattab, R., Lowe, C., Pascal, S., Lessire, R., & Rowland, O. (2010). Three Arabidopsis Fatty Acyl-Coenzyme A Reductases, FAR1, FAR4, and FAR5, Generate Primary Fatty Alcohols Associated with Suberin Deposition1[C][W][OA]. *Plant Physiology*, *153*(4), 1539–1554. https://doi.org/10.1104/pp.110.158238

Duan, H., & Schuler, M. A. (2005). Differential Expression and Evolution of the Arabidopsis CYP86A Subfamily. *Plant Physiology*, *137*(3), 1067–1081. https://doi.org/10.1104/pp.104.055715

Dubos, C., Stracke, R., Grotewold, E., Weisshaar, B., Martin, C., & Lepiniec, L. (2010). MYB transcription factors in Arabidopsis. *Trends in Plant Science*, *15*(10), 573–581. https://doi.org/10.1016/j.tplants.2010.06.005

Enstone, D. E., Peterson, C. A., & Ma, F. (2002). Root Endodermis and Exodermis: Structure, Function, and Responses to the Environment. *Journal of Plant Growth Regulation*, *21*(4), 335–351. https://doi.org/10.1007/s00344-003-0002-2

Fedi, F., O'Neill, C. M., Menard, G., Trick, M., Dechirico, S., Corbineau, F., Bailly, C., Eastmond, P. J., & Penfield, S. (2017). Awake1, an ABC-Type Transporter, Reveals an Essential Role for Suberin in the Control of Seed Dormancy. *Plant Physiology*, *174*(1), 276–283. https://doi.org/10.1104/pp.16.01556

Feng, C., Andreasson, E., Maslak, A., Mock, H. P., Mattsson, O., & Mundy, J. (2004). Arabidopsis MYB68 in development and responses to environmental cues. *Plant Science*, *167*(5), 1099–1107. https://doi.org/10.1016/j.plantsci.2004.06.014

Fich, E. A., Segerson, N. A., & Rose, J. K. C. (2016). The Plant Polyester Cutin: Biosynthesis, Structure, and Biological Roles. *Annual Review of Plant Biology*, *67*(1), 207–233. https://doi.org/10.1146/annurev-arplant-043015-111929

Fodor-Dunai, C., Fricke, I., Potocký, M., Dorjgotov, D., Domoki, M., Jurca, M. E., Ötvös, K., Žárský, V., Berken, A., & Fehér, A. (2011). The phosphomimetic mutation of an evolutionarily conserved serine residue affects the signaling properties of Rho of plants (ROPs). *The Plant Journal*, *66*(4), 669–679. https://doi.org/10.1111/j.1365-313X.2011.04528.x

Fodor-Dunai, C., Fricke, I., Potocký, M., Dorjgotov, D., Domoki, M., Jurca, M. E., Ötvös, K., Žárský, V., Berken, A., & Fehér, A. (2011). The phosphomimetic mutation of an evolutionarily conserved serine residue affects the signaling properties of Rho of plants (ROPs). *The Plant Journal*, *66*(4), 669–679. https://doi.org/10.1111/j.1365-313X.2011.04528.x

Fourcroy, P., Sisó-Terraza, P., Sudre, D., Savirón, M., Reyt, G., Gaymard, F., Abadía, A., Abadia, J., Álvarez-Fernández, A., & Briat, J.-F. (2014). Involvement of the ABCG37 transporter in secretion of scopoletin and derivatives by Arabidopsis roots in response to iron deficiency. *New Phytologist*, *201*(1), 155–167. https://doi.org/10.1111/nph.12471

Franke, R., Briesen, I., Wojciechowski, T., Faust, A., Yephremov, A., Nawrath, C., & Schreiber, L. (2005). Apoplastic polyesters in Arabidopsis surface tissues – A typical suberin and a particular cutin. *Phytochemistry*, *66*(22), 2643–2658. https://doi.org/10.1016/j.phytochem.2005.09.027

Franke, R., Höfer, R., Briesen, I., Emsermann, M., Efremova, N., Yephremov, A., & Schreiber, L. (2009). The DAISY gene from Arabidopsis encodes a fatty acid elongase condensing enzyme involved in the biosynthesis of aliphatic suberin in roots and the chalaza-micropyle region of seeds. *The Plant Journal*, *57*(1), 80–95. https://doi.org/10.1111/j.1365-313X.2008.03674.x

Franke, R., & Schreiber, L. (2007). Suberin—A biopolyester forming apoplastic plant interfaces. *Current Opinion in Plant Biology*, *10*(3), 252–259. https://doi.org/10.1016/j.pbi.2007.04.004

Geldner, N. (2013). The Endodermis. *Annual Review of Plant Biology*, *64*(1), 531–558. https://doi.org/10.1146/annurev-arplant-050312-120050

Geng, Y., Wu, R., Wee, C. W., Xie, F., Wei, X., Chan, P. M. Y., Tham, C., Duan, L., & Dinneny, J. R. (2013). A Spatio-Temporal Understanding of Growth Regulation during the Salt Stress Response in Arabidopsis[W]. *The Plant Cell*, *25*(6), 2132–2154. https://doi.org/10.1105/tpc.113.112896

Gou, J.-Y., Yu, X.-H., & Liu, C.-J. (2009). A hydroxycinnamoyltransferase responsible for synthesizing suberin aromatics in Arabidopsis. *Proceedings of the National Academy of Sciences*, *106*(44), 18855–18860. https://doi.org/10.1073/pnas.0905555106

Graça, J. (2015). Suberin: The biopolyester at the frontier of plants. *Frontiers in Chemistry*, *3*. https://doi.org/10.3389/fchem.2015.00062

Graça, J., Cabral, V., Santos, S., Lamosa, P., Serra, O., Molinas, M., Schreiber, L., Kauder, F., & Franke, R. (2015). Partial depolymerization of genetically modified potato tuber periderm reveals intermolecular linkages in suberin polyester. *Phytochemistry*, *117*, 209–219. https://doi.org/10.1016/j.phytochem.2015.06.010

Graça, J., & Pereira, H. (2000). Methanolysis of bark suberins: Analysis of glycerol and acid monomers. *Phytochemical Analysis*, *11*(1), 45–51. https://doi.org/10.1002/(SICI)1099-1565(200001/02)11:1<45::AID-PCA481>3.0.CO;2-8

Graça, J., & Santos, S. (2007). Suberin: A Biopolyester of Plants' Skin. *Macromolecular Bioscience*, *7*(2), 128–135. https://doi.org/10.1002/mabi.200600218

GWIS weekly digest- January 31st 2022—Almckay@rams.colostate.edu—Colorado State University Mail. (n.d.). Retrieved January 31, 2022, from https://mail.google.com/mail/u/0/?tab=rm&ogbl#inbox/FMfcgzGmthlPTFvdkLfcgwSQkNnXZchN

Harman-Ware, A. E., Sparks, S., Addison, B., & Kalluri, U. C. (2021). Importance of suberin biopolymer in plant function, contributions to soil organic carbon and in the production of bio-derived energy and materials. *Biotechnology for Biofuels*, *14*(1), 75. https://doi.org/10.1186/s13068-021-01892-3

Hoang, M. H. T., Nguyen, X. C., Lee, K., Kwon, Y. S., Pham, H. T. T., Park, H. C., Yun, D.-J., Lim, C. O., & Chung, W. S. (2012). Phosphorylation by AtMPK6 is required for the biological function of AtMYB41 in Arabidopsis. *Biochemical and Biophysical Research Communications*, *422*(1), 181–186. https://doi.org/10.1016/j.bbrc.2012.04.137

Höfer, R., Briesen, I., Beck, M., Pinot, F., Schreiber, L., & Franke, R. (2008). The Arabidopsis cytochrome P450 CYP86A1 encodes a fatty acid ω-hydroxylase involved in suberin monomer biosynthesis. *Journal of Experimental Botany*, *59*(9), 2347–2360. https://doi.org/10.1093/jxb/ern101

Holbein, J., Shen, D., & Andersen, T. G. (2021). The endodermal passage cell – just another brick in the wall? *New Phytologist*, *230*(4), 1321–1328. https://doi.org/10.1111/nph.17182

Huang, C.-N., Cornejo, M. J., Bush, D. S., & Jones, R. L. (1986). Estimating viability of plant protoplasts using double and single staining. *Protoplasma*, *135*(2–3), 80–87. https://doi.org/10.1007/BF01277001

Hydroxycinnamic Acid-derived Polymers Constitute the Polyaromatic Domain of Suberin (Ã¢Ë†â€”) | *Elsevier Enhanced Reader*. (n.d.). https://doi.org/10.1074/jbc.270.13.7382

Jumper, J., Hassabis, D. (2022). Structure predictions to atomic accuracy with AlphaFold. *Nat Methods 19*, 11–12. https://doi.org/10.1038/s41592-021-01362-6

Kolattukudy, P. E. (2001). Polyesters in Higher Plants. In W. Babel & A. Steinbüchel (Eds.), *Biopolyesters* (pp. 1–49). Springer. https://doi.org/10.1007/3-540-40021-4_1

Kosma, D. K., Molina, I., Ohlrogge, J. B., & Pollard, M. (2012). Identification of an Arabidopsis Fatty Alcohol:Caffeoyl-Coenzyme A Acyltransferase Required for the Synthesis of Alkyl Hydroxycinnamates in Root Waxes1. *Plant Physiology*, *160*(1), 237–248. https://doi.org/10.1104/pp.112.201822

Kosma, D. K., Murmu, J., Razeq, F. M., Santos, P., Bourgault, R., Molina, I., & Rowland, O. (2014). AtMYB41 activates ectopic suberin synthesis and assembly in multiple plant species and cell types. *The Plant Journal*, *80*(2), 216–229. https://doi.org/10.1111/tpj.12624

Krishnamurthy, P., Vishal, B., Bhal, A., & Kumar, P. P. (2021). WRKY9 transcription factor regulates cytochrome P450 genes CYP94B3 and CYP86B1, leading to increased root suberin

and salt tolerance in Arabidopsis. *Physiologia Plantarum*, *172*(3), 1673–1687. https://doi.org/10.1111/ppl.13371

Krishnamurthy, P., Vishal, B., Ho, W. J., Lok, F. C. J., Lee, F. S. M., & Kumar, P. P. (2020). Regulation of a Cytochrome P450 Gene CYP94B1 by WRKY33 Transcription Factor Controls Apoplastic Barrier Formation in Roots to Confer Salt Tolerance. *Plant Physiology*, *184*(4), 2199–2215. https://doi.org/10.1104/pp.20.01054

Lashbrooke, J., Cohen, H., Levy-Samocha, D., Tzfadia, O., Panizel, I., Zeisler, V., Massalha, H., Stern, A., Trainotti, L., Schreiber, L., Costa, F., & Aharoni, A. (2016). MYB107 and MYB9 Homologs Regulate Suberin Deposition in Angiosperms. *The Plant Cell*, *28*(9), 2097–2116. https://doi.org/10.1105/tpc.16.00490

Lee, S. B., & Suh, M.-C. (2018). Disruption of glycosylphosphatidylinositol-anchored lipid transfer protein 15 affects seed coat permeability in Arabidopsis. *The Plant Journal*, *96*(6), 1206–1217. https://doi.org/10.1111/tpj.14101

Lee, S.-B., Jung, S.-J., Go, Y.-S., Kim, H.-U., Kim, J.-K., Cho, H.-J., Park, O. K., & Suh, M.-C. (2009). Two Arabidopsis 3-ketoacyl CoA synthase genes, KCS20 and KCS2/DAISY, are functionally redundant in cuticular wax and root suberin biosynthesis, but differentially controlled by osmotic stress. *The Plant Journal*, *60*(3), 462–475. https://doi.org/10.1111/j.1365-313X.2009.03973.x

Li, B., Kamiya, T., Kalmbach, L., Yamagami, M., Yamaguchi, K., Shigenobu, S., Sawa, S., Danku, J. M. C., Salt, D. E., Geldner, N., & Fujiwara, T. (2017). Role of LOTR1 in Nutrient Transport through Organization of Spatial Distribution of Root Endodermal Barriers. *Current Biology*, *27*(5), 758–765. https://doi.org/10.1016/j.cub.2017.01.030

Li, Y., Beisson, F., Koo, A. J. K., Molina, I., Pollard, M., & Ohlrogge, J. (2007). Identification of acyltransferases required for cutin biosynthesis and production of cutin with suberin-like monomers. *Proceedings of the National Academy of Sciences of the United States of America*, *104*(46), 18339–18344. https://doi.org/10.1073/pnas.0706984104

Li, Y., Beisson, F., Ohlrogge, J., & Pollard, M. (2007). Monoacylglycerols Are Components of Root Waxes and Can Be Produced in the Aerial Cuticle by Ectopic Expression of a Suberin-Associated Acyltransferase. *Plant Physiology*, *144*(3), 1267–1277. https://doi.org/10.1104/pp.107.099432

Li-Beisson, Y., Shorrosh, B., Beisson, F., Andersson, M. X., Arondel, V., Bates, P. D., Baud, S., Bird, D., DeBono, A., Durrett, T. P., Franke, R. B., Graham, I. A., Katayama, K., Kelly, A. A., Larson, T., Markham, J. E., Miquel, M., Molina, I., Nishida, I., … Ohlrogge, J. (2013). Acyl-Lipid Metabolism. *The Arabidopsis Book / American Society of Plant Biologists*, *11*, e0161. https://doi.org/10.1199/tab.0161

Líška, D., Martinka, M., Kohanová, J., & Lux, A. (2016). Asymmetrical development of root endodermis and exodermis in reaction to abiotic stresses. *Annals of Botany*, *118*(4), 667–674. https://doi.org/10.1093/aob/mcw047

Lulai, E. C., & Corsini, D. L. (1998). Differential deposition of suberin phenolic and aliphatic domains and their roles in resistance to infection during potato tuber (Solanum tuberosumL.) wound-healing. *Physiological and Molecular Plant Pathology*, *53*(4), 209–222. https://doi.org/10.1006/pmpp.1998.0179

LUX, A., MORITA, S., ABE, J., & ITO, K. (2005). An Improved Method for Clearing and Staining Free-hand Sections and Whole-mount Samples*. *Annals of Botany*, *96*(6), 989–996. https://doi.org/10.1093/aob/mci266

Millar, A. A., & Kunst, L. (1997). Very-long-chain fatty acid biosynthesis is controlled through the expression and specificity of the condensing enzyme. *The Plant Journal*, *12*(1), 121–131. https://doi.org/10.1046/j.1365-313X.1997.12010121.x

Molina, I., Li-Beisson, Y., Beisson, F., Ohlrogge, J. B., & Pollard, M. (2009). Identification of an Arabidopsis Feruloyl-Coenzyme A Transferase Required for Suberin Synthesis. *Plant Physiology*, *151*(3), 1317–1328. https://doi.org/10.1104/pp.109.144907

Molina, I., Ohlrogge, J. B., & Pollard, M. (2008). Deposition and localization of lipid polyester in developing seeds of Brassica napus and Arabidopsis thaliana. *The Plant Journal*, *53*(3), 437–449. https://doi.org/10.1111/j.1365-313X.2007.03348.x

Naseer, S., Lee, Y., Lapierre, C., Franke, R., Nawrath, C., & Geldner, N. (2012). Casparian strip diffusion barrier in Arabidopsis is made of a lignin polymer without suberin. *Proceedings of the National Academy of Sciences*, *109*(25), 10101–10106. https://doi.org/10.1073/pnas.1205726109

Nawrath, C., Schreiber, L., Franke, R. B., Geldner, N., Reina-Pinto, J. J., & Kunst, L. (2013). Apoplastic Diffusion Barriers in Arabidopsis. *The Arabidopsis Book*, *2013*(11). https://doi.org/10.1199/tab.0167

Negrel, J., Pollet, B., & Lapierre, C. (1996). Ether-linked ferulic acid amides in natural and wound periderms of potato tuber. *Phytochemistry*, *43*(6), 1195–1199. https://doi.org/10.1016/S0031-9422(96)00500-6

Neto, C. P., Rocha, J., Gil, A., Cordeiro, N., Esculcas, A. P., Rocha, S., Delgadillo, I., De Jesus, J. D. P., & Correia, A. J. F. (1995). 13C solid-state nuclear magnetic resonance and Fourier transform infrared studies of the thermal decomposition of cork. *Solid State Nuclear Magnetic Resonance*, *4*(3), 143–151. https://doi.org/10.1016/0926-2040(94)00039-F

Nomberg, G., Marinov, O., Arya, G.C., Manasherova, E., & Cohen, H. (2022). The Key Enzymes in the Suberin Biosynthetic Pathway in Plants: An Update. *Plants, 11*, 392. https://doi.org/10.3390/plants11030392

Oemke, Sara. (2020). *Design and quantification of a cell type specific genetic circuit in plants* [Master of Science thesis]. Colorado State University.

Pal, S., Kisko, M., Dubos, C., Lacombe, B., Berthomieu, P., Krouk, G., & Rouached, H. (2017). TransDetect Identifies a New Regulatory Module Controlling Phosphate Accumulation. *Plant Physiology*, *175*(2), 916–926. https://doi.org/10.1104/pp.17.00568

Partial depolymerization of genetically modified potato tuber periderm reveals intermolecular linkages in suberin polyester | Elsevier Enhanced Reader. (n.d.). https://doi.org/10.1016/j.phytochem.2015.06.010

Paul, S., Gable, K., Beaudoin, F., Cahoon, E., Jaworski, J., Napier, J. A., & Dunn, T. M. (2006). Members of the Arabidopsis FAE1-like 3-Ketoacyl-CoA Synthase Gene Family Substitute for the Elop Proteins of Saccharomyces cerevisiae*. *Journal of Biological Chemistry*, *281*(14), 9018–9029. https://doi.org/10.1074/jbc.M507723200

Pecková, E., Tylová, E., & Soukup, A. (2016). Tracing root permeability: Comparison of tracer methods. *Biologia Plantarum*, *60*(4), 695–705. https://doi.org/10.1007/s10535-016-0634-2

Peterson, C., & Enstone, D. (2006). Function of passage cells in the endodermis and exodermis of roots. *Physiologia Plantarum*, *97*, 592–598. https://doi.org/10.1111/j.1399-3054.1996.tb00520.x

Pfister, A., Barberon, M., Alassimone, J., Kalmbach, L., Lee, Y., Vermeer, J. E., Yamazaki, M., Li, G., Maurel, C., Takano, J., Kamiya, T., Salt, D. E., Roppolo, D., & Geldner, N. (2014). A receptor-like kinase mutant with absent endodermal diffusion barrier displays selective nutrient homeostasis defects. *ELife*, *3*, e03115. https://doi.org/10.7554/eLife.03115

Philippe, G., Sørensen, I., Jiao, C., Sun, X., Fei, Z., Domozych, D. S., & Rose, J. K. (2020). Cutin and suberin: Assembly and origins of specialized lipidic cell wall scaffolds. *Current Opinion in Plant Biology*, *55*, 11–20. https://doi.org/10.1016/j.pbi.2020.01.008

Pinot, F., & Beisson, F. (2011). Cytochrome P450 metabolizing fatty acids in plants: Characterization and physiological roles. *The FEBS Journal*, *278*(2), 195–205. https://doi.org/10.1111/j.1742-4658.2010.07948.x

Pollard, M., Beisson, F., Li, Y., & Ohlrogge, J. B. (2008). Building lipid barriers: Biosynthesis of cutin and suberin. *Trends in Plant Science*, *13*(5), 236–246. https://doi.org/10.1016/j.tplants.2008.03.003

Ranathunge, K., & Schreiber, L. (2011). Water and solute permeabilities of Arabidopsis roots in relation to the amount and composition of aliphatic suberin. *Journal of Experimental Botany*, *62*(6), 1961–1974. https://doi.org/10.1093/jxb/erq389

Ranathunge, K., Schreiber, L., & Franke, R. (2011). Suberin research in the genomics era—New interest for an old polymer. *Plant Science*, *180*(3), 399–413. https://doi.org/10.1016/j.plantsci.2010.11.003

Robards, A. W., & Robb, M. E. (1974). The entry of ions and molecules into roots: An investigation using electron-opaque tracers. *Planta*, *120*(1), 1–12. https://doi.org/10.1007/BF00388267

Rowe, J. W. (2014). *Natural Products of Woody Plants Chemicals Extraneous to the Lignocellulosic Cell Wall*. Springer Berlin.

Rupasinghe, S. G., Duan, H., & Schuler, M. A. (2007). Molecular definitions of fatty acid hydroxylases in Arabidopsis thaliana. *Proteins: Structure, Function, and Bioinformatics*, *68*(1), 279–293. https://doi.org/10.1002/prot.21335

Salas-González, I., Reyt, G., Flis, P., Custódio, V., Gopaulchan, D., Bakhoum, N., Dew, T. P., Suresh, K., Franke, R. B., Dangl, J. L., Salt, D. E., & Castrillo, G. (2021). Coordination between microbiota and root endodermis supports plant mineral nutrient homeostasis. *Science*, *371*(6525), eabd0695. https://doi.org/10.1126/science.abd0695

Schreiber, L. (2010). Transport barriers made of cutin, suberin and associated waxes. *Trends in Plant Science*, *15*(10), 546–553. https://doi.org/10.1016/j.tplants.2010.06.004

Schreiber, L., Franke, R., & Hartmann, K. (2005). Wax and suberin development of native and wound periderm of potato (Solanum tuberosum L.) and its relation to peridermal transpiration. *Planta*, *220*(4), 520–530. https://doi.org/10.1007/s00425-004-1364-9

Schreiber, L., Hartmann, K., & Skrabs, M. (n.d.). *Apoplastic barriers in roots: Chemical composition of endodermal and hypodermal cell walls*. 14.

Schwacke R, Schneider A, Van Der Graaff E, Fischer K, Catoni E, Desimone M, Frommer WB, Flu ¨ gge UI, Kunze R. (2003). ARAMEMNON, a novel database for Arabidopsis integral membrane proteins. *Plant Physiology 131*, 16–26.

Serra, O., & Geldner, N. (2022). The making of suberin. *New Phytologist*, *235*(3), 848–866. https://doi.org/10.1111/nph.18202

Serra, O., Hohn, C., Franke, R., Prat, S., Molinas, M., & Figueras, M. (2010). A feruloyl transferase involved in the biosynthesis of suberin and suberin-associated wax is required for maturation and sealing properties of potato periderm. *The Plant Journal*, *62*(2), 277–290. https://doi.org/10.1111/j.1365-313X.2010.04144.x

Serra, O., Soler, M., Hohn, C., Franke, R., Schreiber, L., Prat, S., Molinas, M., & Figueras, M. (2009). Silencing of StKCS6 in potato periderm leads to reduced chain lengths of suberin and wax compounds and increased peridermal transpiration. *Journal of Experimental Botany*, *60*(2), 697–707. https://doi.org/10.1093/jxb/ern314

Serra, O., Soler, M., Hohn, C., Sauveplane, V., Pinot, F., Franke, R., Schreiber, L., Prat, S., Molinas, M., & Figueras, M. (2009). CYP86A33-Targeted Gene Silencing in Potato Tuber Alters Suberin Composition, Distorts Suberin Lamellae, and Impairs the Periderm's Water Barrier Function. *Plant Physiology*, *149*(2), 1050–1060. https://doi.org/10.1104/pp.108.127183

Shanmugarajah, K., Linka, N., Gräfe, K., Smits, S. H. J., Weber, A. P. M., Zeier, J., & Schmitt, L. (2019). ABCG1 contributes to suberin formation in Arabidopsis thaliana roots. *Scientific Reports*, *9*(1), 11381. https://doi.org/10.1038/s41598-019-47916-9

Shi, H., & Bressan, R. (2006). RNA Extraction. In J. Salinas & J. J. Sanchez-Serrano (Eds.), *Arabidopsis Protocols* (pp. 345–348). Humana Press. https://doi.org/10.1385/1-59745-003-0:345

Shukla, V., Han, J.-P., Cléard, F., Lefebvre-Legendre, L., Gully, K., Flis, P., Berhin, A., Andersen, T. G., Salt, D. E., Nawrath, C., & Barberon, M. (2021). Suberin plasticity to developmental and

exogenous cues is regulated by a set of MYB transcription factors. *Proceedings of the National Academy of Sciences*, *118*(39), e2101730118. https://doi.org/10.1073/pnas.2101730118

Soler, M., Serra, O., Molinas, M., Huguet, G., Fluch, S., & Figueras, M. (2007). A Genomic Approach to Suberin Biosynthesis and Cork Differentiation. *Plant Physiology*, *144*(1), 419–431. https://doi.org/10.1104/pp.106.094227

Stracke, R., Werber, M., & Weisshaar, B. (2001). The R2R3-MYB gene family in Arabidopsis thaliana. *Current Opinion in Plant Biology*, *4*(5), 447–456. https://doi.org/10.1016/S1369-5266(00)00199-0

The Biopolymers Cutin and Suberin. (n.d.). Retrieved November 27, 2021, from https://bioone.org/journals/the-arabidopsis-book/volume-2002/issue-1/tab.0021/The-Biopolymers-Cutin-and-Suberin/10.1199/tab.0021.full

The endodermis, a tightly controlled barrier for nutrients | Elsevier Enhanced Reader. (n.d.). https://doi.org/10.1016/j.pbi.2017.06.010

Ursache, R., De Jesus Vieira Teixeira, C., Dénervaud Tendon, V., Gully, K., De Bellis, D., Schmid-Siegert, E., Grube Andersen, T., Shekhar, V., Calderon, S., Pradervand, S., Nawrath, C., Geldner, N., & Vermeer, J. E. M. (2021). GDSL-domain proteins have key roles in suberin polymerization and degradation. *Nature Plants*, *7*(3), 353–364. https://doi.org/10.1038/s41477-021-00862-9

Vishwanath, S. J., Delude, C., Domergue, F., & Rowland, O. (2015). Suberin: Biosynthesis, regulation, and polymer assembly of a protective extracellular barrier. *Plant Cell Reports*, *34*(4), 573–586. https://doi.org/10.1007/s00299-014-1727-z

Waduwara, C. I., Walcott, S. E., & Peterson, C. A. (2008). Suberin lamellae of the onion root endodermis: Their pattern of development and continuity. *Botany*, *86*(6), 623–632. https://doi.org/10.1139/B08-038

Wang, C., Wang, H., Li, P., Li, H., Xu, C., Cohen, H., Aharoni, A., & Wu, S. (2020). Developmental programs interact with abscisic acid to coordinate root suberization in Arabidopsis. *The Plant Journal*, *104*(1), 241–251. https://doi.org/10.1111/tpj.14920

Wunderling, A., Ripper, D., Barra-Jimenez, A., Mahn, S., Sajak, K., Targem, M. B., & Ragni, L. (2018). A molecular framework to study periderm formation in Arabidopsis. *New Phytologist*, *219*(1), 216–229. https://doi.org/10.1111/nph.15128

Xiao, W., Molina, D., Wunderling, A., Ripper, D., Vermeer, J. E. M., & Ragni, L. (2020). Pluripotent Pericycle Cells Trigger Different Growth Outputs by Integrating Developmental Cues into Distinct Regulatory Modules. *Current Biology*, *30*(22), 4384-4398.e5. https://doi.org/10.1016/j.cub.2020.08.053

Yadav, V., Molina, I., Ranathunge, K., Castillo, I. Q., Rothstein, S. J., & Reed, J. W. (2014a). ABCG Transporters Are Required for Suberin and Pollen Wall Extracellular Barriers in Arabidopsis[C][W]. *The Plant Cell*, *26*(9), 3569–3588. https://doi.org/10.1105/tpc.114.129049

Yadav, V., Molina, I., Ranathunge, K., Castillo, I. Q., Rothstein, S. J., & Reed, J. W. (2014b). ABCG Transporters Are Required for Suberin and Pollen Wall Extracellular Barriers in Arabidopsis. *The Plant Cell*, *26*(9), 3569–3588. https://doi.org/10.1105/tpc.114.129049

Yan, B., & Stark, R. E. (1998). A WISE NMR Approach to Heterogeneous Biopolymer Mixtures: Dynamics and Domains in Wounded Potato Tissues. *Macromolecules*, *31*(8), 2600–2605. https://doi.org/10.1021/ma9714880

Yang, W., Pollard, M., Li-Beisson, Y., Beisson, F., Feig, M., & Ohlrogge, J. (2010). A distinct type of glycerol-3-phosphate acyltransferase with sn-2 preference and phosphatase activity producing 2-monoacylglycerol. *Proceedings of the National Academy of Sciences*, *107*(26), 12040–12045. https://doi.org/10.1073/pnas.0914149107

Yang, W., Simpson, J. P., Li-Beisson, Y., Beisson, F., Pollard, M., & Ohlrogge, J. B. (2012). A Land-Plant-Specific Glycerol-3-Phosphate Acyltransferase Family in Arabidopsis: Substrate Specificity, sn-2 Preference, and Evolution. *Plant Physiology*, *160*(2), 638–652. https://doi.org/10.1104/pp.112.201996

Yanhui, C., Xiaoyuan, Y., Kun, H., Meihua, L., Jigang, L., Zhaofeng, G., Zhiqiang, L., Yunfei, Z., Xiaoxiao, W., Xiaoming, Q., Yunping, S., Li, Z., Xiaohui, D., Jingchu, L., Xing-Wang, D., Zhangliang, C., Hongya, G., & Li-Jia, Q. (2006). The MYB Transcription Factor Superfamily of Arabidopsis: Expression Analysis and Phylogenetic Comparison with the Rice MYB Family. *Plant Molecular Biology*, *60*(1), 107–124. https://doi.org/10.1007/s11103-005-2910-y

Zhang, L., Merlin, I., Pascal, S., Bert, P.-F., Domergue, F., & Gambetta, G. A. (2020). Drought activates MYB41 orthologs and induces suberization of grapevine fine roots. *Plant Direct*, *4*(11), e00278. https://doi.org/10.1002/pld3.278

Zhang, P., Wang, R., Yang, X., Ju, Q., Li, W., Lü, S., Tran, L. P., & Xu, J. (2020). The R2R3-MYB transcription factor ATMYB49 modulates salt tolerance in *Arabidopsis* by modulating the cuticle formation and antioxidant defence. *Plant, Cell & Environment*, *43*(8), 1925–1943. https://doi.org/10.1111/pce.13784

Zhang, X., Henriques, R., Lin, S.-S., Niu, Q.-W., & Chua, N.-H. (2006). Agrobacterium-mediated transformation of Arabidopsis thaliana using the floral dip method. *Nature Protocols*, *1*(2), 641–646. https://doi.org/10.1038/nprot.2006.97

Appendix

Media Preparation

Laurel Broth (LB) Media

LB media was used for *E. coli* and *A. tumefaciens* growth. 40g Gibco Tryptone, 20g Gibco yeast extract, and 40g NaCl were added to 3800ml deionized H_2O. The solution was mixed until solids dissolved. The pH was brought to 7 by addition of 3M NaOH. The solution was brought up to 4000ml by addition of deionized H_2O and 3M NaOH added to bring the pH back to 7 if needed. The liquid LB was aliquoted into bottles of 500ml. If preparing solid media, 7.5g Agar II was added to each bottle. Bottles were autoclaved.

Murashige and Skoog (MS) Media

MS media was used for plant growth. For full MS (used unless noted otherwise) 40g sucrose, 17.6g Sigma Aldrich MS Basal Medium, and 2g Sigma Aldrich MES were added to 3200ml deionized H_2O. The solution was mixed until solids dissolved. The pH was brought to 5.7 by addition of 10M or 1M KOH. The solution was brought up to 4000ml by addition of deionized H_2O and 1M KOH added to bring the pH back to 5.7 if needed. The liquid MS was aliquoted into bottles of 500ml. If preparing solid media, 3g Plant Media Phytoagar was added to each bottle. Bottles were autoclaved. For half MS, half the amount of sucrose and MS Basal Medium were used (20g sucrose and 8.8g MS). No other changes were made in preparation of half MS.

New Infiltration Media (NIM)

NIM was used for *Agrobacterium*-mediated transformation of *Arabidopsis thaliana.* 200g sucrose and .812g $MgCl_2$ was added to 3600ml H_2O. The solution was mixed until solids

dissolved. The solution was brought up to 4000ml by addition of deionized H_2O. The NIM was aliquoted into bottles of 500ml and autoclaved.

Primer Sequences

Table A.1. Primer sequences for cloning and mutagenesis.

Primer	*Function*	*Sequence (5'-3')*
MYB49clone-F	cloning	gaaaaagATGGGAAAATCTTCAAGC
MYB49clone-R	cloning	aagacaTTATGATAGATTCAAAGCATTATTATTATG
MYB53clone-F	cloning	caaacATGGGAAGATCTCCTAG
MYB53clone-R	cloning	ataccTTAAGATTGATAAGAAATGTCTGG
MYB107clone-F2	cloning	agatgttataacaaaATGGGGAGATC
MYB107clone-R2	cloning	taatgttttactttcatctCTATTCACGAAAT
MYB84clone-F2	cloning	cactaggagtacaagtATGGGAAG
MYB84clone-R2	cloning	acccccaattaataataatgatgtacg
MYB102clone-F2	cloning	ctgataaacaatcaATGGCAAGGT
MYB102clone-R2	cloning	gaaaactgtatcccactcgagt
MYB49clone-F_BamHI	cloning	acgaatGGATCCgaaaaagATGGGAAAATCTTCAAGC
MYB84clone-F2_BamHI	cloning	acgaatGGATCCcactaggagtacaagtATGGGAAG
MYB102_BglII-F	cloning	acgaatAGATCTtcaATGGCAAGGTCACCTTG
MYB49clone-F_BglII	cloning	acgaatAGATCTgaaaaagATGGGAAAATCTTCAAGC
MYB84_S256-F	mutagenesis	ctatcttgagcgccaacacaaacgatccattgcttaacacaagtaat
MYB84_S256-R	mutagenesis	attacttgtgttaagcaatggatcgtttgtgttggcgctcaagatag
MYB49_S273_T277-F	mutagenesis	cagttcatcaatgctagcgggaacttcagatagcagctcggatccgttgaattcgtcttcga
MYB49_S273_T277-R	mutagenesis	tcgaagacgaattcaacggatccgagctgctatctgaagttcccgctagcattgatgaactg
MYB49_S273-F	mutagenesis	agttcatcaatgctagcgggaacttcagatagcagctcgacacc
MYB49_S273-R	mutagenesis	ggtgtcgagctgctatctgaagttcccgctagcattgatgaact
MYB49_T277-F	mutagenesis	gaacttcatcgagcagctcggatccgttgaattcgtcttcgac
MYB49_T277-R	mutagenesis	gtcgaagacgaattcaacggatccgagctgctcgatgaagttc
MYB107_S253-F	mutagenesis	cagaattttattccgcccttgatttcgacagatcctgatgagtctaag
MYB107_S253-R	mutagenesis	cttagactcatcaggatctgtcgaaatcaagggcggaataaaattctg
MYB49_T277_NEB-R	mutagenesis	AATTCAACGGatcCGAGCTGCTC
MYB49_T277_NEB-F	mutagenesis	CGTCTTCGACTTTTTATG
MYb49_S273_T277_NEB-R	mutagenesis	tgctatcTGAAGTTCCCGCTAGCAT
MYB49_S273_T277_NEB-F	mutagenesis	gctcggatCCGTTGAATTCGTCTTCG

Table A.2. Primer sequences for sequencing and qRT-PCR.

Primer	*Function*	*Sequence (5'-3')*
MYB49sequencing-F	sequencing	CTCCAGCTCTCTTCGTTTCTTACC
MYB49sequencing-R	sequencing	GGTATGATTCGGTCTGAACGTTGTTGA
MYB53sequencing-F	sequencing	CTCAGCTCATGTCTCTGTCTAACCT
MYB53sequencing-R	sequencing	ATGGGAGCAGGAGAAGGTTGAAG
MYB84sequencing-F	sequencing	AGAGACAACACCAACAACAACAAATCC
MYB84sequencing-R	sequencing	GGCTTAACATCTTCTTGGTCGCAAAAC
MYB102sequencing-F	sequencing	TCGTCGTCATCACCAGCAACATC
MYB102sequencing-R	sequencing	CTCCGGTTTGGCTATAAACTGTTTGC
MYB107sequencing-F	sequencing	ACTACTAGCTGCCGCAAATTTCAAC
MYB107sequencing-R	sequencing	TGTGTGATGAATGTCAAAGGAAGAAGAGG
ABCG37-F	genomic DNA check	TTTGTTAAAGGCCTTGTCTGG
ABCG37-R	genomic DNA check	ACTCATCCAGTCTGTGTCC
VacATP-F	genomic DNA check	ACAATATTCAGTCTCAGGTTGC
VacATP-R	genomic DNA check	CTTTCGGTTAATGGCATTGAG
ACT2-F	qRT-PCR	GACCTTTAACTCTCCCGCTATG
ACT2-R	qRT-PCR	GAGACACACCATCACCAGAAT
KCS2-F	qRT-PCR	CCTTTAGTCTCACCGATCTCAC
KCS2-R	qRT-PCR	GAGGACGAGTTGTGAAGTAGAG
FACT-F	qRT-PCR	CGAGGTTCTCGTTCACTACTATC
FACT-R	qRT-PCR	CCACCACTACAACTCCTTCTC
ABCG6-F	qRT-PCR	ATGTTCGCTGCCGAGTTT
ABCG6-R	qRT-PCR	CTTCATCTCCGATCACCGTATTC
GELP51-F	qRT-PCR	CCTCTTATCTCTCACTGCTTCAG
GELP51-R	qRT-PCR	TTATTTCCGGCATCGACTAGAG
MYB84qPCR2-F	qRT-PCR	GGCTGAGGTGGCTTAACTATC
MYB84qPCR2-R	qRT-PCR	GCGATTATAGACCACCTGCTAC